FULL SCALE MODELING OF GEOTEXTILE REINFORCED LIME STABILIZED COHESIVE SOIL RETAINING WALL

MUHANNAD HISHAM ISMEIK

BOĞAZİÇİ UNIVERSITY

1996

FULL SCALE MODELING OF GEOTEXTILE REINFORCED LIME STABILIZED COHESIVE SOIL RETAINING WALL

by

Muhannad Hisham Ismeik

B.Sc. in CE, Boğaziçi University, 1991

M.Sc. in CE, Boğaziçi University, 1992

Submitted to the Institute for Graduate Studies in Science and Engineering in partial fulfillment of the requirements for the degree of

Doctor

of

Philosophy

Boğaziçi University

1996

TO:

MY FATHER AND MOTHER

WHO SACRIFIED A LOT IN ORDER

TO SEE ME IN THIS POSITION

ACKNOWLEDGMENTS

I am deeply indebted to my advisor Dr. Erol Güler for his competent advice, loyal support and unbounded guidance throughout my stay in Turkey. I especially appreciate his knowledge, the valuable suggestions based on many years of experience, the productive discussions and the long hours he dedicated in spite of his busy schedule. I am proud of being one of his students.

I would like to express my sincere gratitude to my advisory committee, Dr. Gökhan Baykal and Dr. Feyza Çinicioğlu, for their efforts and comments.

I also would like to thank all the members of the Civil Engineering Department for their encouragement and help at every stage of my education especially, Dr. Semih Tezcan, Dr. Gülay Altay, Dr. Turan Özturan, İlknur Sargin, Orkun Akkol, and Yasin Fahjan.

The Kilyos geosynthetic wall is a joint research effort between The University of Maryland, The Scientific and Technical Research Council of Turkey and Bogazici University. The financial support provided by US National Science Foundation under grant number Z473401, is greatly appreciated.

The communications with Dr. Deborah J. Goodings at The University of Maryland at every stage were of great benefit.

Ibrahim Boul from the Electrical and Electronics Engineering Department of Boğaziçi university made important contributions in instrumentation of the wall, provided valuable assistance in installing the coils, processing and evaluating the data and development of the computer software.

Dr. Yani Skarlatos at Eti Electrical Industries contributed to the planning, development and production of the electronic materials and coils.

Polyfelt Inc., Austria, kindly provided the geotextiles used as reinforcement and shipped to Istanbul. Alarko Holding provided the compactor equipment, used in the Project.

Dr. Ayşe Edinçliler kindly assisted in running the finite element program.

The contractor was Geta Construction Limited, İsmit Özsavacı and Lemi Hünük provided capable on site surveying and assistance during construction, their cooperation is greatly appreciated.

Tahir Öngür and Hakan Boysan assisted in determining and obtaining undisturbed samples from bore holes, their support is acknowledged.

Anan Al-Shrabati reviewed and checked all electronics problems encountered and assisted in the instrumentation of the coil systems.

Dr. Khaled Ramadan who has been a continuous source of encouragement, provided on site construction inspection and other valuable support assisted in the management of the Kilyos Wall. My valuable brother Mulham Ismeik kindly provided his computer.

Dr. Mehmet Uyan, at The Technical University of Istanbul and Set Concrete Industry provided counter weights and concrete blocks in overloading the Kilyos wall.

The help and cooperation of Rahmi Taşpınar Head of Personnel office, and the technical staff at the Geotechnical Engineering Laboratory is admired.

Very special thanks to all of those real friends who lightened my path, coloured my life and showed me the beautiful dimensions of this world especially Ghassan Khraim, Uğur Bati, Iyad Kayyali, and Anwar Abouqamar. I am deeply proud of this valuable friendship.

Though not mentioned with their names, sincere appreciation and gratitude are extended to all of personnel who administered, coordinated, and provided input and assistance during the course of the research study. Only their loyal and genuine support made this research possible, without of which this work would not be possible.

ABSTRACT

In this research, a reinforced soil retaining structure, "Kilyos Wall" is studied. It is the first known geosynthetic reinforced wall to be instrumented and tested in Turkey.

Lime stabilized cohesive clay is used as a backfill material rather than a pure frictional soil. The wall was designed with a factor of safety of less than one. Measurements include determination of the horizontal and vertical movements of the backfill utilizing an electronic coils developed specially for this project. Vertical and horizontal stresses are determined using Glötzl pressure cells.

A comparison is made between observed behavior and design assumptions and calculations. A Finite Element Analysis study was conducted in order to investigate the stresses and deformations using the CRISP '92 program.

The effect of the facing rigidity on the overall stability of geosynthetic reinforced retaining walls is investigated explicitly for full height concrete facing by using the two wedge mechanism.

A method is proposed to account analytically for the effects of facing thickness to stability of retaining walls with the amount of reinforcement required, using a limit equilibrium analysis with relation to the seismic forces and presented in chart form.

ÖZET

Donatılı zemin yapıların kullanımları gittikçe yaygınlaşmaktadır. Ekonomik olmaları ve inşaat sürelerinin kısa olması, donatılı zemin istinat duvarlarını giderek betonarme istinat duvarlarından daha popüler hale getirmektedir.

Bu araştırmanın amacı, arka dolgu olarak kireçle stabilize edilmiş kil kullanılması ile ilgili olarak geliştirilmiş metodun bir inşaat teknolojisi olarak kullanılabileceğinin gösterilmesidir. Bu amaçla 6 m yüksekliğinde enstrümanlarla teçhiz edilmiş bir donatılı zemin istinat duvarı inşa edilmiştir. Bu duvarda donatılı zemin dolgusu olarak kireçle stabilize edilmiş kil kullanılmıştır. Dolgunun çeşitli yerlerine enstrümanlar yerleştirilmiştir. Bunlar başlıca: yatay ve düşey yöndeki deformasyonları ölçen elektrik bobinleri, yatay ve düşey gerilmeleri ölçen Glötzl hücreleri ve donatı üzerindeki deformasyonları ölçen invar kablolardır.

Duvarın davranışı, CRISP'92-sonlu elemanlar analizi yardımı ile de incelenmiştir. Yapılan ölçümler ve gözlemler sonucunda, geosentetik donatılı istinat duvarlarında kireçle stabilize edilmiş kilin başarı ile kullanılabileceği sonucuna varılmıştır.

Ayrıca donatılı zemin istinat yapılarının genel stabilitesine ön cephenin yapmış olduğu etki, tam boy bir beton ön cephe için iki kama mekanizması kullanılarak incelenmiştir.

Ön cephe kalınlığının, istinat duvarının stabilitesine olan etkisini analitik olarak belirlemek amacı ile bir metod önerilmektedir. Limit denge analizi kullanılarak, kullanılması gereken donatı statik ve dinamik yükler için bulunmuştur. Tüm sonuçlar abak halinde sunulmuştur.

TABLE OF CONTENTS

LIST OF FIGURES

LIST OF TABLES

LIST OF SYMBOLS

c	Cohesion
d	Distance between the two coils
$FS_{sliding}$	Factor of safety against sliding
$FS_{overturning}$	Factor of safety against overturning
$FS_{rupture}$	Rupture safety factor
$Fs_{pullout}$	Pullout safety factor
g	Gravity acceleration
h	Depth of overburden directly
H	Wall height
H_e	Effective wall height
H_f	Horizontal seismic force acting on the face
H_1	Horizontal seismic force acting on wedge 1
H_2	Horizontal seismic force acting on wedge 2
K	Earth pressure coefficient, Ratio of V_2 over V_1
K_1	Cohesion force acting on base of wedge 1
K_2	Cohesion force acting on base of wedge 2
K_{12}	Cohesion force acting on inter wedge boundary
K_a	Coefficient of active lateral earth pressure
K_p	Coefficient of passive lateral earth pressure
K_o	Coefficient of lateral earth pressure at rest
k_h	Horizontal ground acceleration coefficient
k_v	Vertical ground acceleration coefficient
L	Length of reinforcement
L_1	First coil
L_2	second coil
N_1	Normal force on base of wedge 1

N_2	Normal force on base of wedge 2
N_{12}	Normal force on inter wedge boundary
P	Thrust between the facing and the backfill
P_a	Active earth pressure force
q	Surcharge
Q_1	Surcharge load on wedge 1
Q_2	Surcharge load on wedge 2
R_1	Tangential force on base of wedge 1
R_2	Tangential force on base of wedge 2
R_{12}	Tangential force on inter wedge boundary
r_u	Pore pressure ratio
S_v	Vertical spacing
th	Thickness of the face
T_1	Sum of reinforcement forces acting on wedge 1
T_2	Sum of reinforcement forces acting on wedge 2
T_{12}	Inter wedge reinforcement force
T_{tot}	Total quantity of reinforcement
u	Pore water pressure
U_1	Pore water force acting on base of wedge 1
U_2	Pore water force acting on base of wedge 2
U_{12}	Pore water force acting on inter wedge boundary
V_f	Vertical seismic force acting on the face
V_1	Vertical seismic force acting on wedge 1, Voltage at the first coil
V_2	Vertical seismic force acting on wedge 2 Voltage at the second coil
W_1	Weight of wedge 1
W_2	Weight of wedge 2
X	x coordinate of two-wedge node
Y	y coordinate of two-wedge node
α	Percentage coefficient
δ	Inter wedge angle of friction

ϕ	Soil friction angle
ϕ_{12}	Inter wedge angle of friction
γ	Unit weight of the soil
γ_c	Unit weight of concrete = 24 kN/m^3
λ	Non dimensional base sliding factor
θ_1	Angle at the base of wedge 1
θ_2	Angle at the base of wedge 2
θ_{12}	Angle of inter wedge boundary
σ_h	Horizontal stress
σ_v	Vertical stress

1 INTRODUCTION

Soil is a natural construction material, which can be strong to a certain extent in compression and shear when at a suitable density and water content, but totally incapable of carrying any tension. With the inclusion of tensile reinforcing elements of some sort, a composite structure is produced to combine the best load carrying features of both reinforcement and soil. The resultant composite is called *Reinforced Soil.*

In order to understand the behavior of reinforced soil retaining structures, small laboratory and centrifugal models were studied throughout the literature. However they can not represent the actual stress and strain distribution of actual cases. Therefore, the requirement to study full scale reinforced soil walls is important. Unlike, reduced models, full scale construction of walls is not as simple and economical as reduced models. These walls mainly consist of: geosynthetic reinforcement elements; backfill soil; and some type of facing elements

Theoretical work based on Finite Element Analysis and Centrifuge model tests indicated that using on site soil that is stabilized with lime can be successfully used. So to be able to get a real experience with this technique, the aim of this research was chosen as to construct a full size geosynthetic reinforced soil retaining structure with lime stabilized clay backfill.

So the backfill used in this structure is a lime stabilized clay. Lime is known to be one of most common additives for improving the physical characteristics of in situ soils. When proper amount of lime is mixed with clayey soils, it improves not only their mechanical properties, but also their hydraulic properties. Namely it increase the permeability so the dissipation of the pore water pressure will occur faster and thus reduce the imposed hydraulic static loads. The reaction of lime with the soil is mainly a function of the water content and the temperature and most importantly, its quantity.

To understand the behavior of the wall better, it was equipped with instrumentation to measure stresses and deformations both in the soil and reinforcement and loaded with surcharge loads to overstress the structure.

The results obtained showed that the current design methods are too conservative. It neither considers a possible cohesion nor the effect of facing elements if present. To further improve the economy of geosynthetic reinforced soil walls, it was looked into an analytical way to incorporate the effect of facing elements into the design procedure.

Here in this research, the relationship between the function of the facing and stability is investigated analytically using the two wedge failure mechanism. Full height precast or cast in place concrete facings were considered. A new method is developed to account for the facing thickness and the reduction to reinforcement required.

In seismically active areas, earthquake forces may have severe damages to reinforced walls if these forces are not considered in the design. Therefore, static and dynamic conditions were considered for design. The results and comparisons are presented in chart form so as to be more easily used by engineers and will allow comparisons with other methods.

2 LITERATURE REVIEW

2.1 General

Geosynthetics have found some use in reinforced soil walls in the past 10 to 20 years and are becoming increasingly popular as their behavior becomes better understood. Reinforced walls are made of some type of reinforcement layers, embedded in a backfill soil to construct a free standing structure. These walls tend to be quite flexible when compared with conventional structural retaining walls.

The main types of reinforced soil structures are classified in two broad categories as earth structures and load supporting structures:

1. *Earth structures* include slopes, walls, embankments, low permeability soil layers used in dams and waste containment facilities, and some soil layers on non uniform foundations such as roads and embankments over karst topography. Earth structures do not normally support significant external loads, and primary design consideration is stability of the structure under its own weight.

2. *Load supporting* structures include flexible pavements, unpaved roads, railroad track structures, and load supporting pads such as drilling pads, fabrication yards and construction staging areas. These structures are usually stable under their own weight, and the primary consideration is the structure's ability to support the applied loads (usually traffic loads) with limited deformation.

Generally, some type of facing is usually required. The exposed face of the wall may consist of a variety of building materials, such as cast in place concrete, masonry, timber, precast concrete panels, or the reinforcement may be wrapped at the face and left exposed or provided with protection such as sprayed on asphalt or gunite.

Geosynthetic reinforced soil walls also frequently tend to be less costly than more conventional retaining structures. Reasons behind their economy are due to the fact that geosynthetics are relatively inexpensive reinforcing element; the use of on site available soil can save much compared to soil transported with the added benefit of preserving the aggregate resources; geosynthetic walls can usually be sited on or near the ground surface, which reduces costly sub excavation and reduces total wall height; and shorter fabric lengths can be used in some cases near the base of the wall.

2.2 History and Development of Reinforced Soil

Soil reinforcement is not a new concept. Early examples of soil reinforcement include the ancient ziggurats found in Iraq, which are more than 3000 years old, the tower of babel which was completed around 550 BC, and the great wall of china. The Romans have also used earth reinforcing techniques, and a first century Roman army project of a port which was discovered shows that past construction techniques are very similar to present day methods.

However, the first successful application of soil reinforcement concept is developed by the French Architect and Engineer Henry Vidal (1969) during the late 1950's. Metal strips were used to anchor facing panels at the wall's face and to reinforce the backfill soil mass. The design of these early soil reinforced walls was expressed very simply in terms of conventional soil mechanics. This same design procedure has proven to be both applicable to geosynthetically reinforced retaining walls. Then this art is developed continuously elsewhere in Europe and in USA.

2.3 Backfill Selection

Generally, the mechanism of soil to reinforcement stress transfer is mainly friction developed between the soil and the reinforcement surfaces which is a function of:

- The nature of the soil
- The effective overburden stress
- The rigidity of the reinforcements
- The location of ground water table

Task Force 27 specifications (1990), foresee that the backfill soil used for reinforced structures has to be a granular backfill. However, in many countries, granular frictional materials are rare and very expensive. Barrett (1992) showed that the greatest economy is obtained by using on site soils for backfill. Tall wall costs are so totally governed by the backfill cost that economy is principally a function of whether on site soils can be utilized as backfill or not. Therefore it might be a good idea to improve the strength properties of the available on site backfill, which is generally a low quality cohesive backfill. The limitations of such soils are:

a) low shear strength parameters;
b) low permeability.

The technique of improving poor soils by adding admixtures is very powerful tool in using available on site soil as back fills. Lime for example, if added to cohesive soils, it produces substantial improvement in soil strength. It has the further beneficial effect of reducing the deformation and of improving the workability as well.

As it is known, short-run reaction with lime include replacement of monovalent adsorbed cations by Ca^{++}, adsorption of $Ca(OH)_2$ by particles, cementation in a long term reaction at interparticle contacts, and establishment of a high pH (12.4) environment. In the long-run a high pH environment causes a breakdown of the crystal lattice of clay and formation of cementitious products (Mitchell, 1981). Brandl (1981) stated that the compressive strength first increases with growing dosage of lime but declines after reaching a maximum. Also, an increase in tensile strength is observed in lime stabilized clays. He also reported that the deformation resistance after adding lime is much significant than the increase in compressive strength, and that an increase of 20 to 40 times in the elastic modules is not seldom.

Bulut (1986) run different tests on determining the ultimate strength, mechanical properties of clay-lime treated and untreated with lime mixtures. He verified that with the addition of lime in the clay up to certain extend resulted in a significant increase in the ultimate strength at failure for clay lime treated specimens than untreated samples. In parallel to the increase in strength, modules of elasticity for lime-treated soil samples increase as well. He showed also that for a clay sample, lime-untreated, would have no shear strength if the confined pressure is zero. However, this is not the case for lime-treated samples. For them, even with zero confining pressure, they would possess a shear strength due to the fact that there have been cementation bonds between clay particles which arises from the pozzolanic chemical reaction of clay and lime. The cemention bond between clay particles generated by lime need to be distracted before the sample fails, and therefore a significant strength increase is required to shear the clay to failure.

Iyidil (1988) investigated the hydraulic properties of the clay mixed with 2 to 6 % lime by running permeability tests. He concluded that lime stabilization causes an increase in the permeability of the untreated clay. So this is an additional benefit of lime stabilization.

Burwash and Frost (1991) discussed that the clay used as a backfill for reinforced walls would behave satisfactory as long as it did not reach saturation. The saturation of the clay which may occur by the pounding of surface runoff of water, may result in significant loss in strength and let the clay behave like a cohesionless backfill. Thus the wall behaviour would be fine as long as drainage is provided so as saturation is not developed.

Najefzadeh (1981) argued that lime stabilized clay could be used as a backfill material instead of granular material for reinforced retaining walls. Mitchell and Villet (1987) reported that clays were used as backfills materials for many low height retaining walls. Güler (1990) verified by means of Finite Element Analysis, that lime stabilized cohesive soil could be used successfully as a backfill material for geotextile reinforced retaining structures. He also showed that horizontal deformation of the wall could be reduced as well.

At the University of Maryland, a two-year experimental research was carried out about the possibility of using lime stabilized cohesive soils as a backfill material in reinforced soil retaining structures. Centrifuge models by Güler and Goodings (1992) confirmed that further improvement in wall stability could be achieved by using lime in the cohesive soil backfill.

In addition, the centrifuge modeling research, carried out by Porbaha (1994) confirmed and gave depth to earlier similar research that cohesive soil retaining structures can be constructed economically and with a satisfactory performance. Porbaha investigated the stability of geotextile reinforced cohesive soil retaining systems. He conducted 60 reduced centrifuge tests models. He stated that failure of the geotextiles in the all models was always by breakage of the reinforcements and pullout failure was never observed. The lime treated backfill models collapsed suddenly in a brittle type of failure, when compared to untreated clay backfill models which collapsed gradually and endured large deformations prior to failure.

Field instrumentation (Floss and Thamm 1979), full scale experiments (Wu 1992a), centrifugal model tests (Bolton et al. 1978), and reduced scale laboratory model test results (Lee et al. 1973; Boden et al. 1977; Juran and Schlosser 1978) have provided insight in understanding of the behavior of reinforced earth systems.

Billiard and Wu (1992) loaded a large scale geotextile reinforced wall till failure. They verified that that the Forest Service method yields a very conservative design where a classic failure condition was not developed at surcharge load three times that of the calculated load.

2.4 Facing Rigidity

The stability of a geosynthetic wall is highly dependent on the type of facing system used and the care with which it is designed and constructed, as well as its ability of transforming the stresses from the soil to the facing system.

New variety of facing systems have been used for geosynthetic walls. Typical examples are: segmental and full height precast concrete panels, interlocking precast concrete blocks, welded wire panels, gabion baskets and treated timber facing. Aesthetic often determine the type of facing systems. Anticipated deflection of the wall face, both laterally and downward, may place further limitations on the type of facing system selected. (Allen and Holtz, 1991).

The effects of facing rigidity are not taken into account explicitly in most of the current stability analysis methods used for reinforced structures, probably based on the assumption that the facing of a reinforced structure does not play a major role in overall structure stability justified from its relatively short history of actual performance.

Wu (1992b), Claybourn and Wu (1992) and Wu et al. (1992) compared wrapped facing predictions with the results of the loading tests on two 3 m high plane strain geosynthetic reinforced retaining wall models with a sand or clay backfill, (Denver Walls). Wooden block facings were used and the length of reinforcement was relatively short (L/H=55 per cent). All of the six limit equilibrium methods Steward (1977), Broms (1978), Collin (1986), Bonapart et al. (1987), Leshchinsky and Perry (1987) and Schmertman et al. (1987), currently used in the United States underpredicted the actual failure load by 4 - 40 times. This disagreement was largely because the effects of facing rigidity was not taken into account in these design methods.

In many methods, it is always assumed that the whole horizontal outward thrust by earth pressure activated at the failure plane is resisted by the tensile resistance of reinforcement. However, for full height precast facings which are connected to reinforcement at the back face having both local rigidity, and overall axial, shear and bending rigidities can effectively carry partially a percentage of that active earth pressure thrust, thus reducing the amount of reinforcements in terms of quantity and length. Field tests results show that as a facing becomes more rigid, the earth pressure acting on the back face of facing increases. It has also observed that this large earth pressure confines the soil immediately behind the facing, which decreases the deformation and increases the ultimate stability of the wall (Tatsuoka 1993).

In Japan, geosynthetic reinforced retaining walls having a cast in place concrete facing were constructed as important permanent railway structures. This type of facing was adopted not only for better durability and aesthetics of the wall face and easier construction, but also by expecting contributions of local and overall rigidities of facing to the stability of the wall. (Tatsuoka et al. 1992, Murata et al. 1993).

Tateyama et al. (1994) showed that the use of rigid facing application for geosynthetic reinforced retaining walls has performed satisfactory as bridge abutment for rail ways. Measurement and observations of geosynthetic reinforced walls was very stable without showing great noticeable deformation with both clay and sand both used as backfill materials. This led to adopt this system in Japan.

Tatsuoka (1992) studied the effect of facing systems to the stability of reinforced walls. He concluded that full height rigid facing is better than a facing of discrete panels in reducing face deformations as well reducing the length of the reinforcement required. He also showed that local and overall facing rigidity can help in increasing the stability of the structure. Tatsuoka stated that the structure of facing and its related design issues become more important:

a) as the slope becomes steeper;
b) as the soil becomes weaker;
c) as the load on the crest of slope or wall becomes larger;
d) as the vertical spacing becomes larger;
e) as the density and length of reinforcement becomes shorter;
f) as the allowable deformation of wall becomes smaller;
g) as the structure becomes more important;
h) as the designed life time of structure becomes longer.

2.5 Failure Type

Generally speaking, the failure of a soil structure as shown in Figure 2.1 is always more or less progressive starting from a local failure. Therefore, as stress concentration and the resulting initiation of premature local failure can be restrained effectively by using a rigid facing resulting in larger failure load and large stability of the structure.

Tatsuoka (1993) reported that the failure of a warped face 4 m high test reinforced retaining wall backfilled with clay as due to the lack of confinement to the soil near the face. The failure started from a local compression failure in zone immediately behind the wall face in lowest soil layer which progressed toward the deeper zone and in turn triggered every where. Similar type of failures in centrifuge tests of 152 mm high geosynthetic reinforced clay models were reported by Goodings (1989).

2.6 Summary

With the help of the above results, it was possible to consider the use of the developed method in real structures. Since the method was developed by using theoretical models and centrifuge tests it was necessary to check the design method on a real structure.

So the aim of this research work was to show that the proposed method can be successfully used in real applications. It was important to know the stress distribution and the deformations in the structure at specific locations. Consequently the structure was instrumented and real stress and deformations were recorded.

Also the a new proposed design method to take the effects of the facing rigidity to the overall stability of geosynthetic reinforced walls, and thus make an attempt to reduce the conservative current design methods, which do not at all account for the effect of facing rigidity.

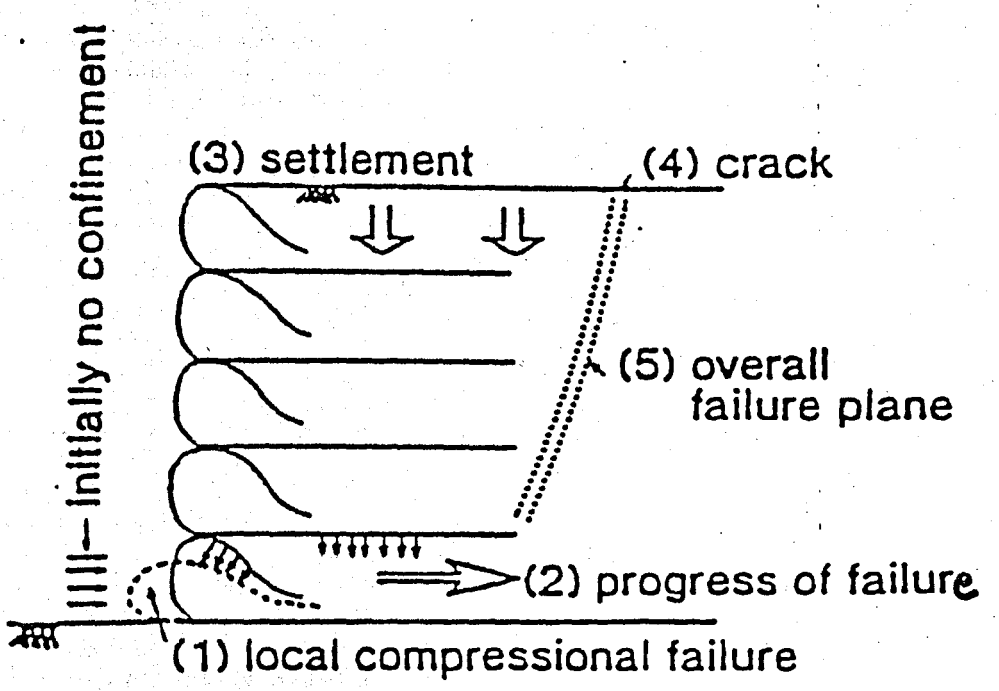

FIGURE 2.1 Progressive failure starting from a local compression failure of soil immediately behind the wall face (Tatsuoka, 1993)

3 METHODOLOGY OF KILYOS WALL CONSTRUCTION

3.1 Introduction

In 1991 a geosynthetic reinforced soil retaining wall with cohesive backfill was constructed in Istanbul, to support the research work of centrifuge tests results conducted on model walls.

The six-layer wall was constructed at the university campus at Kilyos. The wall reinforcement consisted of a low strength geotextile, Polyfelt TS 21 spaced roughly at 1 m intervals.

Naturally available clay mixed with 4 per cent lime was used as a backfill. Foundation soil consisted of stable sand with the ground water table well below the ground surface.

Deformations were measured using special type of electrical coils developed for this purpose. Pressures through the profile of the wall were measured with the help of Glötzl pressure cells.

The design, construction, and the placement of the surcharge load performed on a 6 m high geotextiles reinforced retaining wall are presented here as well in Appendix 1. The Forest Service design method was followed.

3.2 Material Properties

3.2.1 Soil Properties

a) Measured before the Construction

In November 1993, just before the start of the project, preliminary design and some determination of the specific properties of the soil that will be used were investigated. So samples of the soil were taken and tested in the laboratory. A standard unconfined compression test of the clay with and without lime treatment was carried out with 0,4, 5, 6, 7 lime percentage. The results are shown in Table 3.1.

TABLE 3.1 Results of the unconfined compression test

Lime Percent (%)	Ultimate Strength (kPa)
0	147.70
4	385.23
5	415.33
6	252.53
7	342.65

As it is seen the strength is substantially increased by the addition of lime. However, this is true up to a certain limit. The selection of 4 per cent lime mixed with the clay was chosen as an optimum and economical lime mixture. After selecting this as a base, for that mixture the optimum water content of the untreated soil and treated soil were determined. Also, the liquid and plastic limits were determined. The results are shown in Table 3.2. Shear strength parameters of the treated soil are determined and shown in Table 3.3.

TABLE 3.2 Soil properties of the treated and untreated clay

	Clay with 0 % lime	Clay with 4 % lime
Plastic Limit (PL)	18 %	21 %
Liquid Limit (LL)	41 %	47 %
Plasticity Index	23 %	26 %
Optimum Water Content	17 %	18 %

TABLE 3.3 Soil strength parameters determined before construction

Strength Parameter	Value
φ	26°
c	55 kPa
ω_{opt}	18 %

b) Measured during the Construction

A series of laboratory tests were conducted on samples of the lime stabilized clay backfill recovered during the construction time in December 1993. Unconsolidated Undrained triaxial tests were conducted on these samples. The test results are given in Table 3.4 and the shear strength properties are given in Table 3.5. The water contents of the samples were measured as 20 per cent. It is believed that the tested samples were not really homogenous, and may not represent exactly 4 per cent lime mixture. This was due to random way of mixing the lime with clay at site.

TABLE 3.4 Results of the triaxial tests conducted on samples taken from site

σ_3(kN/m^2)	σ_1(kN/m^2)	p (kN/m^2)	q (kN/m^2)
149.15	738	443.575	294.425
49.05	473	261.025	211.975
89.1	568.1	333.1	235
147.15	706	426.575	279.425

TABLE 3.5 Soil strength parameters determined while construction

Strength Parameter	Value
φ	20 °
c	103 kPa
ω	20 %

c) Measured after the Construction

In July 1994 before the overloading stage, two boreholes, spaced 3m from each other, were opened behind the face of the wall at different locations. The aim of conducting these bore holes was to investigate the long term shear strength parameters. Samples were taken out from different depths from the wall and Unconsolidated Undrained triaxial test, were conducted and their water contents were determined.

Construction records showed that the average moisture content of the soil right after construction, was 20 per cent which was 2 per cent wet of the optimum value of 18 per cent. In comparison, the moisture content determined on samples taken from the boreholes 7 months after completion of construction showed a water content of 24 per cent

which was 6 per cent wet of optimum. This result was possible due to the heavy rains which took place during the previous winter season.

The results of the triaxial test conducted on samples taken from boreholes are presented in Table 3.6 while shear strength parameters are given in Table 3.7. Unit weights of the lime stabilized soil were determined by the Cone Sand Test and shown in Table 3.8.

TABLE 3.6 Results of the triaxial tests conducted on samples taken from the bore holes

σ_3(kN/m^2)	σ_1(kN/m^2)	p (kN/m^2)	q (kN/m^2)
98	336	217	119
98	384	241	143
196	552	374	178
196	626	411	215

TABLE 3.7 Soil strength parameters determined from bore holes

Strength Parameter	Value
φ	24°
c	44 kPa
ω	24 %

TABLE 3.8 Unit weights of the lime stabilized soil

Property	Value
γ	15 kN/m^3
γ_s	26 kN/m^3
γ_{dry}	12.4 kN/m^3

d) Summary of the Soil Properties

A summary of all shear strength properties obtained at different stages is presented in Table 3.9.

TABLE 3.9 Summary of the results

	Measured Before the Construction November 1993	Measured During the Construction December 1993	Measured After the Construction July 1994
φ°	26	19	23
c (kPa)	55	95	43
ω (%)	18	20	24

3.2.2 Geosynthetic Reinforcement

The geotextile used in this project as reinforcement was a non woven needle punched Polyfelt TS 21. The geotextile was chosen to be a weak one and has strip tensile strength of 5.9 kN/m. This gives an equivalent force per unit width of approximately 35.4 kN/m for the 6 layers wall. No safety factor is applied to this strength, just directly used in the design. Technical data of the geotextile used is shown in Table 3.10 as obtained from the manufacture. No specific tests were conducted on the geotextile. No special site equipment or expertise was required for the installation of the geotextiles.

TABLE 3.10 Technical data of Polyfelt TS 21 geotextile

TEST	MAGNITUDE
Weight	95 g/m^2
Thickness under pressure	
2 kN/m^2	1.0 mm
20 kN/m^2	0.6 mm
200 kN/m^2	0.4 mm
CBR-puncture resistance	980 N
Strip tensile strength	5.9 kN/m
Elongation at break	70/40 %
Grab-tensile strength	340 N
Cone drop test	25 mm
E.O.S.	0.13 mm
Vertical permeability under pressure (10 cm water head)	
2 kN/m^2	450 l/m^2 s
200 kN/m^2	150 l/m^2 s
Horizontal permeability under pressure (hydr. gradient 1)	
2 kN/m^2	40 l/m h
20 kN/m^2	9 l/m h
200 kN/m^2	1.4 l/m h

3.3 Construction Phase

3.3.1 Selection of the Site

Preliminary investigations have shown that the most suitable place of such a retaining wall was the University Campus at Kilyos. Reasons behind this selection were the availability of the required clay, equipments and space.

3.3.2 Dimensions of the Wall

Figures 3.1 and 3.2 illustrate a view of the wall geometry after construction. The face of the wall has a trapezoidal section with upper and lower bases of 8.8 m and 18.2 m, respectively. The wall height is 5.25 m. The inclinations of the right and left sides from the horizontal are 46° and 50° respectively. Total quantities for the wall are as follows: 74 m^2 face.

3.3.3 Wall Construction

In the construction phase of the wall naturally available clay was mixed with 4 per cent lime at the site. It was not possible to determine the exact weight of soil precisely which was going to be used as a backfill, however its volume was determined. So indirectly, the weight is determined and accordingly lime was added. After mixing it by a bulldozer, the treated soil was then laid down in layers of roughly 100 cm thickness. The intention was to build a wall 6 m high. Due to some variation of layer thickness it ended up to be 5.25 m. Layers were compacted using a smooth-wheeled roller in the first two meters height. Despite the winter season, the natural moisture content of compacted clay was suitable to allow fair good compaction. The smooth-wheeled roller had two disadvantages: the compaction energy was quite low and secondly since there was no barrier at the edge of the wall, it was getting more and more risky as the wall height was increasing. So for the remaining part of the wall a Wacker Vibro Rammer type compactor was used instead. The rammer type compactor proved to be very efficient in terms of operation and as well as in terms of the compaction degree achieved.

The six layer reinforced soil mass construction was completed in one month using a seven-man labour crew, a supervisor, a rubber tired front - end loader, a vibratory compactor and following the typical sequential construction practice suggested by US Forest method of construction illustrated in Figure 3.3.

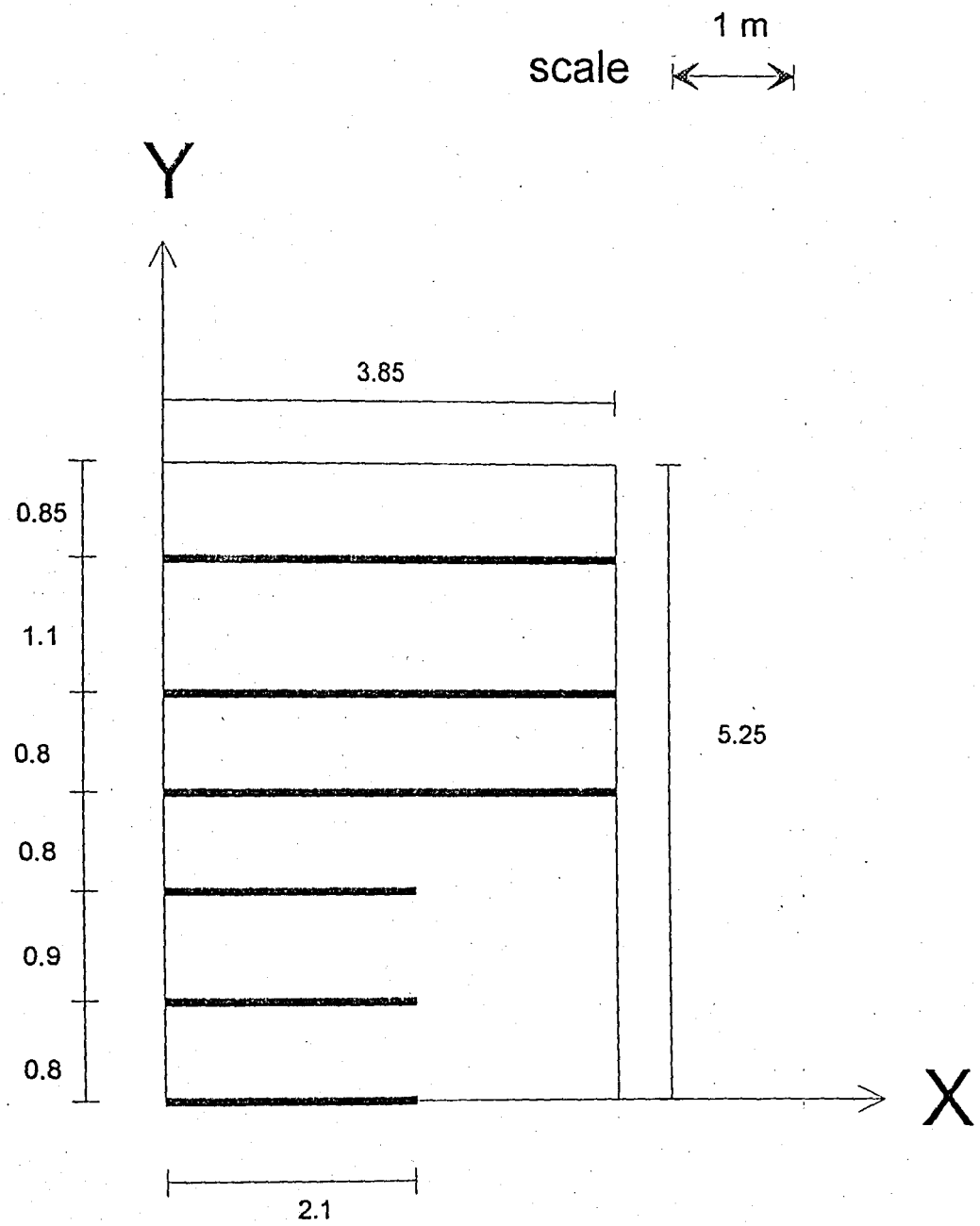

FIGURE 3.1 Dimensions of the wall (side view)

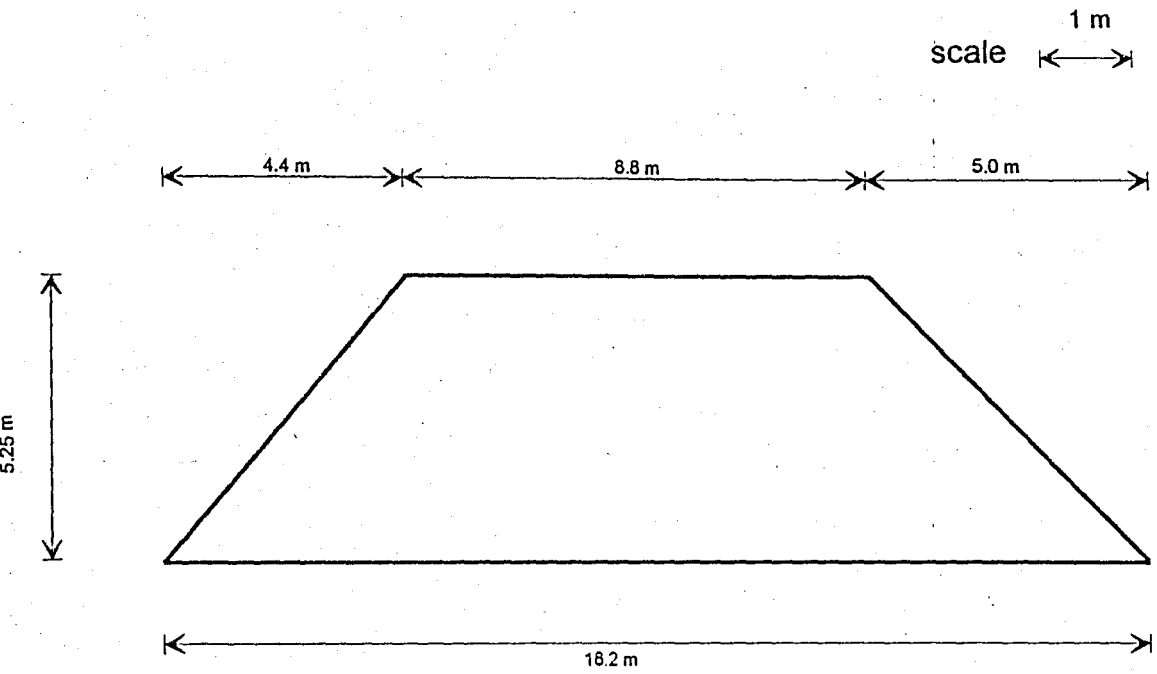

FIGURE 3.2 Dimensions of the wall (front view)

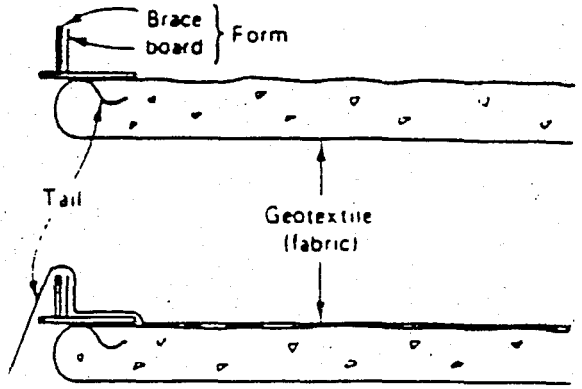

1. Set form completed lift.

2. Unroll fabric and position so that a 3 ft wide tail drapes over the form.

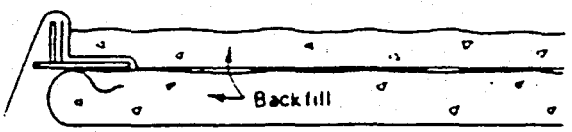

3. Place backfill to about half of the total lift height.

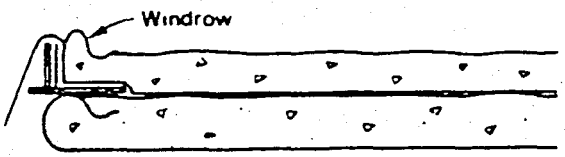

4. Make a window to slightly greater than full lift height against the form.

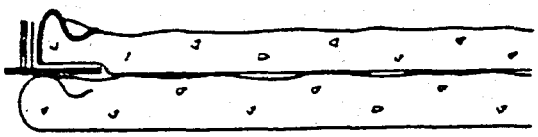

5. Place the fabric tail over the window and lock into place with backfill.

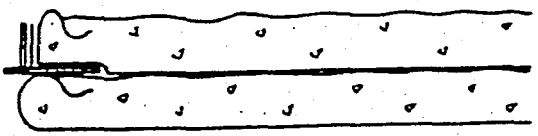

6. Complete back firing for planned lift thickness.

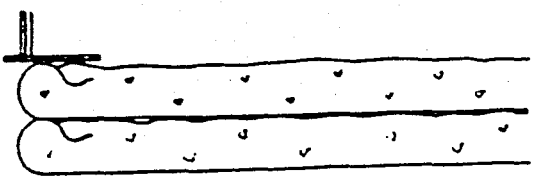

7. Reset the form and repeat the sequence.

FIGURE 3.3 Construction sequence for geotextile wall followed by US Forest Service (Koerner 1994)

3.4 Instrumentation

3.4.1 Glötzl Pressure Cells

Glötzl pressure cells are special type of hydraulic measuring system, which are based upon the compensation method. They work by pressurizing oil through pipes and measure the required pressure through the system. The oil is pumped by the means of a hydraulic pump, and a gage reads the contact pressure where a Glötzl pressure cell is placed. The pressure cell could be placed anywhere in the soil and is capable of reading either the overburden vertical or horizontal stress.

Vertical and horizontal Glötzl pressure cells were used to determine the pressure distribution within the wall. Six of the used to measure the vertical pressure illustrated in Figure 3.4 while the other five are used to measure the horizontal pressure illustrated in Figure 3.5. The exact locations, x and y coordinates of these Glötzl cells are given in Table 3.11. These pressure cells can not feel small pressures, therefore had to be placed at the lower layers of the wall, since placing them at the upper layers would not allow to make readings. Measurements of the pressure values read from the Glötzl cells started to be taken after the construction of the wall until the termination of the project.

Each gauge would not function or feel the pressure below a minimum pressure value of 14 kPa. This means that lower pressure would not be measured had the gauges been placed at the upper layers of the reinforced wall, therefore, all of them have been placed deeply at the lower layers.

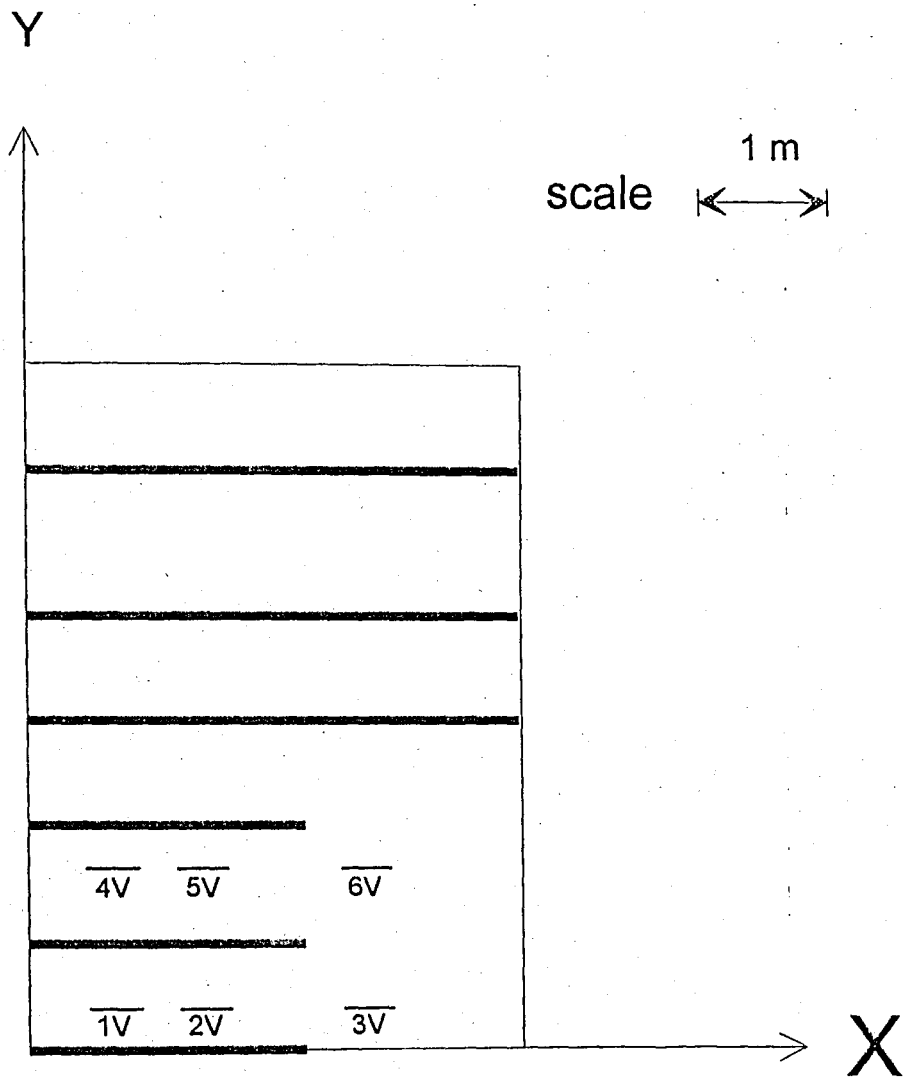

FIGURE 3.4 Locations of the vertical pressure cells

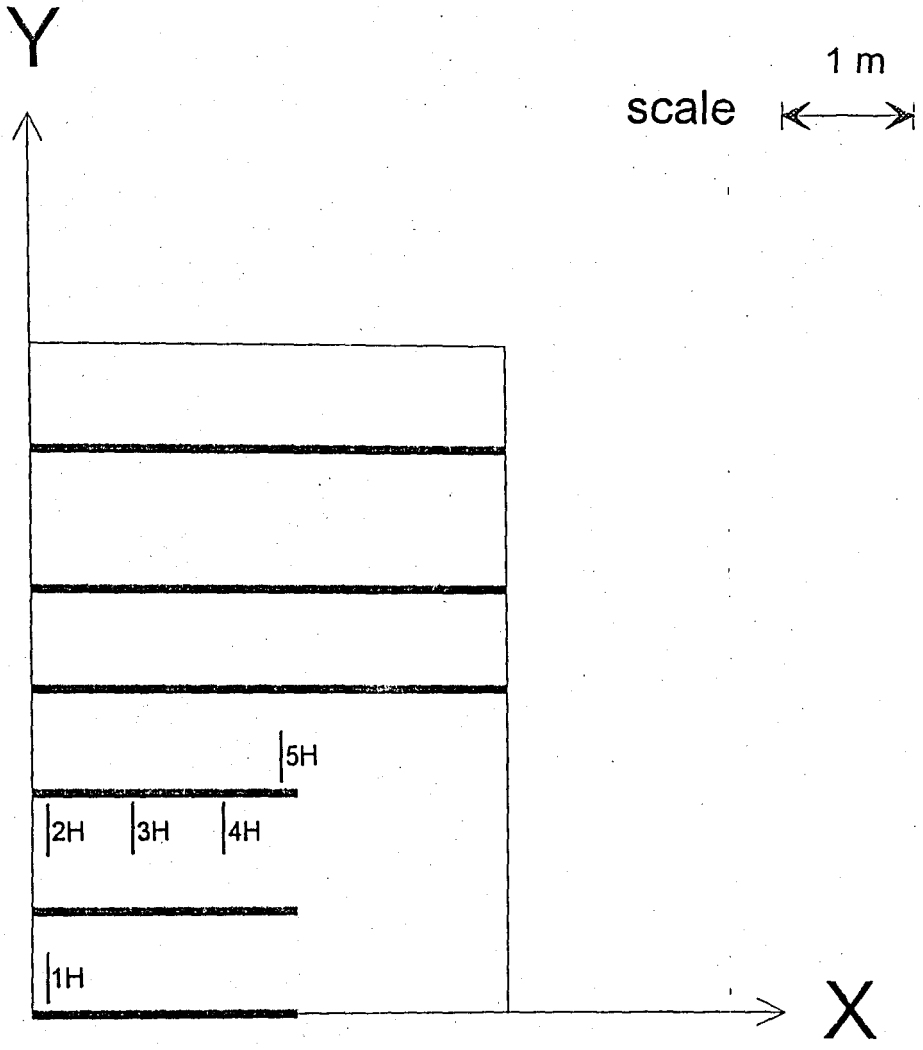

FIGURE 3.5 Locations of the horizontal pressure cells

TABLE 3.11 Locations of Glötzl pressure cells

	X	Y
1 Vertical	0.66	0.3
2 Vertical	1.33	0.3
3 Vertical	2.66	0.3
4 Vertical	0.66	1.4
5 Vertical	1.33	1.4
6 Vertical	2.66	1.4
1 Horizontal	0.16	0.3
2 Horizontal	0.16	1.4
3 Horizontal	0.8	1.4
4 Horizontal	1.5	1.4
5 Horizontal	2.0	1.9

3.4.2 Deformation Measurements by Inductance Displacement Transducer Method

The basic idea of the transducer is that the mutual inductance of two mutually coupled inductors change as a function of their separation (distance) as well as their mutual when they are concentrically aliened. If a voltage is supplied to L1, as shown in Figure 3.6, an induced voltage will be produced across the terminals of L2. This voltage will be a function of the current passing through L1, the permeability at the medium, the alignment of the two coils, (Chua 1987, Tompkins 1988).

Taking the separation as the independent variable and fixing all other parameters in the experiment, a ratio factor K defined as the applied voltage V2 over the induced voltage V1 in L2 is obtained as a function of the coil's separation. So a calibration curve is plotted between the K variable, and the distance between the two coils, d.

Once this relationship is established, as presented in Figure 3.7, the deformation in the soil is obtained as a change in distance between the two coils, placed in the soil, could be measured by measuring the change of the K ratio, and then indirectly from the calibration curve, the distance change is calculated, (Boul 1993).

Applying this idea in measuring the horizontal and vertical deformations inside the retaining wall, the change of the distance between two coils results in a measurable change in the induced voltage. So twelve sets of coils were placed vertically and horizontally in the structure at specific places in order to determine the deformations. Each set is made of a main primary coil, and two secondary coils placed above and below the main one, or right and left in the case of horizontal deformation measurement. This means that each set is made of the three coils, and this will help to check displacement from both sides of the primary coil. The voltages of these coils were recorded frequently, by a data acquisition card connected to a computer, where all data are stored in the hard disk for processing. Now after developing the mentioned system, it would be possible to measure the vertical displacement or the horizontal displacement with the help of these coils. The exact configuration of the coil sets and the location of each set is shown in Table 3.12 and Figure 3.8.

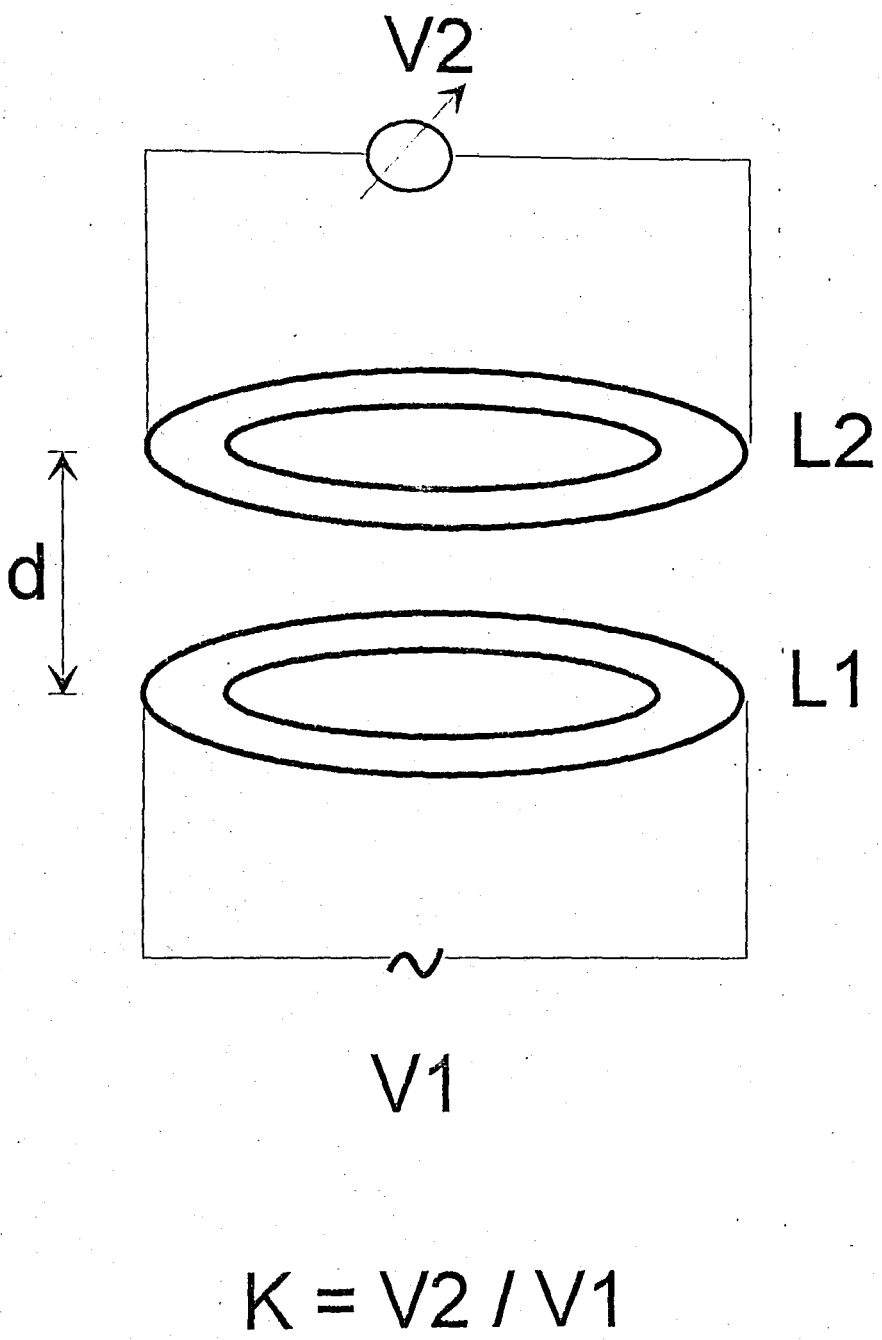

FIGURE 3.6 Typical configuration of the coils

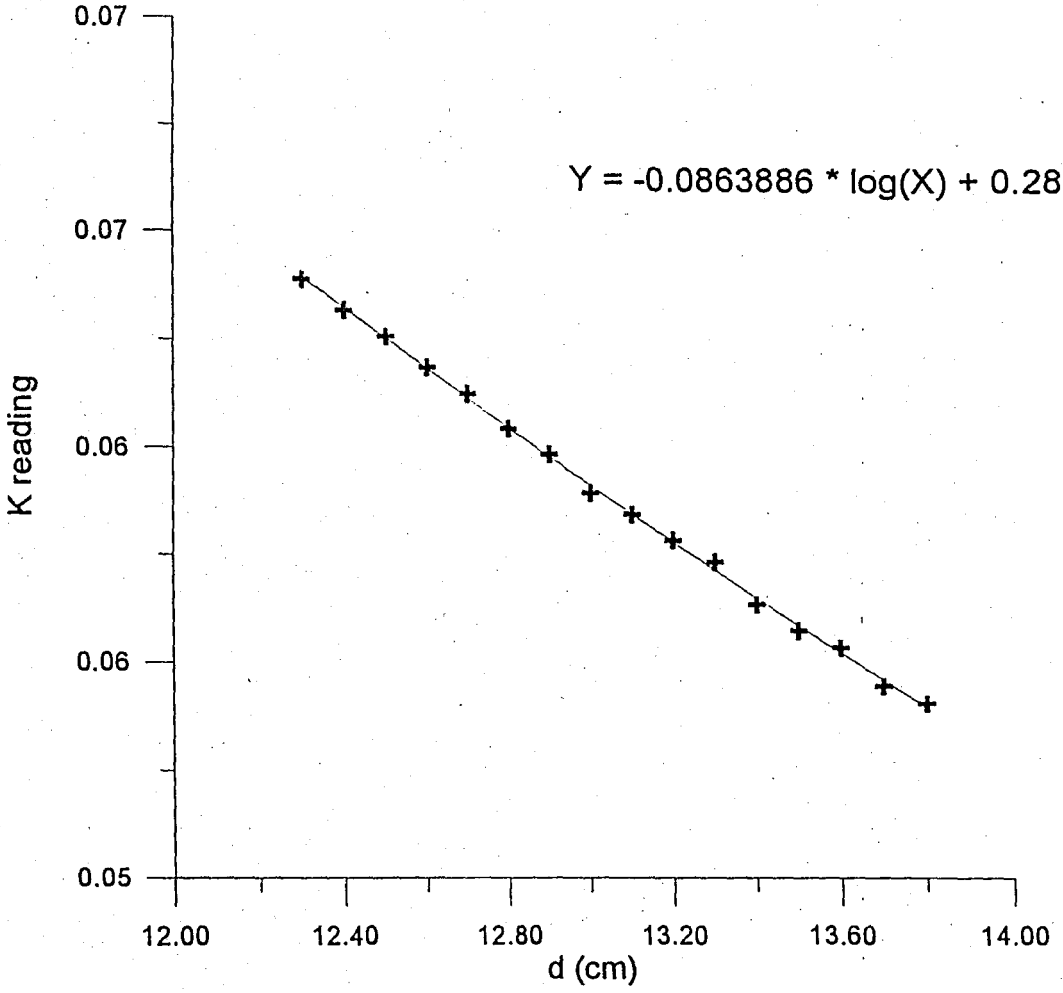

FIGURE 3.7 Typical calibration curve for the coils

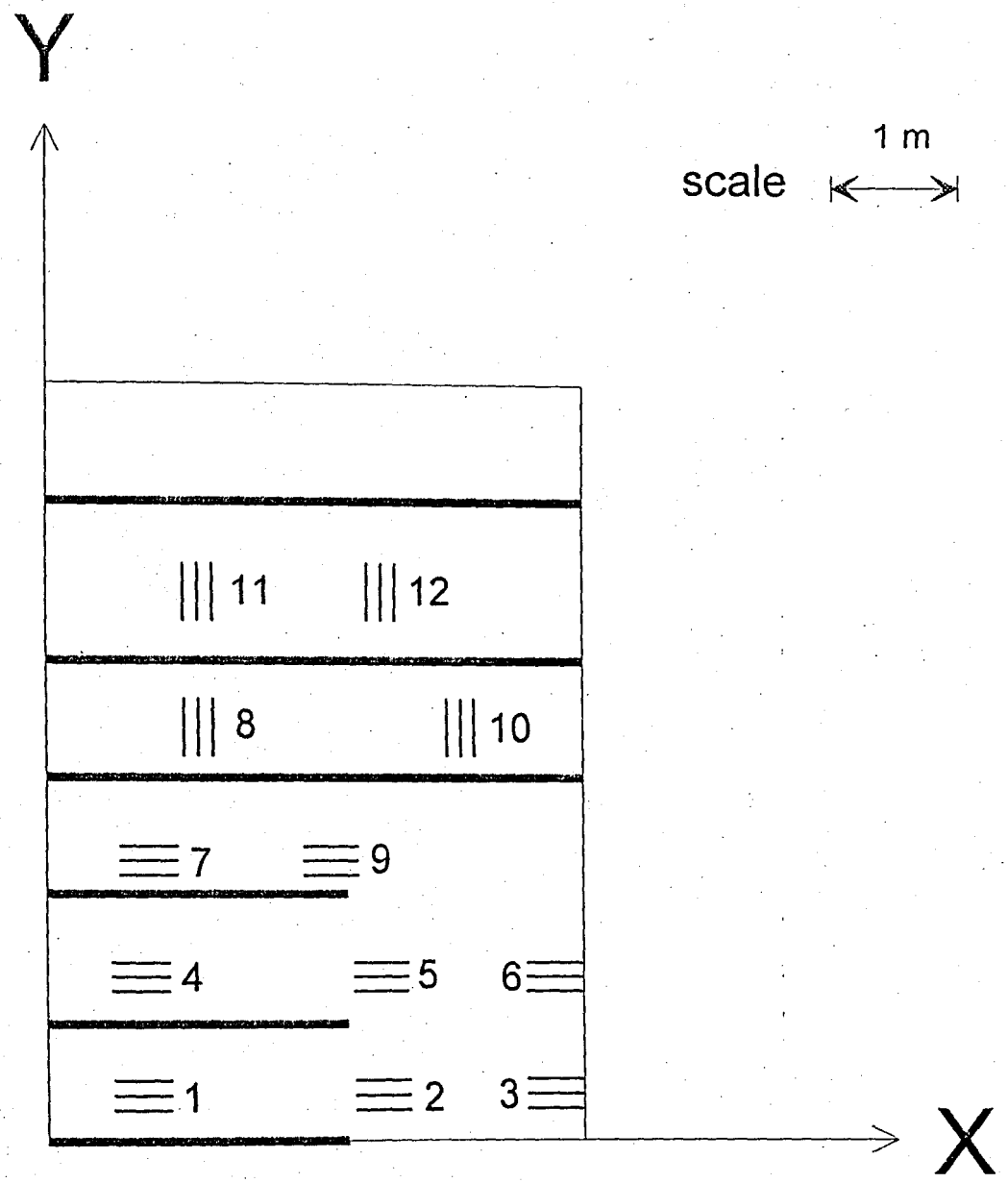

FIGURE 3.8 Locations of the coil sets

TABLE 3.12 Locations of coil sets

Coil Set Number	X (m)	Y (m)
1	0.66	0.30
2	2.33	0.30
3	3.66	0.30
4	0.66	1.10
5	2.33	1.10
6	3.66	1.10
7	0.70	1.90
8	1.00	2.90
9	2.00	1.90
10	3.00	2.90
11	1.00	3.85
12	2.30	3.85

3.4.3 Measurement of Reinforcement Strains

In an effort to measure the reinforcement strains for every geotextile layer, invar cables were attached to every geotextile reinforcement at 4 points. The locations of the attachment of the invar cable was chosen so that they are almost aligned in the direction perpendicular to the wall front but are at various distances from the front of the wall. These invar cables were put into a semi rigid plastic pipe so that the friction between the soil and the cable would not effect the deformation readings. The aim was to measure the deformation of the geotextile at 4 different locations, and consequently obtaining the strain at 3 different intervals of the geotextile. The invar cables were connected to a fixed reference with the dial gages before the over loading stage and the readings were taken daily in order to determine the strains of the geotextiles.

3.5 Overloading Phase

An incremental surcharge load was exerted over an effective area at the top surface. The way this was done was by the placement of concrete blocks next and above each other until the required area is covered. Then increasing the height subsequently layer after layer of concrete. This led to a gradual increase of the load while readings were being taken at each step as the load was increased.

The aim of overloading was to bring the structure to failure condition or at least to strain the wall somehow. For this purpose, the wall was overloaded twice. The first time was in August 1994 with the maximum load of 315 kN which was applied to an effective area of 2.25 m * 3.42 m = 7.69 m^2 . This produced a uniform surcharge pressure of 41 kPa as illustrated in Figure 3.9. The second time was in June 1995 after the removal of the upper two layers with a load of 223 kN applied to an effective area of 2.25 m * 3.00 m = 6.75 m^2 . This resulted a surcharge pressure load of 33 kPa as illustrated in Figure 3.10. The incremental load increase for each case is shown in Table 3.13 and Table 3.14 respectively.

The above mentioned surcharged loads were the maximum ones that could be obtained. The limiting factor was the risk of the instability of the blocks above each other and the difficulty of increasing the height by the labor.

TABLE 3.13 The incremental load increase for the first overloading stage

Layer No	Incremental Load (kN)	Total Load (kN)	Surcharge Load (kPa)
1	86	86	11.0
2	36	122	15.8
3	27	149	19.3
4	26	175	22.7
5	92	267	34.7
6	48	315	41.0

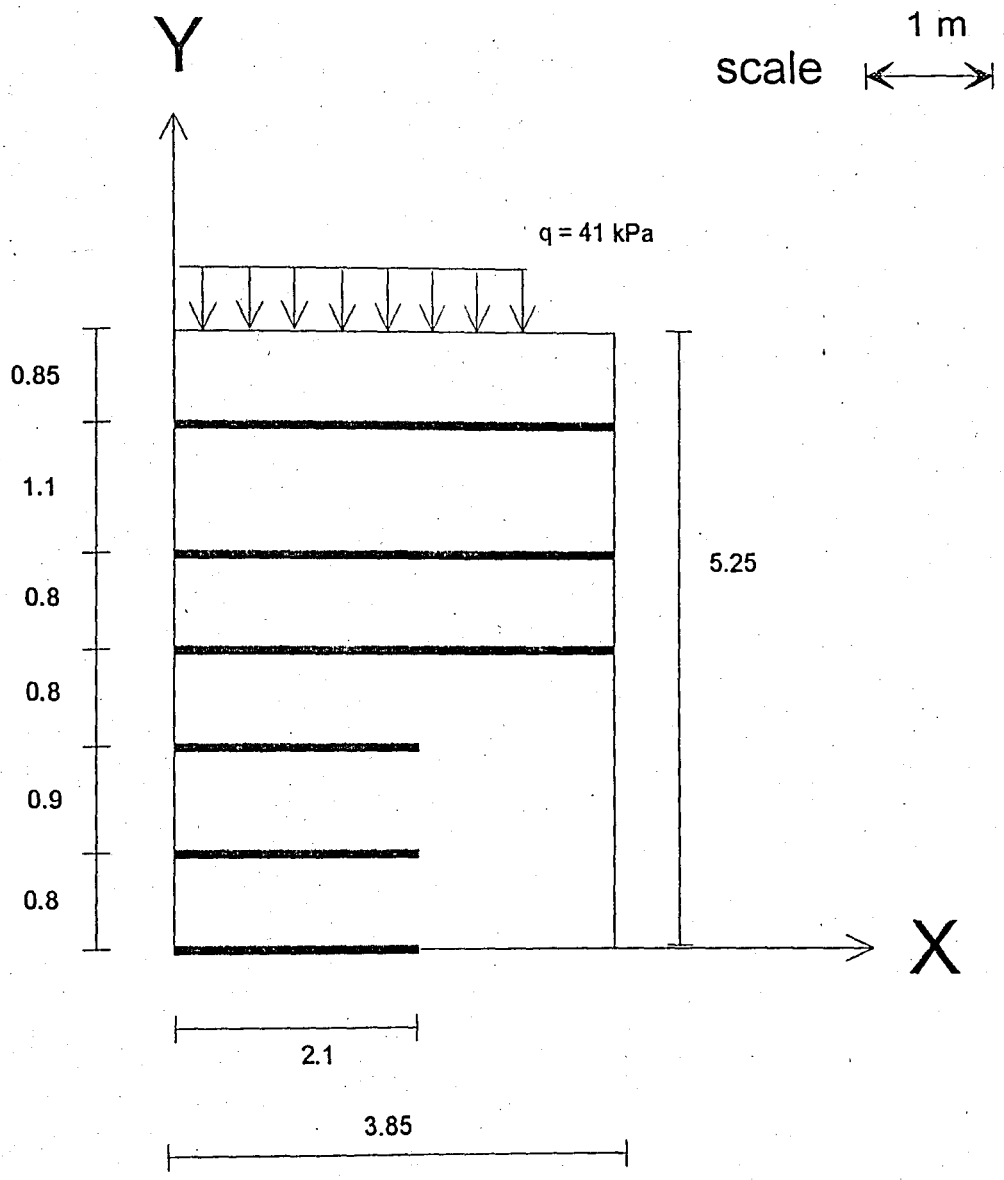

FIGURE 3.9 The first overloading stage

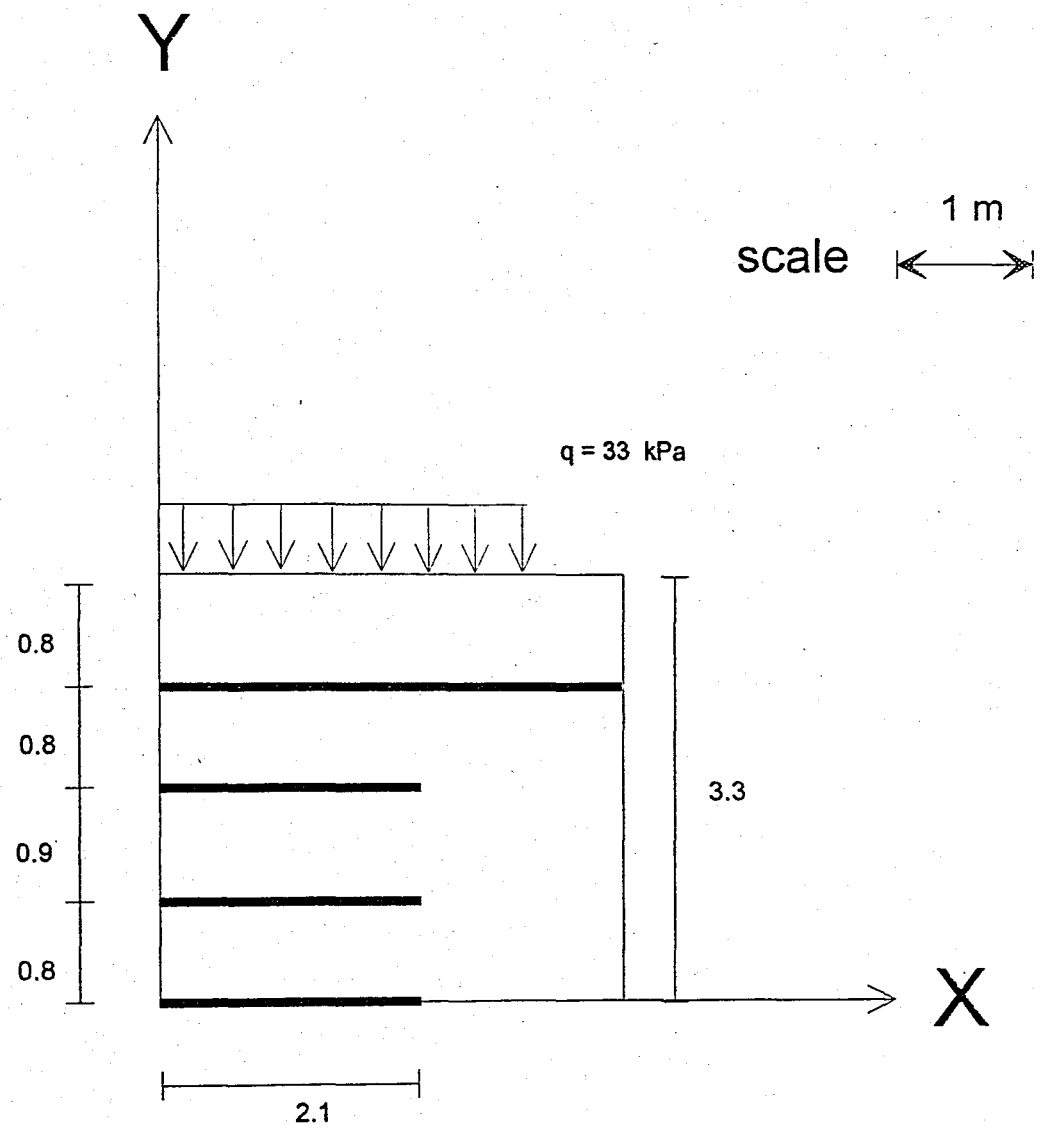

FIGURE 3.10 The second overloading stage

TABLE 3.14 The incremental load increase for the second overloading stage

Layer No:	Incremental Load (kN)	Total Load (kN)	Surcharge Load (kPa)
1	13	13	1.9
2	13	26	3.85
3	13	39	5.7
4	22	61	9.0
5	20	81	12.0
6	12	93	13.7
7	14	107	15.8
8	11	118	17.4
9	11	129	19.1
10	17	146	21.6
11	14	160	23.7
12	13	173	25.6
13	15	188	27.8
14	12	200	29.6
15	23	223	33.0

3.6 Termination of the Project

It was impossible to load the wall till failure. Many methods were tried in order to achieve this purpose. For instance, the surcharge load could not be increased more than the mentioned values. The stability of the blocks above each other became a critical problem after a certain height.

Burwash and Frost (1991) verified that the saturation of the clay used as backfill for reinforced walls may result in significant loss in strength and caused a significant reduction in cohesion value.

Following this idea, two big holes were excavated at the surface of the wall and filled continuously with water. The goal was to increase the pore water pressure and wet the soil. It was thought that this way the wall could be brought to failure easier.

However, this did not happen. The water immediately escaped through the first layer of geotextile and drained in the horizontal direction. Thus, no pore water pressure is developed and reduction in the shear strength was not achieved since no saturation occurred

Therefore, the project was terminated at this stage leaving the wall unfailed.

3.7 Summary of All Events

A summary of all events from completion of the wall until the end is discussed below and is given in abbreviated form in Table 3.15.

TABLE 3.15 Summary of events

Date	Time from Initial Start of Construction	Event
November 1993	0	Beginning of Construction
December 1993	1 month	End of Construction
July 1994	7 months	Bore Hole Sampling
August 1994	8 months	First Overloading Stage
February 1995	14 months	Removal of the Upper Two Layers
June 1995	18 months	Second Overloading Stage
August 1995	20 months	Termination of the Project

The construction of the wall started in November 1993 and was completed in December 1993. Then the wall was left for natural atmospheric conditions like snow, heavy rain, strong wind and strong sunshine and high temperature conditions till July 1994, when

samples were taken away from the boring holes and tested in the laboratory. The placement of the first surcharge load of 41 kPa was in August 1994 in order to determine long term shear strength parameters. The surcharge was left for 6 months and was removed with the upper two layers of soil in February 1995. Again the wall was left unloaded till June 1995 where another surcharge load of 33 kPa was placed. Finally in August 1995 the surcharge is removed and all the electrical and mechanical equipment were taken away, thus the project was terminated.

4 ANALYSIS OF THE KILYOS WALL

4.1 Introduction

The design philosophy and methodology developed for reinforced earth retaining structures derives primarily from research related to strip reinforced retaining structures. Methods of evaluating the internal and external stability of reinforced earth walls have been developed in various stages. They evolved from applying basic earth pressure theories, through altering and complementing results obtained from information on the distribution of tensile forces in reinforcing strips at working stress levels obtained from field and laboratory studies. Different numerous methods were proposed for designing reinforced walls structures. Among many, Christopher and Holtz (1985), Mitchell and Villet (1987) and Christopher, et al. (1990). For the design of the experimental wall, the FHWA method was adopted.

4.2 Brief Description of FHWA Method

The Federal Highway Administration design method (Christopher, et al. 1990), was incorporated for this study of a geotextile reinforced earth retaining structures. The design method is chosen for its popularity in practice.

In this method, the design permits only close to vertical retaining walls, granular backfill, and no hydrostatic water pressure with either segmented of flexible facing systems. The extensibility of the reinforcement controls the state of the assumed failure plan.

In this method only the frictional resistance of the soil is taken into consideration. The cohesion is ignored in both short and long term considerations. Therefore the cohesion value is assumed always to be zero as a conservative approach.

The stability of such structures are classified into internal and external ones.

4.3 Internal Stability

The internal stability analysis ensures that the reinforced soil mass is self supporting under the action of its own weight and any external applied forces. This self support is accomplished through stress transfer from the soil to the reinforcements only. It addresses the structural integrity of the reinforced zone of the wall and deals with the resistance to pullout failure within the reinforced soil zone resulting from interaction between soil and reinforcement, and the capability of a reinforcement layer to rupture against the breakage forces resulting from the horizontal stresses, as depicted in Figure 4.1. Therefore, two independent safety factors are determined for each layer of reinforcement.

Limit equilibrium analysis is used to equate the horizontal forces due to lateral earth pressures tending to cause instability to the stabilizing tensile forces in the horizontal reinforcement. The only stresses considered are vertical and lateral earth pressures, the horizontal tensile stresses in the reinforcement, and the horizontal resistance to pullout of the geotextiles from behind a Rankine failure plane which is defined as a straight line with an inclination of $(45 + \phi/2)$ as shown in Figure 4.2.

The reinforcement could be selected and spaced to preclude tension rupture and to prevent pullout from the soil mass beyond the assumed failure surface. The method provides the layer thickness, given a factor of safety in rupture, or conversely, provides a factor of safety against rupture, given a layer thickness.

(a) Rupture Failure

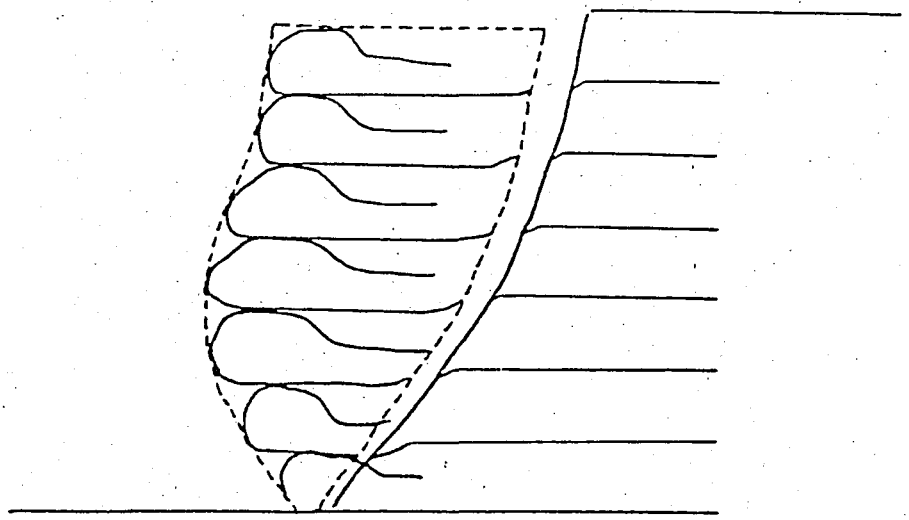

(b) Pullout Failure

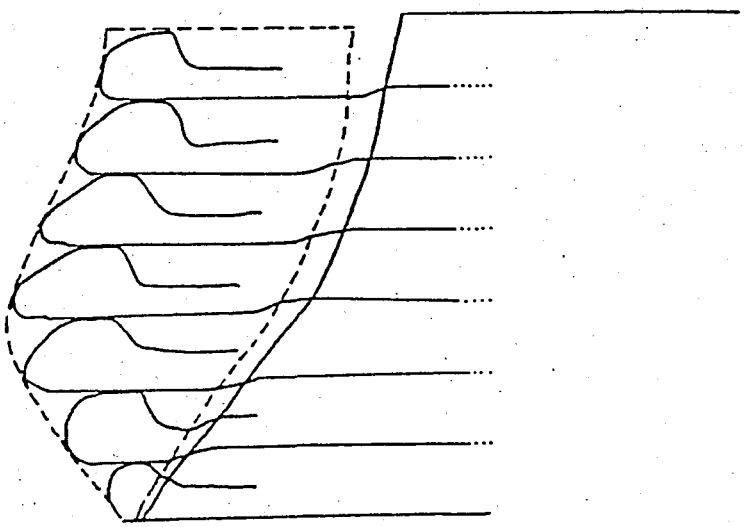

FIGURE 4.1 Internal failure modes of geosynthetic reinforced walls

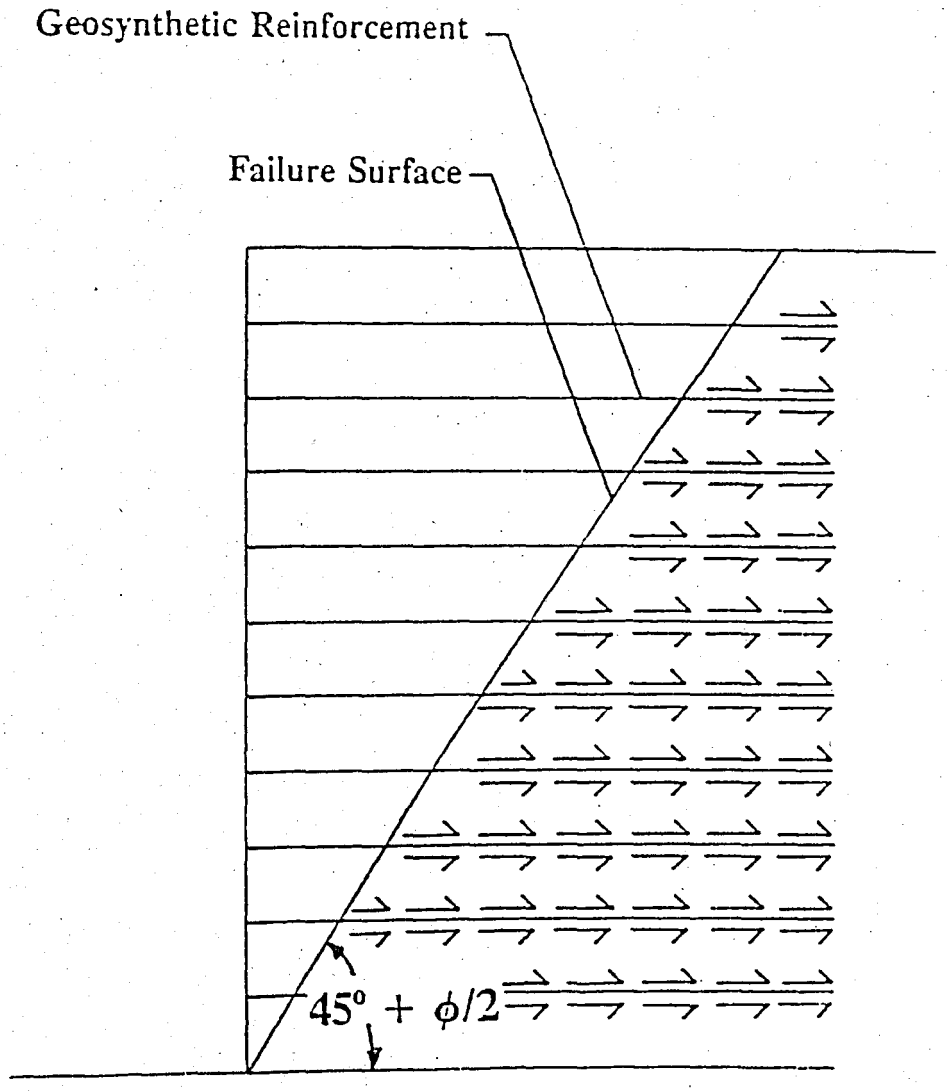

FIGURE 4.2 Assumed failure surface inclination

4.3.1 Rupture

The reinforcement tensile stress must be greater than the applied soil shearing forces. The ratio of the ultimate tensile force of the reinforcement over the soil shearing forcing defines the factor of safety against rupture for each layer as follows:

$$FS_{rupture} = \frac{T_{ult}}{\sigma_h S_v} \qquad (4.1)$$

$$= \frac{T_{ult}}{K_a S_v (\gamma Z_m + q)}$$

4.3.2 Pullout

Pullout resistance is provided by horizontal shear stresses resulting from the soil to reinforcement interface friction under the vertical confining stress where only the reinforcements which extend beyond the assumed Rankine failure surface are considered to be tension resistant. The factor of safety for pullout is the ratio of pullout resistance to the lateral earth pressure thrust for the layer. This is shown clearly as:

$$FS_{pullout} = \frac{2\tau}{\sigma_h S_v} \qquad (4.2)$$

$$= \frac{2(\gamma Z_b + q)\tan\delta L_e}{K_a S_v (\gamma Z_m + q)}$$

4.4 External Stability

Evaluation of external stability, typically consider the reinforced zone of the wall to be a semi rigid structure. It addresses situations where a portion may slid horizontally as a block, or the overturning of an equivalent retaining wall over its toe. Bearing capacity failure and slope instability beneath or behind the wall are also evaluated. as shown in Figure 4.3.

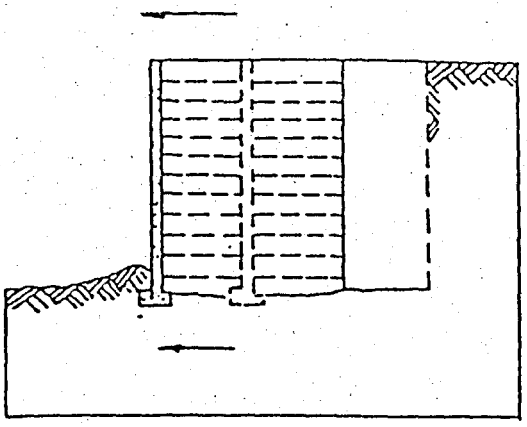

(a) sliding

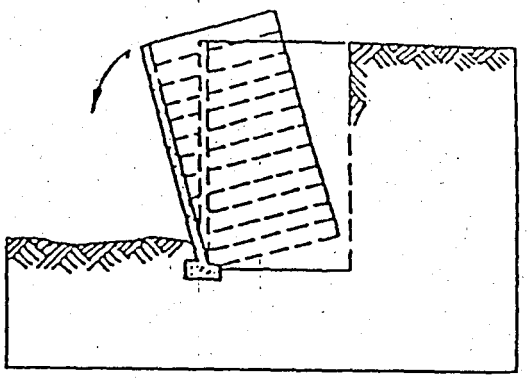

(b) overturning

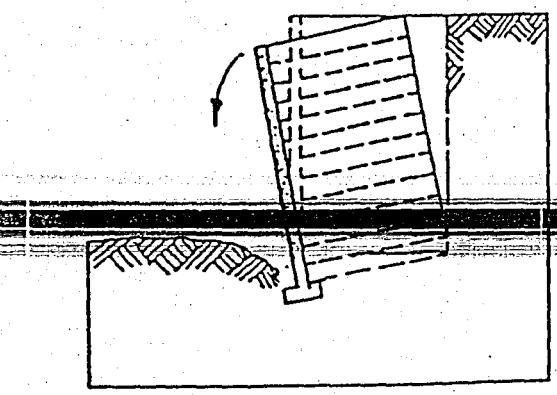

(c) bearing capacity

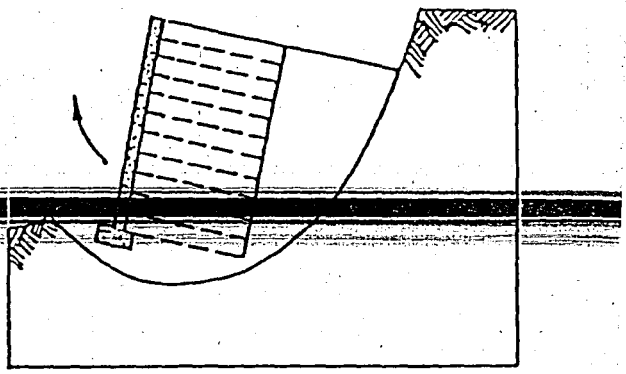

(d) rotational slip - surface failure

FIGURE 4.3 Potential external failure mechanisms

The reinforced geotextile wall must satisfy the same external stability criteria as conventional gravity retaining walls. These are:

4.4.1 Sliding

The factor of safety against sliding is defined as the ratio of resisting forces over the sliding forces as:

$$FS_{sliding} = \frac{\text{Resisting Forces}}{\text{Sliding Forces}}$$

$$= \frac{(L\,H\,\gamma + q\,H)\tan\Phi}{K_a\left(\frac{1}{2}\gamma H^2 + q\,H\right)} \qquad (4.3)$$

4.4.2 Overturning

Similarly, the resisting moments over the driving moments defines the overturning safety factor follows:

$$FS_{overturning} = \frac{\text{Resisting Moments}}{\text{Driving Moments}}$$

$$= \frac{\left(\frac{1}{2}\gamma H L^2 + \frac{1}{2}q L^2\right)}{K_a\left(\frac{1}{6}\gamma H^3 + \frac{1}{2}q H^2\right)} \qquad (4.4)$$

4.4.3 Bearing Capacity

It is required that the vertical stress at the base calculated with the Meyerhof distribution does not exceed the allowable bearing capacity of the foundation soil, determined considering a safety factor of 2 with respect to the ultimate bearing capacity.

4.4.4 Global Stability

Overall stability is determined using a classical slope stability analysis method. The reinforced soil wall is considered as a rigid body and failure surfaces completely outside the reinforced mass are considered.

4.5 Details of Kilyos Wall Analysis

External and Internal stability checks were carried out before and during the project was taking place. Four analysis are presented. The initial design before construction, and three analysis corresponding to three stages of loading and unloading of the structure presented below in Table 4.1.

TABLE 4.1 The loading and unloading stages

Stage Number	Description
I	The placement of a surcharge load of 41 kPa
II	The removal of the upper two layers (this correspond to 35 kPa load removal) and the mentioned surcharge load
III	The placement of a second surcharge load of 33 kPa above the left 4 layer reinforced retaining wall

presented below in Table 4.1.

Keeping this in mind, the layer spacing were accordingly calculated. The layer thickness used in the wall was designed as 1 m. However due to compaction of the clay the

layer thicknesses varied from 0.8 m thick at the layer number 1 to 1.1 m thick at layer number 5. No factor of safety was used to reduce the allowable fabric strength.

A factor of safety at least 1.5 was provided to prevent the possibility of sliding of the entire reinforced mass.

A minimum factor of safety of 2.0 is used to prevent the possibility of overturning about the toe. This was achieved and no problem of overturning occurred. In fact, this is generally true for most reinforced soil structures.

A circular arc stability analysis including the effects of geotextiles reinforcement were carried out as a conventional stability analysis (Ismeik, 1992). The results indicated that the minimum factor of safety with respect to global or deep seated shear failure was 2.45 therefore, exceeded the conventional minimum factor of safety of 1.5.

bearing capacity of that foundation exceeds the imposed pressure of the wall thus practically no bearing capacity problems was expected.

Polyfelt TS 21 was used in the Kilyos wall which has a strip tensile strength of 5.9 kN/m. Upper and lower layers were 5.45 m long and 3.85 m of reinforcement length thus both give length to height ratios (L/H) of 0.73 and 0.4 respectively and 0.75 m of construct the warp around face. The lengths of the geotextile used in the wall are shown in Table 4.2.

TABLE 4.2 Geotextiles lengths used in the retaining wall

Layer No:	Overlap Length (m)	Spacing (m)	Inside Length (m)	Total Length (m)
VI	0.75	0.85	3.85	5.45
V	0.75	1.10	3.85	5.70
IV	0.75	0.80	3.85	5.40
III	0.75	0.80	2.10	3.65
II	0.75	0.90	2.10	3.75
I	0.75	0.80	2.10	3.65

A Computer spread sheet program was written and used for applying the FHWA design method to this case study. As a result, the wall was designed only to fail by tension failure of reinforcement with and without surcharge load. All the four analysis calculations

No:	Length (m)	(m)	Length (m)	Length (m)

All the four analysis calculations

TABLE 4.3 Initial design before construction

Used Data

H =	5.25 m
L_{upper} =	3.85 m
L_{lower} =	2.10 m
φ =	26 °

Internal Stability

Layer	S_v	Z_b	Z_m	L_e	Δ q	$FS_{pullout}$	$FS_{rupture}$
6	0.85	0.85	0.43	1.10	0	4.1	2.8
5	1.10	1.95	1.40	1.78	0	3.6	0.7
4	0.80	2.75	2.35	2.28	0	5.3	0.5
3	0.80	3.55	3.15	1.03	0	2.3	0.4
2	0.90	4.45	4.00	1.60	0	3.2	0.3
1	0.80	5.25	4.85	2.10	0	4.5	0.3

External Stability

$FS_{sliding}$ = 1.83 > 1.5

$FS_{overturning}$ = 4.13 > 2

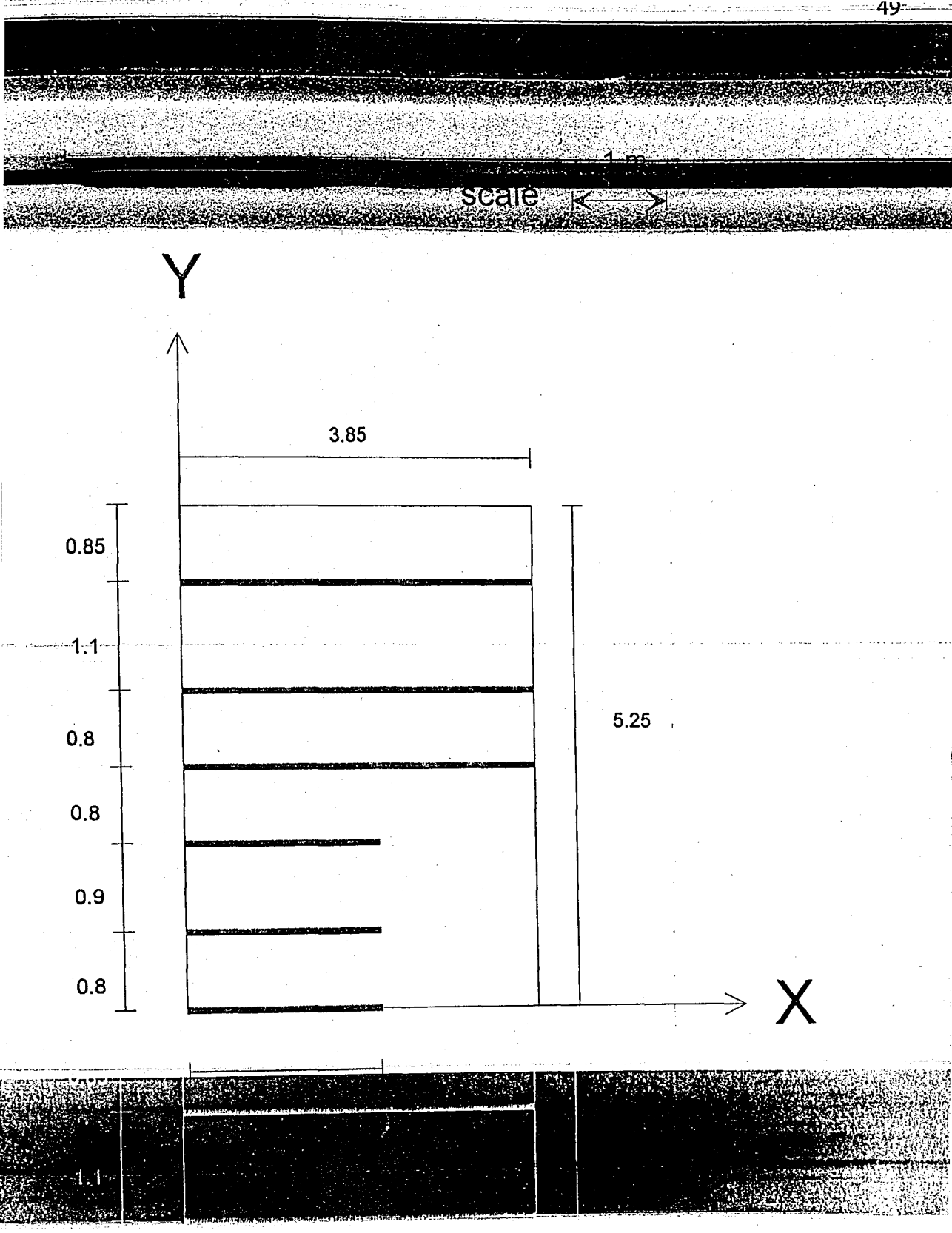

FIGURE 4.4 Configuration of initial design before construction

TABLE 4.4 Stage I: Overloading the wall with a surcharge of 40 kPa

$H =$	5.25 m
$L_{upper} =$	3.85 m
$L_{lower} =$	2.10 m
$\varphi =$	26 °
$\gamma =$	15 kN/m^3
$q =$	40
$T_{all} =$	5.9 kN/m

Internal Stability

		5.25 m					rupture
L_{upper} =		3.85 m					0.4
5	1.10	1.95	1.40	1.78	17.6	3.6	0.2
4	0.80	2.75	2.35	2.28	11.6	4.8	0.3
3	0.80	3.55	3.15	1.03	8.7	1.9	0.2
2	0.90	4.45	4.00	1.60	6.6	2.5	0.2
1	0.80	5.25	4.85	2.10	5.2	3.6	0.2

External Stability

$FS_{sliding} = 1.37 < 1.5$

$FS_{overturning} = 2.47 > 2$

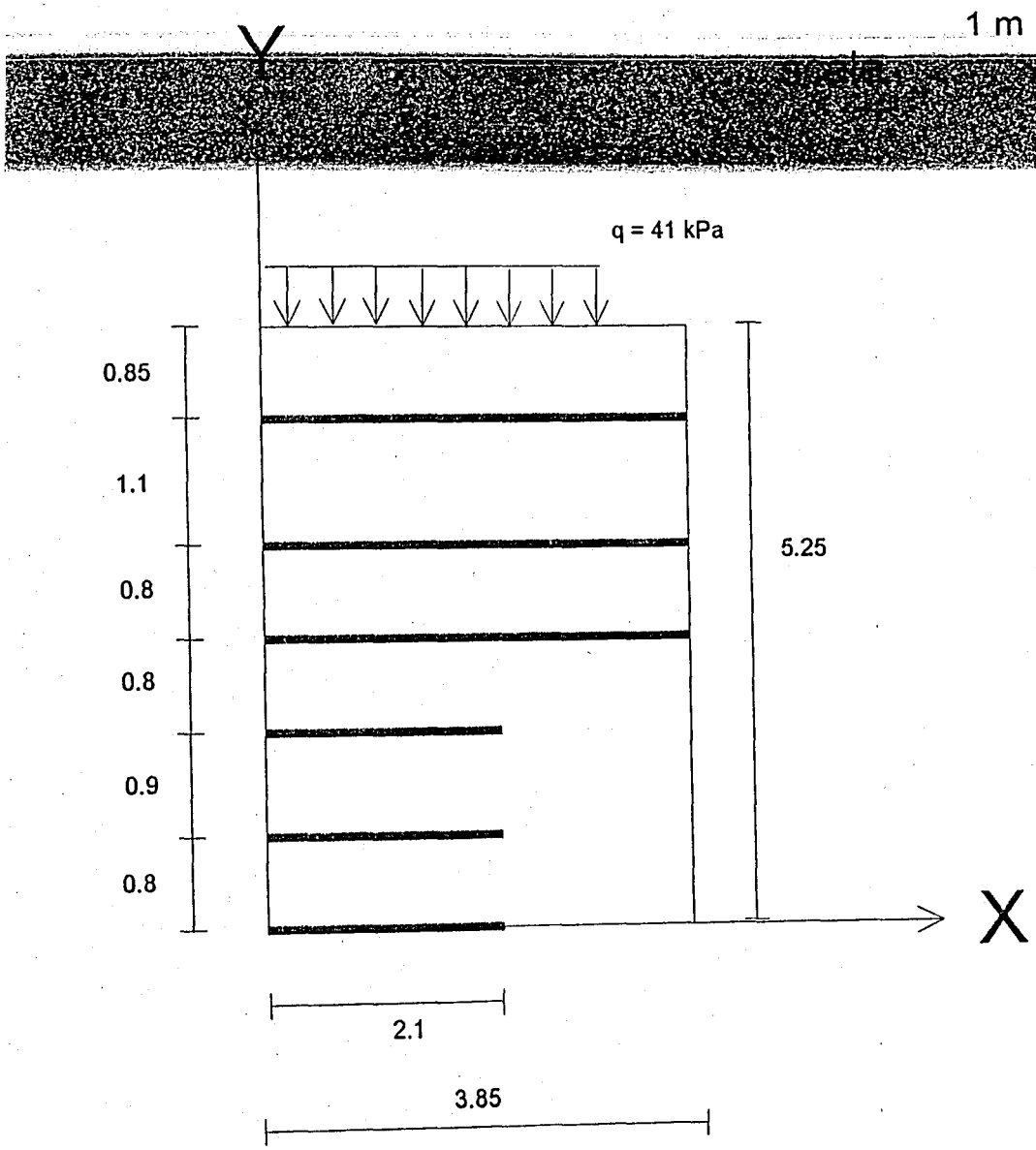

FIGURE 4.5 Stage I configuration after overloading the wall with a surcharge of 40 kPa

TABLE 4.5 Stage II Removal of the upper two layers and surcharge

Used Data

$H =$	3.30 m
$L_{upper} =$	3.85 m
$L_{lower} =$	2.10 m
$\varphi =$	26 °
$\gamma =$	15 kN/m^3
$q =$	0
$T_{all} =$	5.9 kN/m

Internal Stability

Layer	S_v	Z_b	Z_m	L_e	Δq	$FS_{pullout}$	$FS_{rupture}$
4	0.80	0.80	0.40	2.28	0	9.1	3.1
3	0.80	1.60	1.20	1.03	0	2.7	1.0
2	0.90	2.50	2.05	1.60	0	3.5	0.5
1	0.80	3.30	2.90	2.10	0	4.8	0.4

External Stability

$FS_{sliding} = 2.91 > 1.5$

$FS_{overturning} = 10.46 > 2$

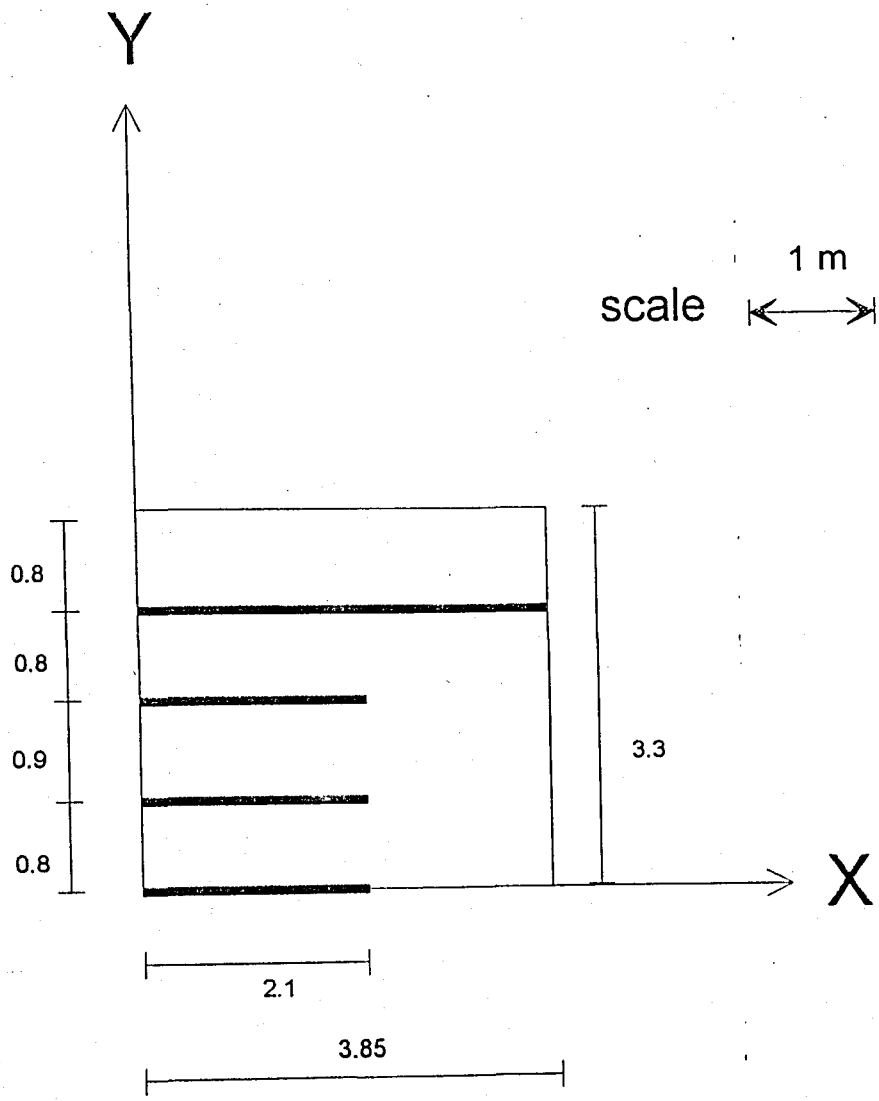

FIGURE 4.6 Stage II configuration after the removal of the upper two layers and surcharge

TABLE 4.6 Stage II: Overloading the 4 layer wall again with a surcharge of 32.2 kPa

Used Data

H =	3.30 m
L_{upper} =	3.85 m
L_{lower} =	2.10 m
φ =	26 °
γ =	15 kN/m^3
q =	32.2
T_{all} =	5.9 kN/m

Internal Stability

Layer	S_v	Z_b	Z_m	L_e	Δq	$FS_{pullout}$	$FS_{rupture}$
4	0.80	0.80	0.40	2.28	24.1	10.7	0.5
3	0.80	1.60	1.20	1.03	15	3.0	0.4
2	0.90	2.50	2.05	1.60	10	3.1	0.3
1	0.80	3.30	2.90	2.10	7.1	4.0	0.2

External Stability

$FS_{sliding}$ = 2.09 > 1.5

$FS_{overturning}$ = 5.85 > 2

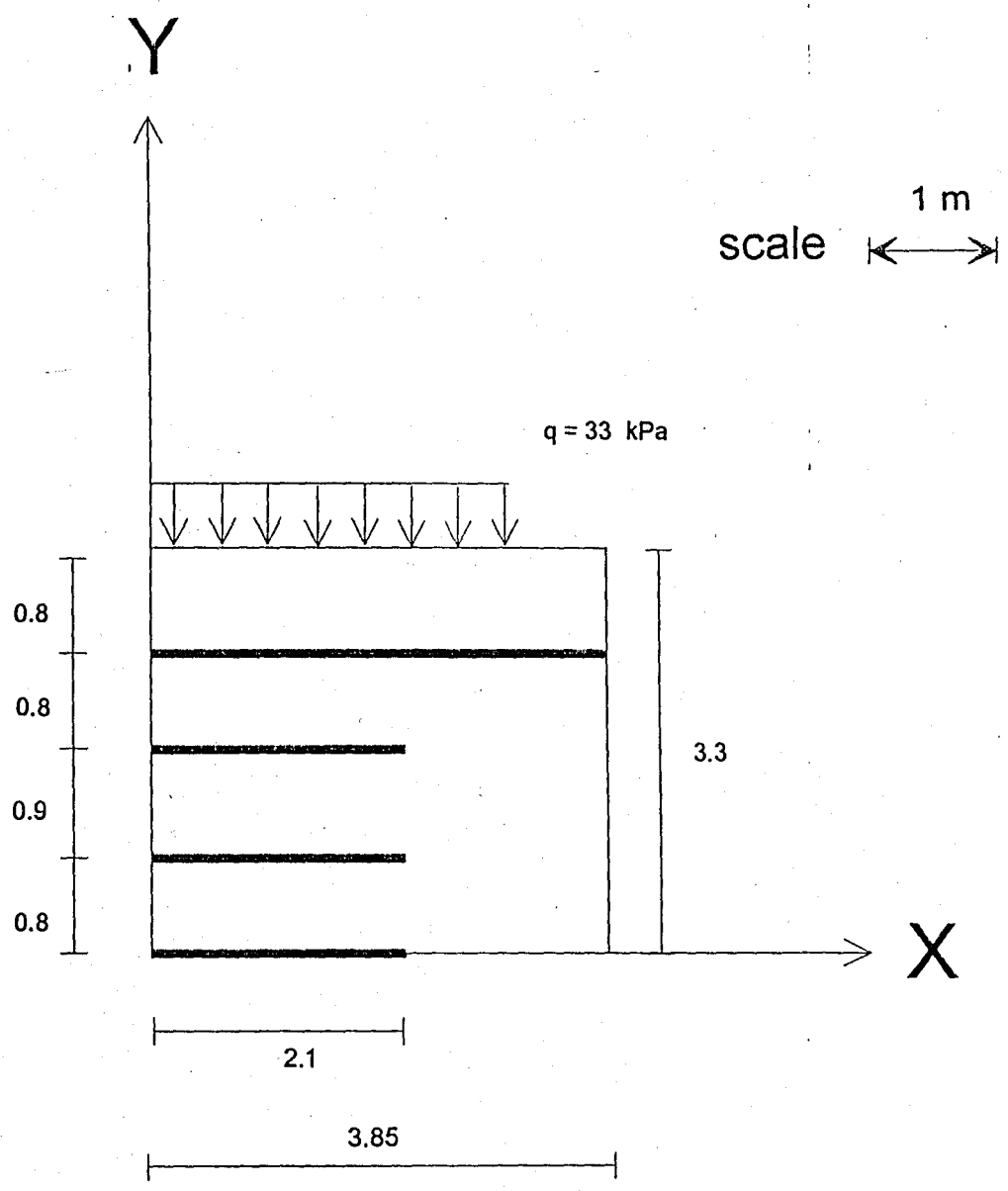

FIGURE 4.7 Stage III configuration after overloading the 4 layer wall again with a surcharge of 32.2 kPa

5 EFFECT OF WALL FACING

5.1 Introduction

Reinforced soil is a composite construction material in which the strength of engineering fill is enhanced by the addition of some type of reinforcements. The basic three components of reinforced soil are namely: engineering fill; reinforcements; as well as some form of facing which prevents surface erosion and give an aesthetically pleasing finish. Until recently, the effect of the facing element to strength of the wall was neglected. Recently there are trends to take the effect of facing elements into account while determining the stability.

The success of a geosynthetic wall is highly dependent on the type of facing system used and the care with which it is designed and constructed, as well as its stability and the ability of transforming the stresses from the soil to the facing system safely.

Geosynthetic face wraps can degrade with time due to ultraviolet exposure, and they are subject to fire and vandalism and generally limited to short design life applications. The deformation of the wall face may not be aesthetically pleasing, and the construction can be relatively slow and labor intensive and the geosynthetic reinforcement may be damaged too much during the compaction of soil layers.

5.2 Classification of Facing Types

The facing rigidity is categorized in to the following four items:

a) Local rigidity, by which the earth pressure on the back facing can be activated

b) Overall vertical rigidity, by which the axial force in the facing can be activated

c) Overall shear rigidity, by which the shear stress on the horizontal planes in facing can be activated

d) Overall bending rigidity, by which the bending moment in the facing can be activated.

Various facing types are classified according to the degree of facing rigidity summarized in Table 5.1 and Figure 5.1, adopted from Tatsuoka (1993). They range from Type A facing those for which a flat soil face is wrapped around with geotextiles sheet to extreme rigid facing as type D and E of full height precast or cast in place concrete facings which are connected to reinforcement at the back face.

Tatsuoka (1993) verified that type D and E facing , have increased the stability and is better than all other previous facing types. Many data obtained from laboratory and case studies indicated that under otherwise identical conditions, geosynthetic reinforced soil retaining walls with type D or E facing are more stable than those having a less rigid facing against the self weight of soil and load applied on the crest of backfill or the top of facing.

Facing rigidity reduce the soil stress behind the facing when stiff rather flexible facing panels were used, Jaber (1989) Bolton and Pang (1982). It should be pointed out that a full height continuous rigid facing to be used for an important permanent reinforced retaining wall can be much simpler and lighter than a conventional reinforced concrete retaining wall structure. This is because large earth pressure which may be activated on the back face of the facing is supported by many reinforced layers with a small span.

In summary, the use of geosynthetic reinforced wall with rigid facing have the following advantages:

a) Permit the use of most on site soils as the backfill soil, which results in a considerable large cost saving;
b) It can be used for reconstruction of existing embankment making a gentle slope near vertical so as to produce a wider crest area without a large amount of excavation work;
c) It exhibits very small deformations specially near the wall face so that it could be used as bridge abutment;
d) Wall face is sufficiently durable against natural and artificial damaging actions as well aesthetically acceptable which is practically important when constructed in urban areas.

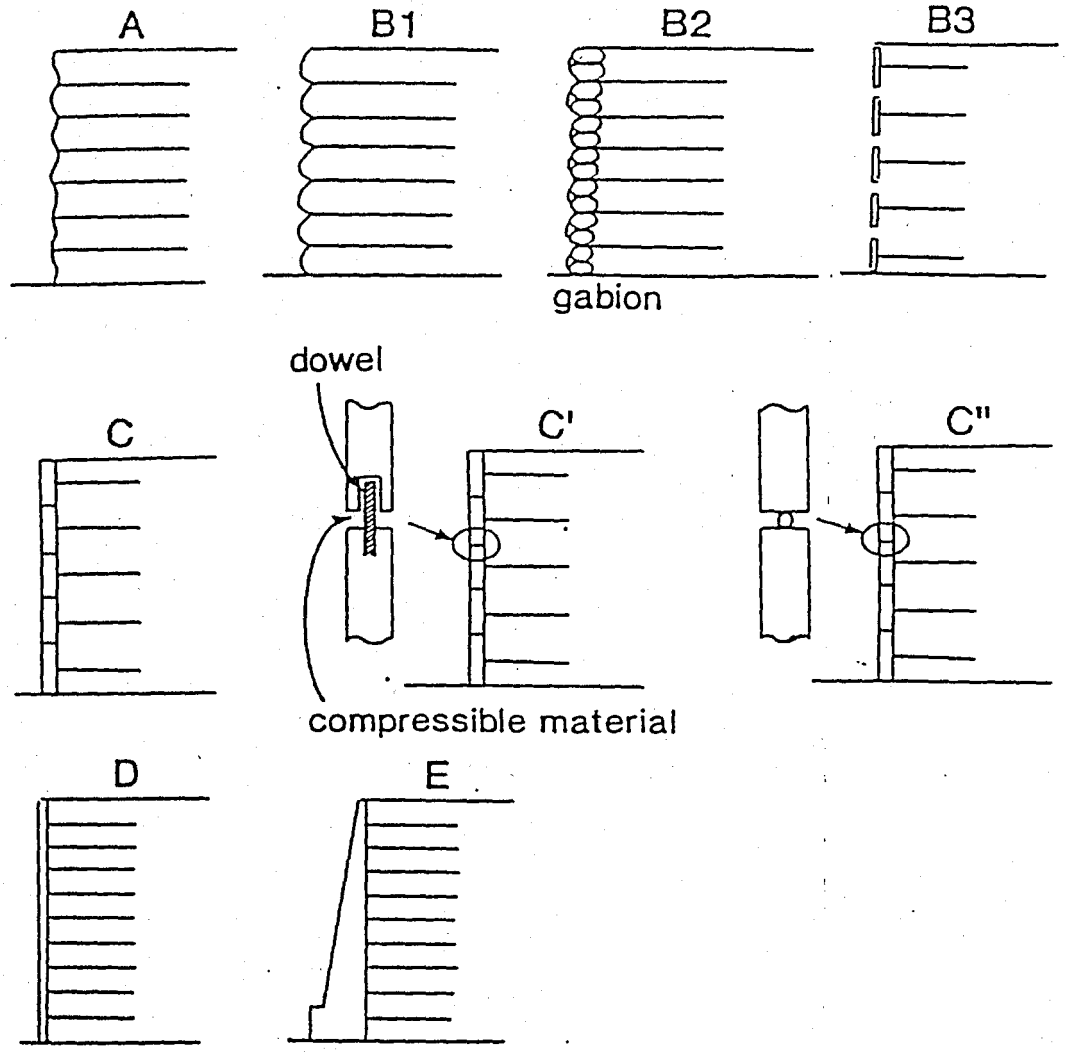

FIGURE 5.1 Schematic diagram showing various facing types (Tatsuoka, 1993)

TABLE 5.1 Classification of facing types according to the facing rigidity (Tatsuoka, 1993)

FACING TYPE / FACING RIGIDITY	A	B1	B2	B3	C	C'	C"	D	E
Local rigidiy	×	△	□	○	○	○	○	○	○
Overall axial rigidity	×	×	×	×	○	×	○	○	○
Overall shear rigidity	×	×	×	×	○	○	×	○	○
Overall bending rigidity	×	×	×	×	×	×	×	○	○
Gravity resistance	×	×	×	×	×	×	×	×	○

× means that this facing type lacks this kind of facing rigidiy.
△ means that this facing type has this facing rigidiy only slightly.
□ means that this facing type has this facing rigidiy moderately.
○ means that this facing type has this facing rigidiy sufficiently.

5.3 Theory of Two-wedge Method

Tatsuoka (1993) used the two wedge method in considering the effect of facing rigidity on overall stability. Based on his approach with slight modifications, the relationship between the developed active stresses behind the face of the wall and the total amount of reinforcement required is investigated. A new method is proposed to account for the effects of facing thickness to stability of retaining walls with the amount of reinforcement required, using a limit equilibrium analysis with relation to the seismic forces and presented in chart form.

The two-wedge mechanism shown in Figure 5.2 is adopted among many of the limit equilibrium approaches in analyzing reinforced retaining walls. The two-wedge mechanism which is one of its many variation, is preferred because it provides a simple method for obtaining safe and economical solutions and is practically suitable to reinforced soil problems. Simple hand check calculations may be carried out where other design approaches using relatively more complicated analysis are amenable to hand calculations. Also it gives relatively close solutions compared to other methods.

The forces acting on the two wedges with the schematic model for the analysis are shown in Figure 5.3 and Figure 5.4. The forces acting on each wedge are the wedge weights W_1 and W_2, resultants of surcharge loads on top of each Q_1 and Q_2, friction forces at the base of the wedges R_1 and R_2 as well the cohesion forces K_1 and K_2, normal forces N_1 and N_2, pore water pressures U_1 and U_2 and the resultant of the reinforcement forces at the base of each wedge T_1 and T_2. The inter wedge forces are exactly defined in the same manner, namely: R_{12}, K_{12}, N_{12}, U_{12} and T_{12}.

An overall equilibrium is performed to evaluate the value of T_1 and T_2. By resolving forces parallel and perpendicular to the lower surface of each wedge in turn, and assuming limiting friction $R = N \tan \phi$ a general formula is derived for total quantity of reinforcement force required T_{tot}, which is the sum of T_1 and T_2.

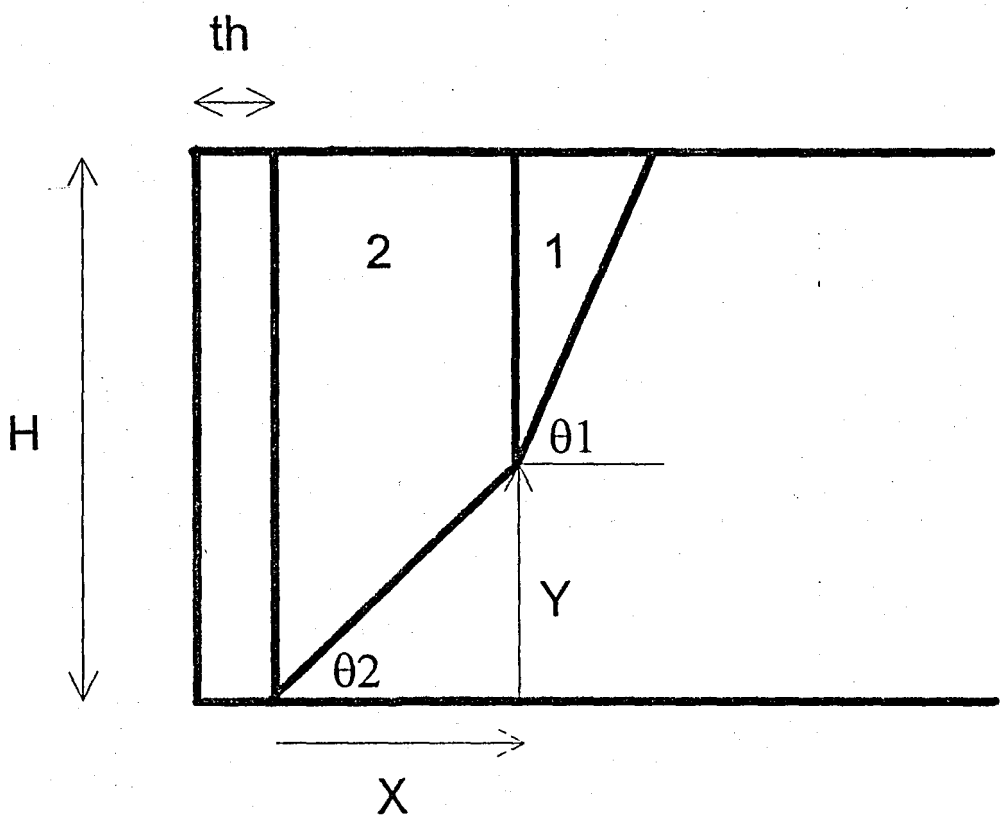

FIGURE 5.2 General overview of the two wedge mechanism

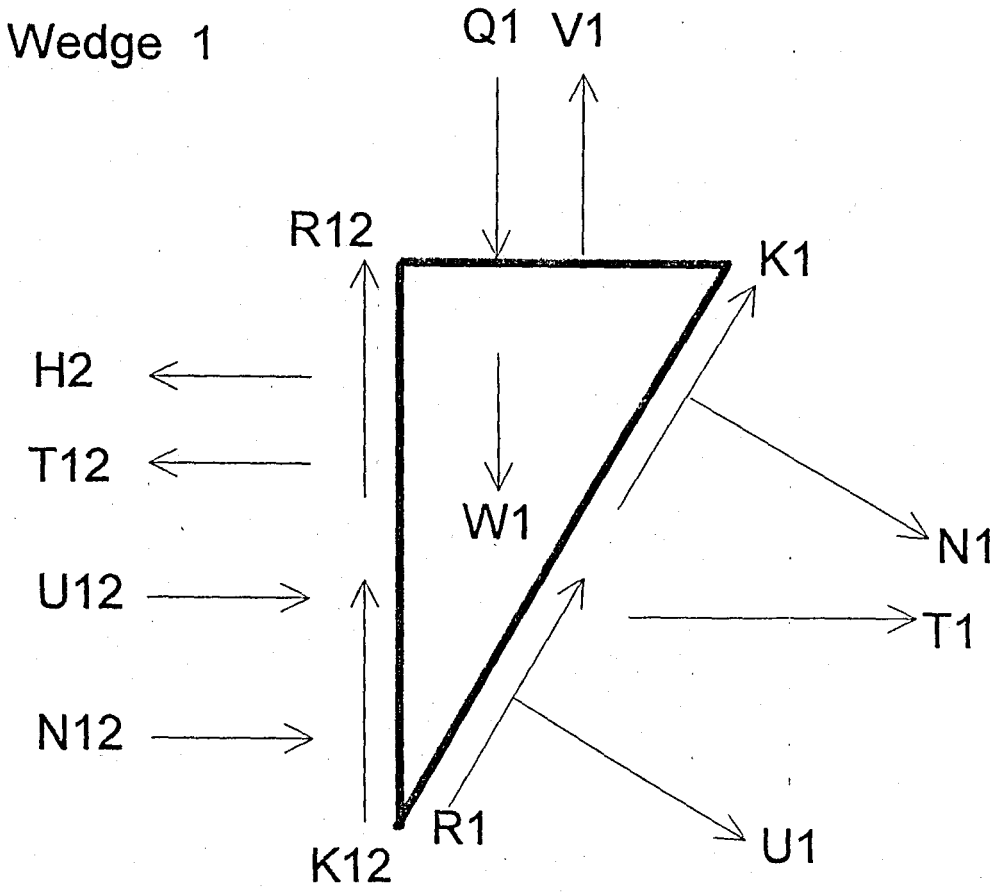

FIGURE 5.3 Forces acting on the first wedge

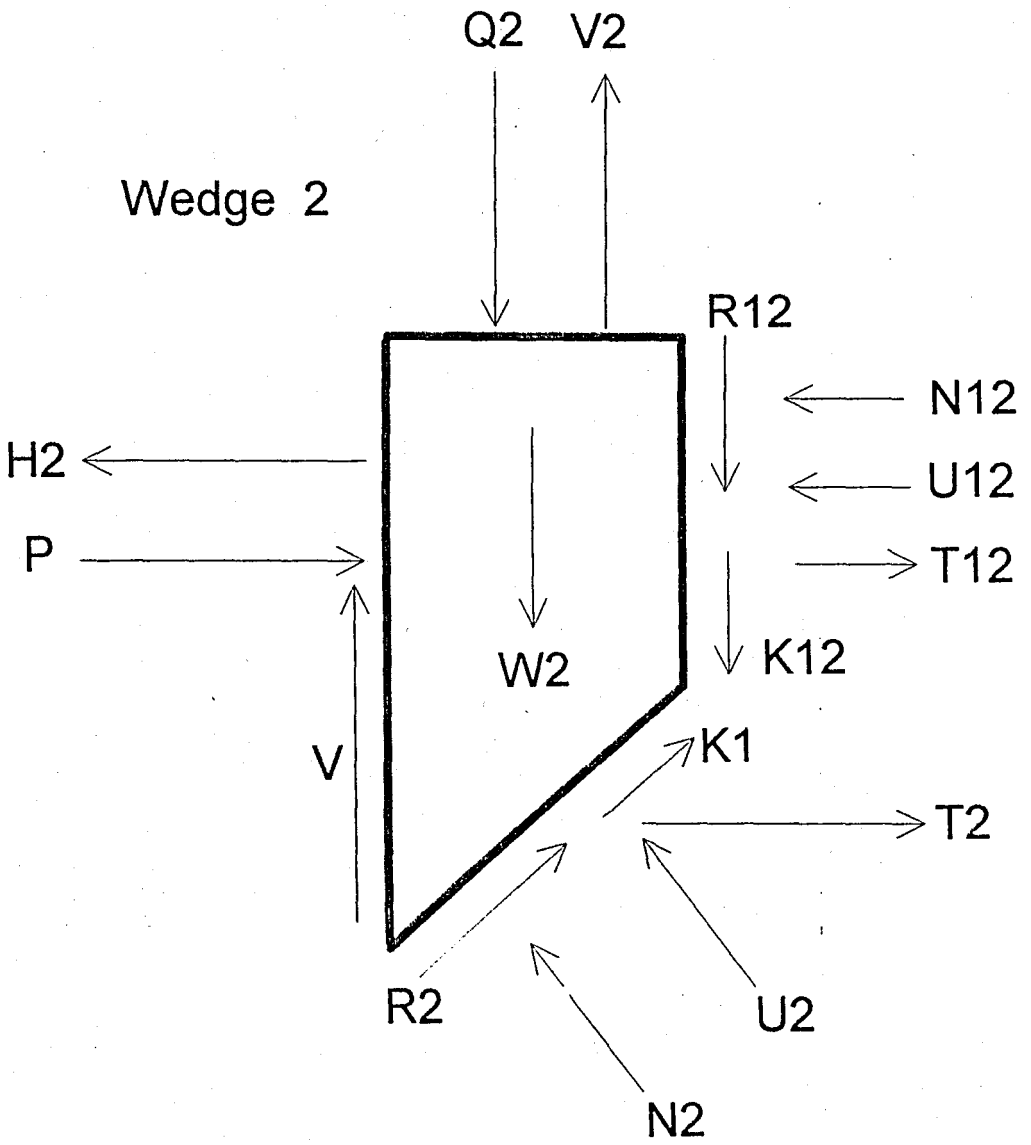

FIGURE 5.4 Forces acting on the second wedge including the inter thrust force P

Based on horizontal and vertical equilibriums, the expressions for the total quantity of horizontal reinforcement force required T_{tot}, as well T_1 and T_2 are derived after lengthy derivation and cancellations to be:

$$T_1 = \frac{(W_1 + Q_1 - K_{12} - V_1)(\tan\theta_1 - \tan\phi) + (U_1 \tan\phi - K_1)/\cos\theta_1}{1 + \tan\theta_1 \tan\phi} \quad (5.1)$$

$$T_2 = \frac{(W_2 + Q_2 + K_{12} - V_2 - V)(\tan\theta_2 - \lambda \tan\phi) + (U_2 \tan\phi - K_2)/\cos\theta_2}{1 + \lambda \tan\theta_2 \tan\phi} \quad (5.2)$$

$$T_{tot} = T_1 + T_2 + H_1 + H_2 - P \quad (5.3)$$

where the term λ is a nondimensional base sliding factor that has a value of unity for all cases except when sliding over a layer of the reinforcement takes place ($\theta_2 = 0$), a value of 0.8 is incorporated. H_1 and H_2 are the horizontal seismic forces acting on wedge 1 and 2 respectively. P is the inter thrust force between the facing and the face.

The force coefficient K which determine the quantity of reinforcement required, is defined in non dimensional form as:

$$K = \frac{T_{tot}}{0.5\,\gamma\,H^2} \quad (5.4)$$

The Tensile force T_{tot} obtained in the analysis described above depends on the value of the interwedge angle of friction ϕ_{12} adopted. It was observed that the maximum tensile force T_{tot} decreases as the value of ϕ_{12} increases and also the general formula may be considerably simplified by the conservative consumption that the inter wedge angle of friction is zero thus $\phi_{12} = 0$ is selected conservatively.

The procedure consisted in finding the critical bi-linear sliding surface which required the maximum tensile force T_{tot}, which is similar to that proposed by Jewell et al. (1984) and Jewell (1990). This critical mechanism is unique and will determine the total reinforcement force required for which forces equilibrium is maintained. The search is done by varying the position of the surface and the angles θ_1 and θ_2 at the bases of the wedges as well the x coordinate of inter wedge boundary.

The constrains on the mechanism are that the inter wedge boundary should be vertical, and the base of the lower wedge intersects the toe of the wall. The mechanism may take any form provided that these two constrains are observed.

The length of the reinforcement L required for the reinforcement zone is determined by reinforcing all possible wedge failures which are unstable under their own weights. Generally the size of the reinforcement zone should be such no wedge requiring reinforcement can pass completely outside the reinforced zone.

5.4 Seismic Loading

For a geosynthetic reinforced soil retaining wall, the use of continuous rigid facing was experimentally found to increase the stability of the wall. Shaking table test results, on large geosynthetic reinforced soil retaining wall model indicated that these walls with a continuous rigid facing could be very stable against severe earthquake loading including foundation liquefaction. (Murata et al. 1993, 1994)

The seismic stability of reinforced retaining walls is evaluated here by the two-wedge method. In seismically active areas, an analysis of stability of the geosynthetic reinforced wall under seismic conditions should be carried out. Checks include the wall as well the facing system. The pseudo-static Mononobe-Okabe analysis is followed to calculate the extra dynamic forces acting on the two wedges and the face. The analysis assumes coefficient forces, namely, k_h and k_v horizontal and vertical ground acceleration ratios

expressed as fractions of the gravitational constant are used as accelerations multiplied by the weight of each wedge as well the facing.

Thus, the extra vertical and horizontal seismic forces acting on the face are:

$$V_f = k_v W_f \tag{5.5}$$

$$H_f = k_h W_f \tag{5.6}$$

and the ones acting on the first wedge are:

$$V_1 = k_v W_1 \tag{5.7}$$

$$H_1 = k_h W_1 \tag{5.8}$$

and the ones acting on the second wedge are:

$$V_2 = k_v W_2 \tag{5.9}$$

$$H_2 = k_h W_2 \tag{5.10}$$

5.5 The New Design Approach

The design method developed by Tatsuoka (1993) is modified to determine the analytical relation for the inter trust force P. The effects of facing rigidity on the stability of reinforced retaining walls are considered herein based on a two-wedge method as described. Here, the contribution from the facing is accounted for as follows. The face has a rectangular shape and has a weight of W_f. P is the thrust between the backfill and the face and expressed as a percentage α of the active earth pressure. V is the shear force between the face and the backfill and S is the shear at the base.

In a more mathematical form:

$$P = \alpha P_a \tag{5.11}$$

$$V = P \tan \phi_w \tag{5.12}$$

$$S = (V + W_f - V_f) \tan \phi_f \tag{5.13}$$

where ϕ_w and ϕ_f are wall and foundation friction angles respectively.

In this approach, it is considered that the facing rigidity increases the stability of the wall in the following way. For full concrete panel having a sufficient amount of overall bending and axial rigidities part of the weight of backfill is transmitted to the facing through the frictional force V, on the back face.

The laboratory and field tests (Tatsuoka et al., 1992, Murata et al., 1991, 1993) showed that the coefficient α is nearly equal to zero for a flat soil face wrapped around with the geotextile sheet, while it is nearly equal to one for facing having sufficient local rigidity as full concrete panel. The coefficient α increases as the thickness increases.

The physical meaning of α means that less force P would be carried out by the reinforcements. Also, as the facing thickness increases, the rigidity of the wall increases as well, thus a higher percentage of the P force is transmitted to the facing.

Uniform vertical surcharge on the top of the wall may be treated as an equivalent additional height of fill. An effective wall height H_e could be used in the calculations defined as:

$$H_e = H + \frac{q}{\gamma} \tag{5.14}$$

Pore water pressures, acting at the base of the failure surfaces and at the interface between wedges, could be taken into account, however only dry conditions are considered here, therefore the pore pressure quantities U_1 and U_2 are identically zero.

5.6 Analytical Determinations of Inter-thrust Force P

Considering the face as a single unit having sufficient amount of bending rigidity, the forces acting on it are shown in Figure 5.5. As described above, theses forces are self weight of the facing W_f, inter thrust force between the soil and the face P, shear force V, and slid shear force S.

Recalling equations 11, 12 and 13 and defining W_f, P_a, and K_a as

$$W_f = th\, H\, \gamma_c \tag{5.15}$$

$$P_a = \frac{1}{2} K_a \gamma H^2 \tag{5.16}$$

$$K_a = \tan^2\left(45 - \frac{\phi}{2}\right) \tag{5.17}$$

and then summing up the forces in the vertical and horizontal directions, one can end up with following equation for α including the seismic forces as follows:

$$\alpha = \left\{ \left(\frac{2}{K_a}\right) \left(\frac{\gamma_c}{\gamma}\right) \left(\frac{(1 - k_v)\tan\phi_f - k_h}{1 - \tan\phi_f \tan\phi_w}\right) \right\} \left(\frac{th}{H}\right) \tag{5.18}$$

The coefficient α distributes the total active force as a percentage to facing system as well to the reinforcement. This also means that the stability of the facing has achieved its maximum resisting capacity by resisting the released thrust from the soil.

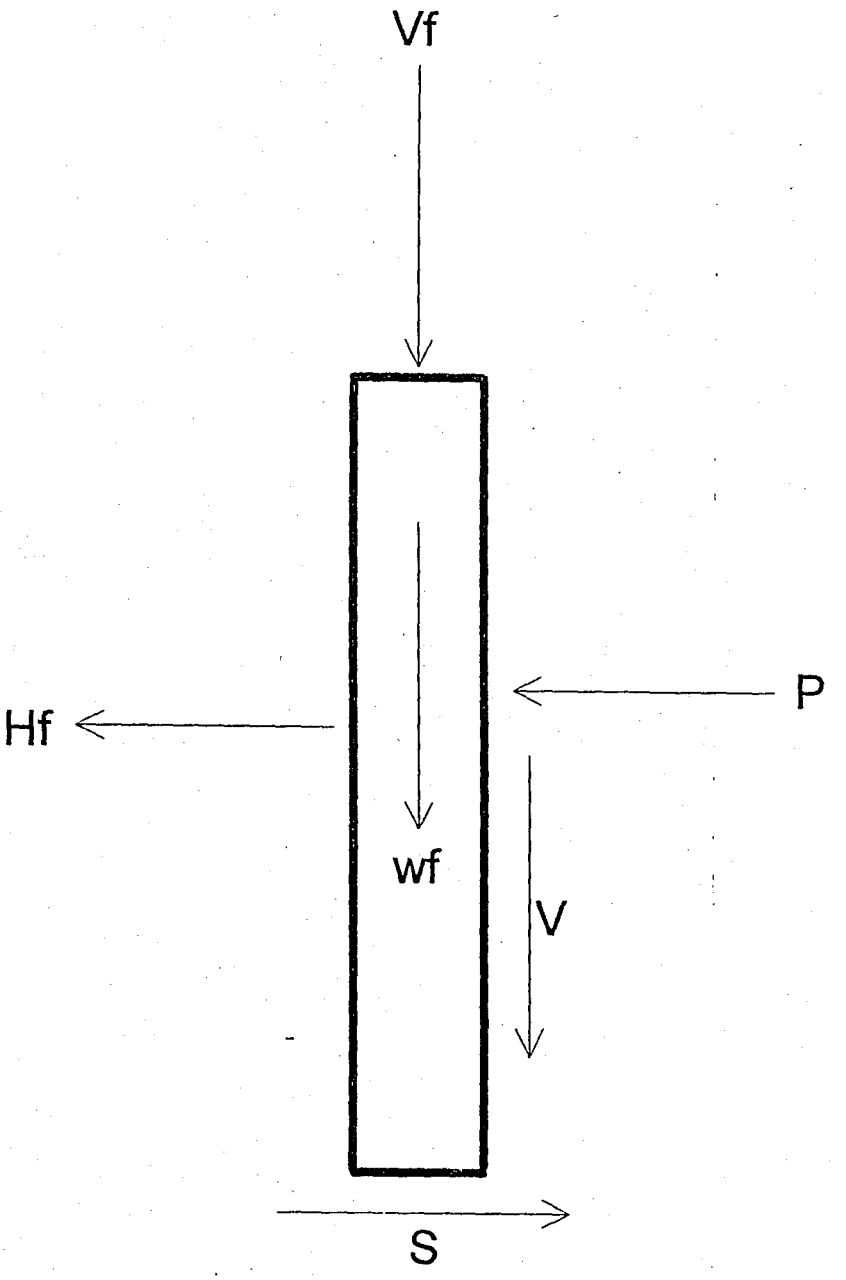

FIGURE 5.5 Forces acting on the facing including the inter thrust force P

The above equation is dependent of only one variable (th/H). Careful examination of the above expression leads absolutely to the fact that as the wall thickness ratio increases the capacity of carrying a larger quantity of active earth pressure increases till to the point that all the active force is carried out by rigid facing and thus no need for reinforcement as in classical concrete retaining structures.

5.7 Development of Design Charts

Now, after presenting the basic outlines of the two-wedge method, and the seismic forces, it is possible to develop a new design method presented in chart form for determining the total amount of reinforcement as well their lengths as a function of face thickness, with respect to three cases of horizontal seismic loading for $k_h = 0$, 0.1 and 0.2.

Recalling equation (5.4) the amount or reinforcement required is expressed in a non dimensional form as the force coefficient defined as:

$$K = \frac{T_{tot}}{0.5\,\gamma\,H^2} \qquad (5.4)$$

In the above equation, K is evaluated according to the geometrical and loading conditions assumed for the design where a wider range of loading conditions including seismic loading has been taken into account with different wall thicknesses. All the equations are modified to include the inertial forces $k_h W_1$, $k_h W_2$, and $k_h W_f$.

The direction of the seismic forces is always taken in the direction of decreasing stability, i.e. towards the outside, since this is the most critical case. Other combinations of possible directions, i.e. towards the backfill, will not lead to the maximum tensile force required for design since they will help to increase the stability of the reinforced wall by supporting the unstable wedge, thus are not considered here.

6 RESULTS AND DISCUSSIONS

6.1 Kilyos Wall

6.1.1 General

The behavior of the Kilyos reinforced retaining wall with emphasis on the obtained measurements is studied. This includes review of the theoretical analysis method, results of an instrumentation program, and comparison of field measurements with values of stresses and deformations predicted by using the equations used in designing of the wall and finite element analysis results obtained from CRISP (CRItical State Program).

6.1.2 Behavior of the Wall

Instrument readings were taken during construction of the wall and at intervals throughout a period of two years after the construction of the wall. The readings of all measurements are grouped into three stages. These stages are classified according to loading and unloading stages as illustrated in Table 6.1.

TABLE 6.1 The loading and unloading stages

Stage Number	Description
I	The placement of a surcharge load of 41 kPa
II	The removal of the upper two layers (this correspond to 35 kPa load removal) and the mentioned surcharge load
III	The placement of a second surcharge load of 33 kPa above the remaining 4 layer reinforced soil retaining wall

Readings of all pressure cells with respect to time are presented in Appendix 2. All measurements are shown in a single graph in Figure 6.1.

From the end of construction till the first stage of loading the readings were fluctuating with average values increasing. Although not all of the readings increased at the same rate, they in general showed an increase in the pressures. This is assumed to be mainly due to the settlement of soil around the gages.

Then although a surcharge load of 41 kPa is placed above the retaining wall, from the first stage till the second one, readings were almost constant. No great changes were observed at all.

Then the upper two layers and the surcharge were removed. Almost all readings were constant and / or showed slight increase during this stage. At this stage, one of the pressure reading showed incredible increase, while others did not function properly.

In fact, all of them should had decreased since the removal of the upper two layers and the surcharge should decrease the load above the pressure cells, however the pressure cells could not feel the decrease in load. This can indicate that residual stresses remained around the gages.

At the third and last stage, where another surcharge to 33 kPa was placed above the four layer reinforced wall, a small increase of pressure was observed. This is due to the increase of load coming from the surcharge.

The pressure cells were not very sensitive to the effect of increasing and decreasing loads above the wall. This may be due to the fact that all of the increase of load is transferred to lateral soil particles and non is transferred to bottom of the wall where the pressure cells were deep and could not sense these changes.

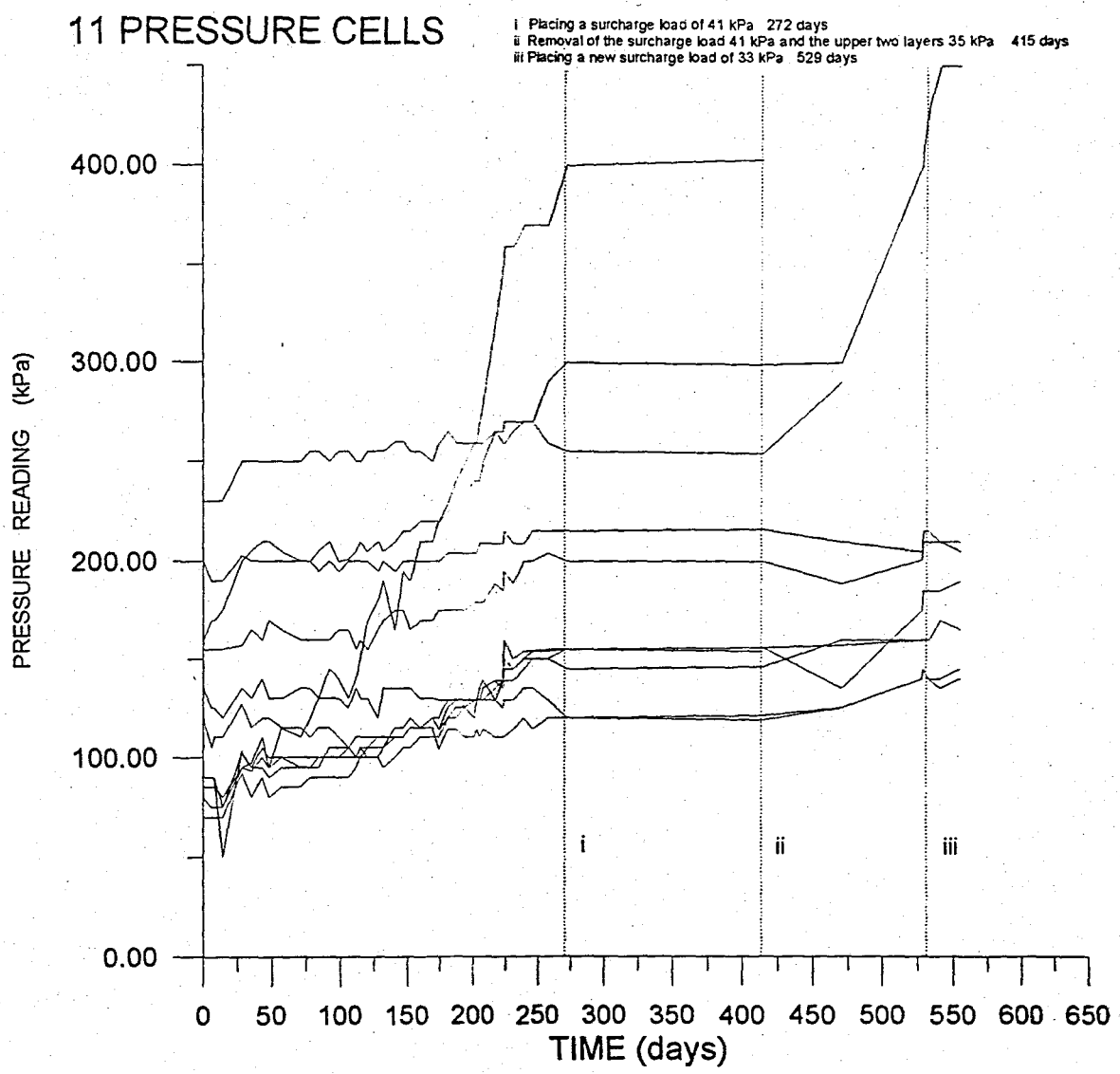

FIGURE 6.1 Readings of all pressure cells

6.1.3 Theoretical Distribution of Vertical Pressure

The stress distribution of the soil is assumed to be proportional to depth. Thus the overburden vertical stress is constant at equal elevations.

Since the unit weight of the compacted soil is known to be 15 kN/m^3 , this means the overburden pressures could be calculated theoretically as the product of depth and unit weight.

6.1.4 Comparison Between the Theoretical and Obtained Results of Pressure Readings

Following construction of the wall, a detailed finite element analysis of the wall has been carried out using the program CRISP and the results have been presented in Appendix 3 (Edinçliler, 1994) and compared with the measured readings below.

A) Vertical Soil Pressures

Typical results of the vertical pressure acting on the first and second layers of the retaining wall obtained from pressure cells at elevations 0.3 m and 1.4 m are shown in Figures 6.2, 6.3, 6.4, and 6.5 respectively. The analysis is divided into two cases. The first one is before applying the surcharge and the second one is after applying the surcharge load of 41 kPa.

Each case has two components of readings at the first layer and the second layer. The obtained results are compared with the finite element analysis and the theoretical ones. The results in the above mentioned four graphs demonstrated that both the measured readings and finite elements results are greater than the theoretical assumed value of stress distribution. This implies that either the pressure cell are reading locally high pressures or due to the long pipes the dial gages is reading artificially high value due to frictional resistance of oil with pipe surface.

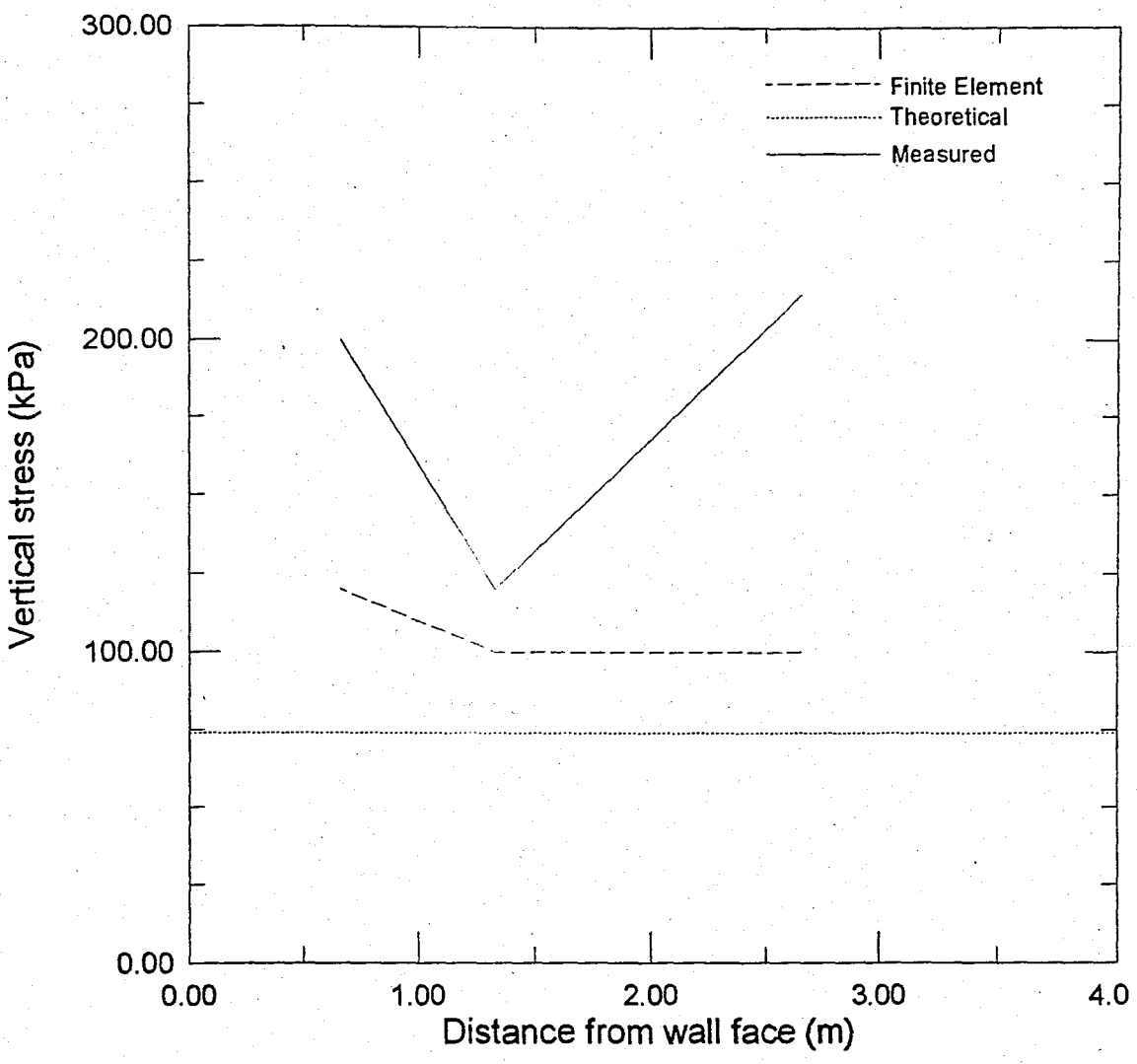

FIGURE 6.2 Measured distribution of vertical stress before applying the surcharge load for the layer I at elevation 0.3 m

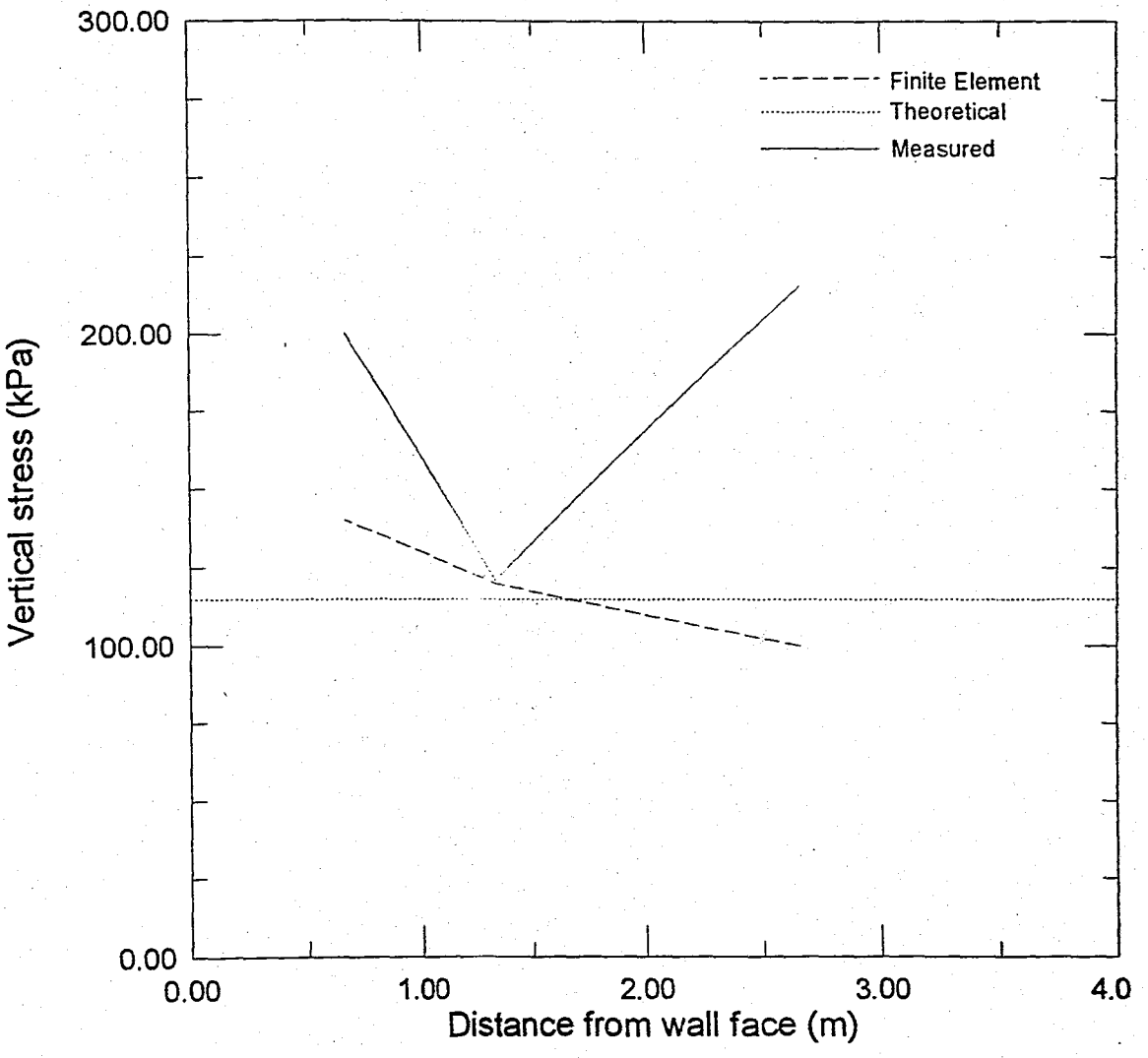

FIGURE 6.3 Measured distribution of vertical stress after applying the surcharge load for the layer I at elevation 0.3 m

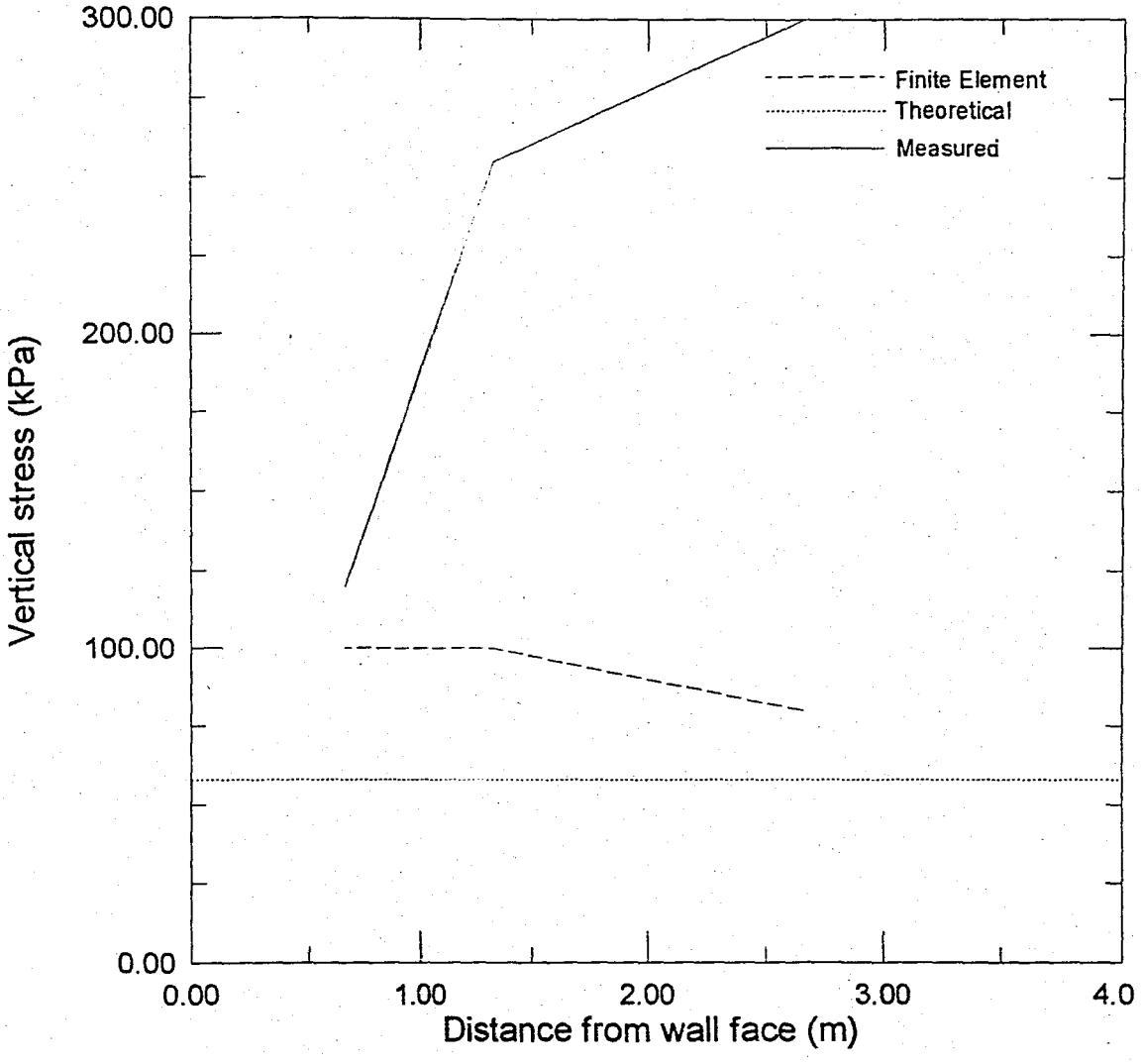

FIGURE 6.4 Measured distribution of vertical stress before applying the surcharge load for the layer II at elevation 1.4 m

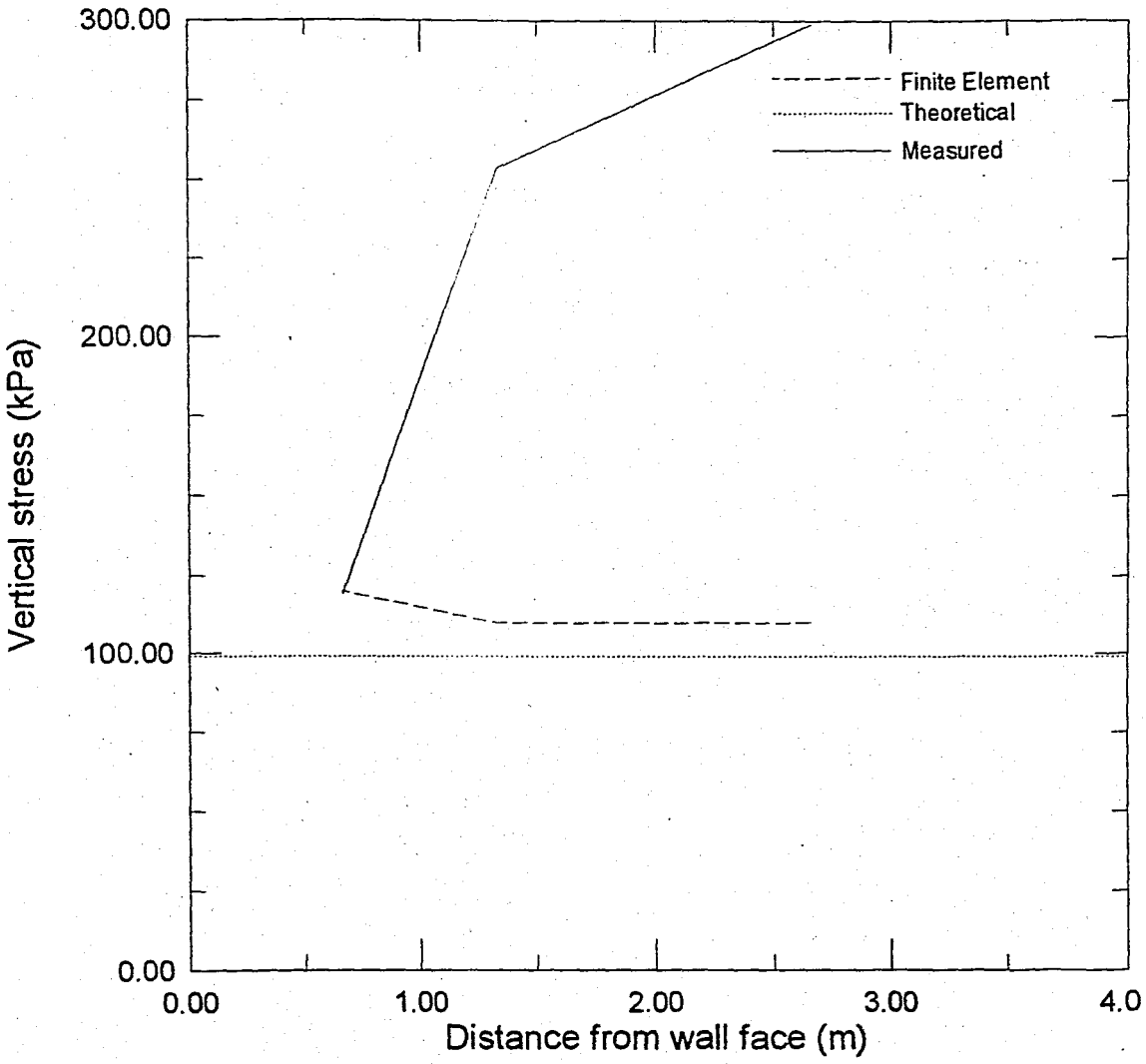

FIGURE 6.5 Measured distribution of vertical stress after applying the surcharge load for the Layer II at elevation 1.4 m

To eliminate the effect of oil friction with pipes, a calibration procedure has been applied. Oil was pressurized into the pipe without passing the pressure cell in order to determine the effect of friction and see how this would shift the readings. The assumed friction was low. The friction only contributed to real readings by an amount of 1 per cent. Thus it was concluded that long or short pipes might not alternate the readings significantly.

The graphs indicated that the measured distribution of the vertical stress along the depth is nonlinear or not changing smoothly. Only after the application of the surcharge load quite close agreement between all analysis is observed as can be seen in Figure 6.4.

A bilinear distribution is almost observed in all cases. There appears to be a distinct difference in the vertical pressure distribution between the measured values and the geostatic one, however this difference is less compared to the results of finite element method.

B) Lateral Earth Pressures

Lateral earth pressures near the back side of the face obtained from the Kilyos test site are presented with respect to the two cases. Figures 6.6 and 6.7 present results from pressure cells placed to measure lateral earth pressure in layer 2 before and after the placement of the surcharge load.

The pressure is almost constant throughout the depth. Measured values did not show significant changes in lateral earth pressure in either case. Measurements of wall lateral pressures were not consistent with behavior predicted with the finite element analysis as well the linear distribution.

Reasons behind this could be the same as described above as well it is believed that the high values of these obtained lateral pressures depends not only on backfill properties but also on the construction process. High compaction effort induces considerable lateral pressures that should be considered in the analysis and design of reinforced earth structures.

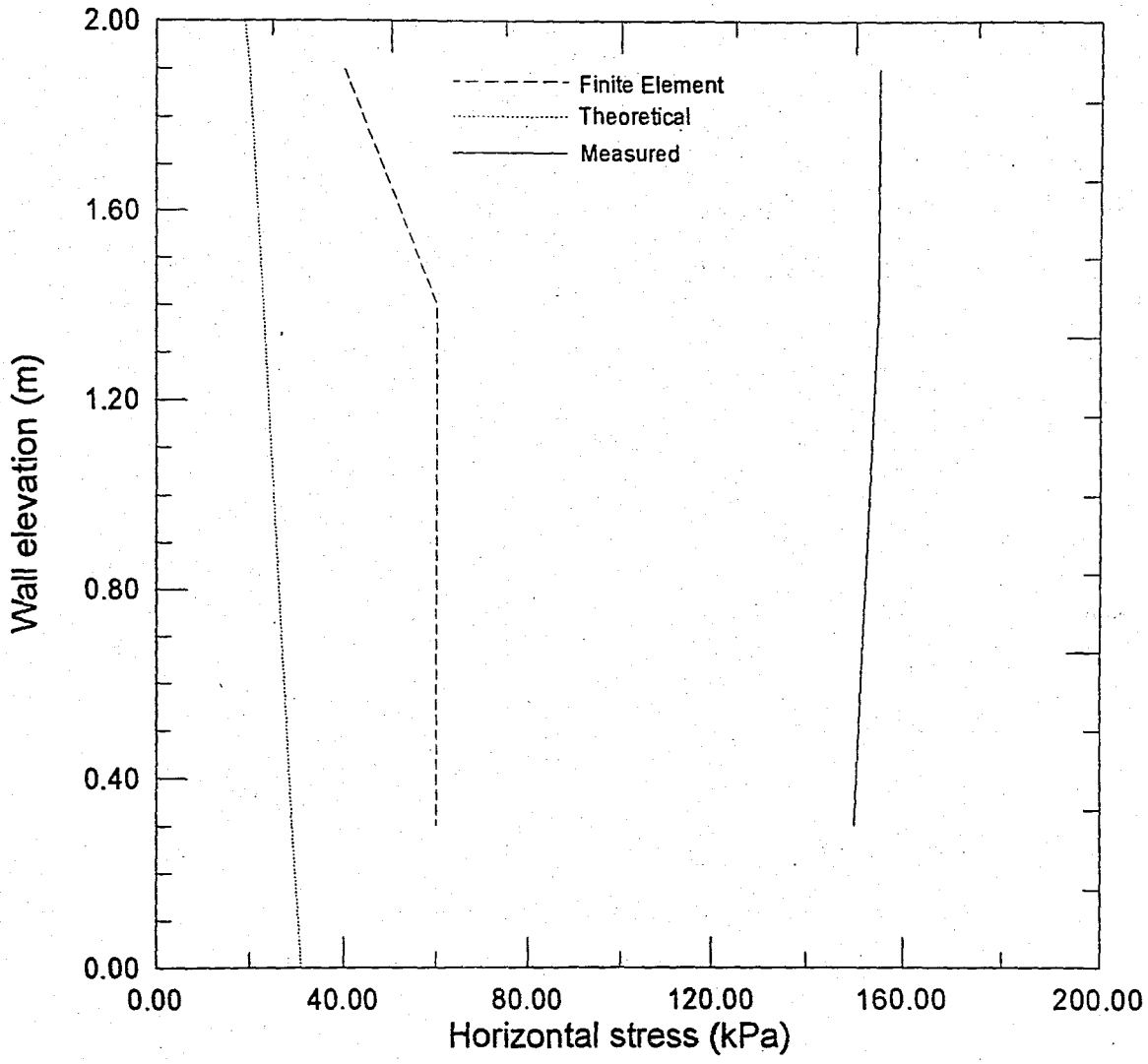

FIGURE 6.6 Measurement of lateral earth pressure near wall facing before applying the surcharge load for the layer II at elevation 1.4 m

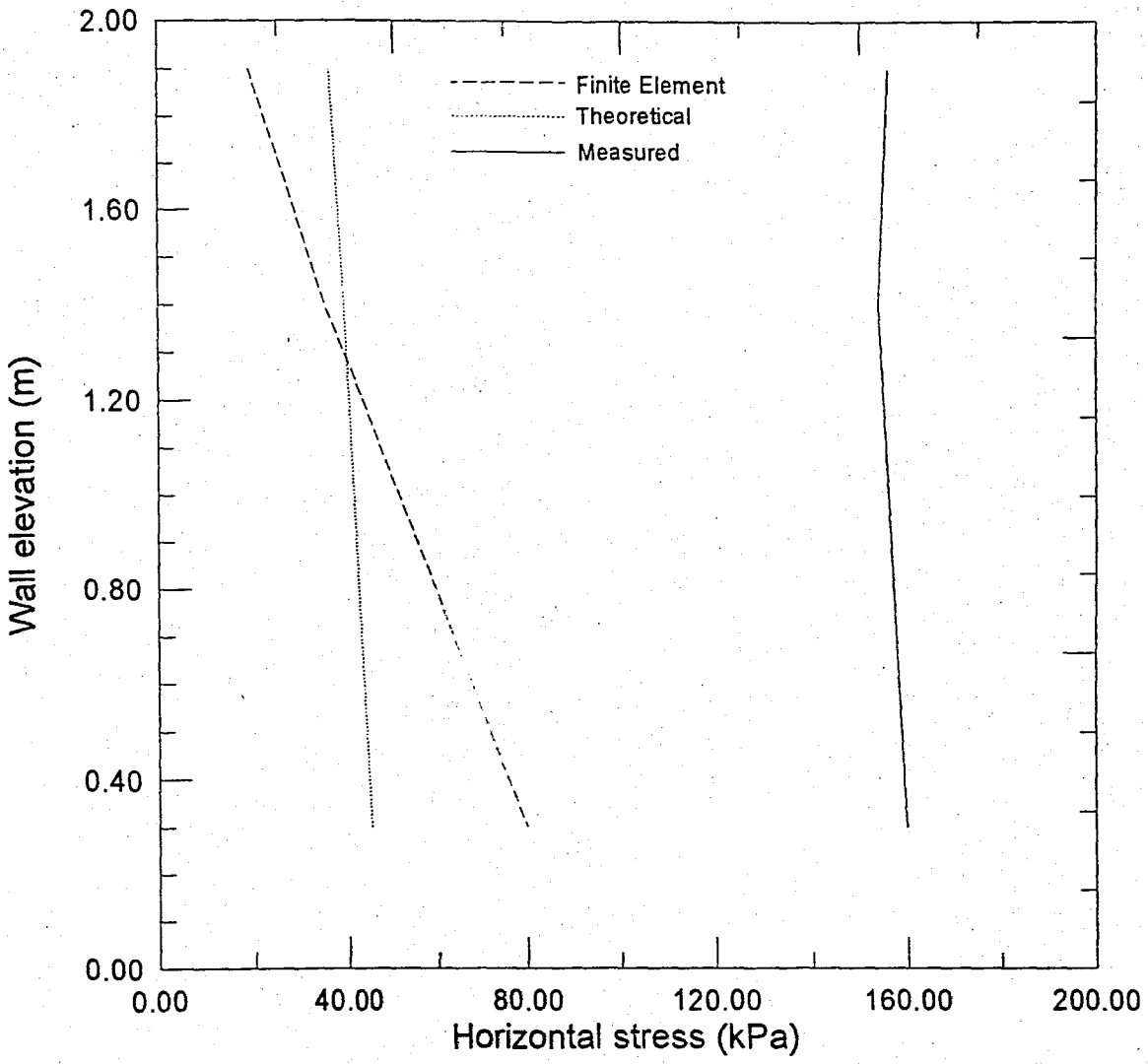

FIGURE 6.7 Measurement of lateral earth pressure near wall facing after applying the surcharge load for the layer II at elevation 1.4 m

6.1.5 Coefficients of Earth Pressures

The angle of internal friction of stabilized clay was determined to be 23°, so it is possible to calculate the theoretical at rest and active earth pressure coefficients as follows:

$$K_o = 1 - \sin\phi = 1 - \sin 23^\circ = 0.609 \qquad (6.1)$$

$$K_a = \tan^2(45 - \phi/2) = \tan^2(45 - \phi/2) = 0.438 \qquad (6.2)$$

Now, it is interesting to compare the measured three lateral earth pressure coefficients with the calculated theoretical ones above. Since the locations of the group pressure cells 4V and 3H, 5V and 4H have the same coordinates, it is therefore possible, to calculate numerically the lateral earth pressure coefficients of earth pressure as the ratios of the horizontal pressure above the vertical one determined from real field measurements as:

$$K = \sigma_h / \sigma_v \qquad (6.3)$$

The lateral earth pressure coefficients calculated from measured pressures are given in Table 6.2 and Table 6.4 respectively. Since the gauges 3H and 4V are within the theoretical active zone, it is assumed that here active pressure should be present and since 4H and 5V are within the theoretical resistive zone so it is assumed that in situ conditions exist here.

Comparison between the theoretical and measured values are shown in Table 6.3 and 6.5 respectively for both, after construction and at the termination of the project.

TABLE 6.2 Measured lateral earth pressure coefficients (end of construction, December 1993)

Horizontal pressure reading (kPa)	Vertical pressure reading (kPa)	K ratios
3 H = 70	4 V = 120	70 / 120 = 0.583
4 H = 80	5 V = 230	80 / 230 = 0.347

TABLE 6.3 Comparison between the theoretical and measured lateral earth pressure coefficients (End of Construction, December 1993)

Lateral earth pressure coefficients	Theoretical	Measured	Difference
K_o	0.609	.347	42 %
K_a	0.438	.583	33 %

TABLE 6.4 Measured lateral earth pressure coefficients (termination of the project, August 1995)

Horizontal pressure reading (kPa)	Vertical pressure reading (kPa)	K ratios
3 H = 154	4 V = 145	154 / 145 = 1.062
4 H = 403	5 V = 290	403 / 290 =1.389

TABLE 6.5 Comparison between the theoretical and measured lateral earth pressure coefficients (Termination of the Project, August 1995)

Lateral earth pressure coefficients	Theoretical	Measured	Difference
K_o	0.609	1.389	128 %
K_a	0.438	1.062	142 %

Measured lateral earth pressure coefficient values are lower at end of construction. In August 1995 the values have increased well above the theoretical values.

6.1.6 Deformations

Deformation measurements taken during the three mentioned stages showed so low deformations that they remained beyond the sensitivity of the measuring coils. Therefore, theoretically the deformations appeared to be almost zero.

Besides the type of backfill material, there are, many factors affecting the deformations of the backfill. More important factors include the height, stiffness of soil, design and stiffness of reinforcing system, compaction process, construction method, and elapsed time. Therefore, it is difficult, if not possible, to quantify why so small deformations were obtained, among these influencing factors.

It is believed that the wall had the rate of consolidation was high that almost a great percentage of it took place during the construction, since the construction rate was low, little deformation left at the long run, which could not be measured by the developed system.

6.1.7 Strains of Geotextiles

The dial gages connected to the invar cables, did not show any change in reading. It was not clear that if this means that the geotextiles did not have any deformation or possible due to some other source of error, this technique did not function properly.

6.1.8 Drainage of Geotextiles

Observations on Kilyos wall with respect to the horizontal drainage under the addition of extra water through the excavated holes gave important clues with regard to stability. It is of interest to note that in spite of significant amount of water fed, the reinforcement was especially useful for cohesive backfills since the drainage capabilities of the geosynthetic dissipate the developed excess pore water pressure thus enhancing stability during and after construction phases. In this way, the geosynthetic layers work not only as reinforcements but also as lateral drains.

Since the drained friction strength of cohesive soils is usually low the dissipation of the built-up of pore water pressure results in increase of the backfill soil strength parameters. Consequently, the design of a safe and economical structure should address an important aspect to the reinforcement drainage characteristics embedded in clayey backfills. Also another aspect of the drainage of water through the geotextile is the increase of consolidation process. This is so important when dealing with clays used as backfills in for reinforced wall since this will allow to construct any structure rapidly.

6.1.9 Performance

The performance of the wall was checked by instrumenting it by Glötzl pressure cells, and specially developed coil sets installed into the soil. Long term data were gathered approximately 20 months after completion of the wall.

As of the end of August 1995, when the project was terminated, the performance has been entirely satisfactory. No decrease of stability has been encountered and expectations have been met with no signs of settlement or cracking.

6.2 Effect of Facing Thickness

6.2.1 Overview

The two-wedge method for a typical vertical retaining wall without any surcharge load is applied. It is assumed that the soil is of cohesionless type, though cohesion could be included. Seismic effects are simulated introducing pseudo static forces applied horizontally on the two wedges as well to the facing, thus the vertical seismic coefficient kv is assumed to be zero. The seismic force is resisted by tensile force in the reinforcement and partially by the facing system.

6.2.2 Results

The results presented in chart form are demonstrated through Figure 6.8 to Figure 6.13, which give the force coefficient K and the length of reinforcement as a function of the face thickness for different kind of soils and different seismic accelerations. The analysis was carried out for a practical face thickness ratio (th/H) varying from 0 to 0.25 and for horizontal seismic accelerations varying from 0 to 0.2g.

The graphs demonstrate clearly that the facing system can play a very important role in increasing the stability of vertical reinforced walls. This is achieved by directly reducing the amount of required reinforcements represented by the force coefficient K.

The graphs roughly represent a reduction in K coefficient between 20 per cent to 70 per cent depending on the soil type had the wall thickness increased from 0 (no facing) to 0.25 (th/H). Similar reduction is obtained in length ratios.

A parallel reduction is also observed for the cases of seismic loading. This show the importance of facing even in seismically active zones. Figure 6.14 and Figure 6.15 present a comparison on the effect of seismic loading for soil with friction angle of 25°. The increase of horizontal ground acceleration leads to the increase of reinforcement required as well the their corresponding lengths. However, it is still observed that the facing rigidity reduces the amount of reinforcement required in all cases. This demonstrate the importance of facing rigidity even in actively seismic zones.

6.2.3 Remarks

The refinements in the design procedure which were made here, lead to an estimate of lateral earth pressure against the facing, thus designers will enhance extra confidence in choosing wall facing thicknesses which increase the stability of the wall.

Other failure criteria must be checked to have a global stability. Extra internal and external checks should be carried out to have a global stability of the system as a single unit. Overall stability, overturning as well sliding must be checked specially when the reinforcement are short.

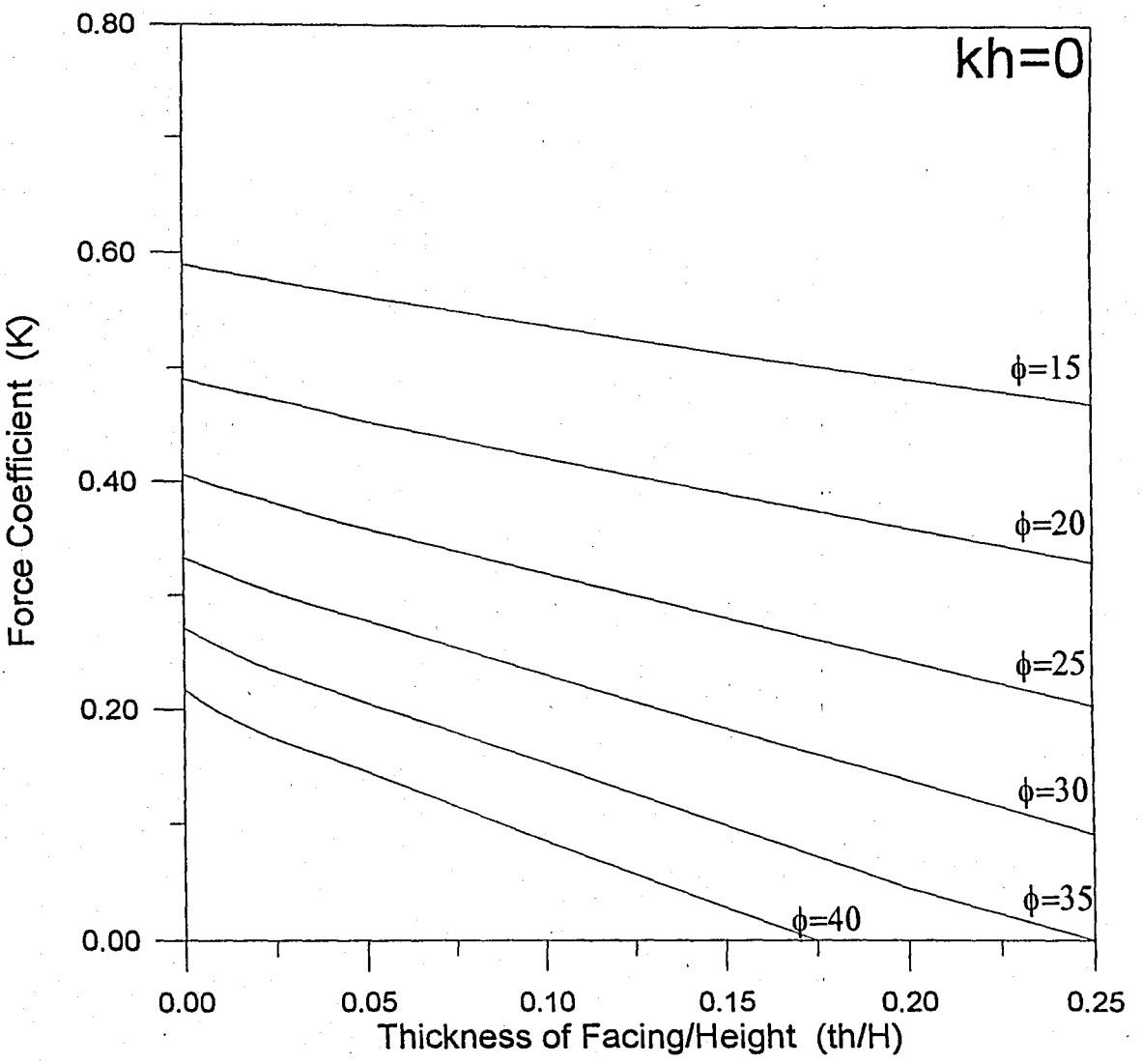

FIGURE 6.8 Force coefficients for different soil types ($k_h = 0$)

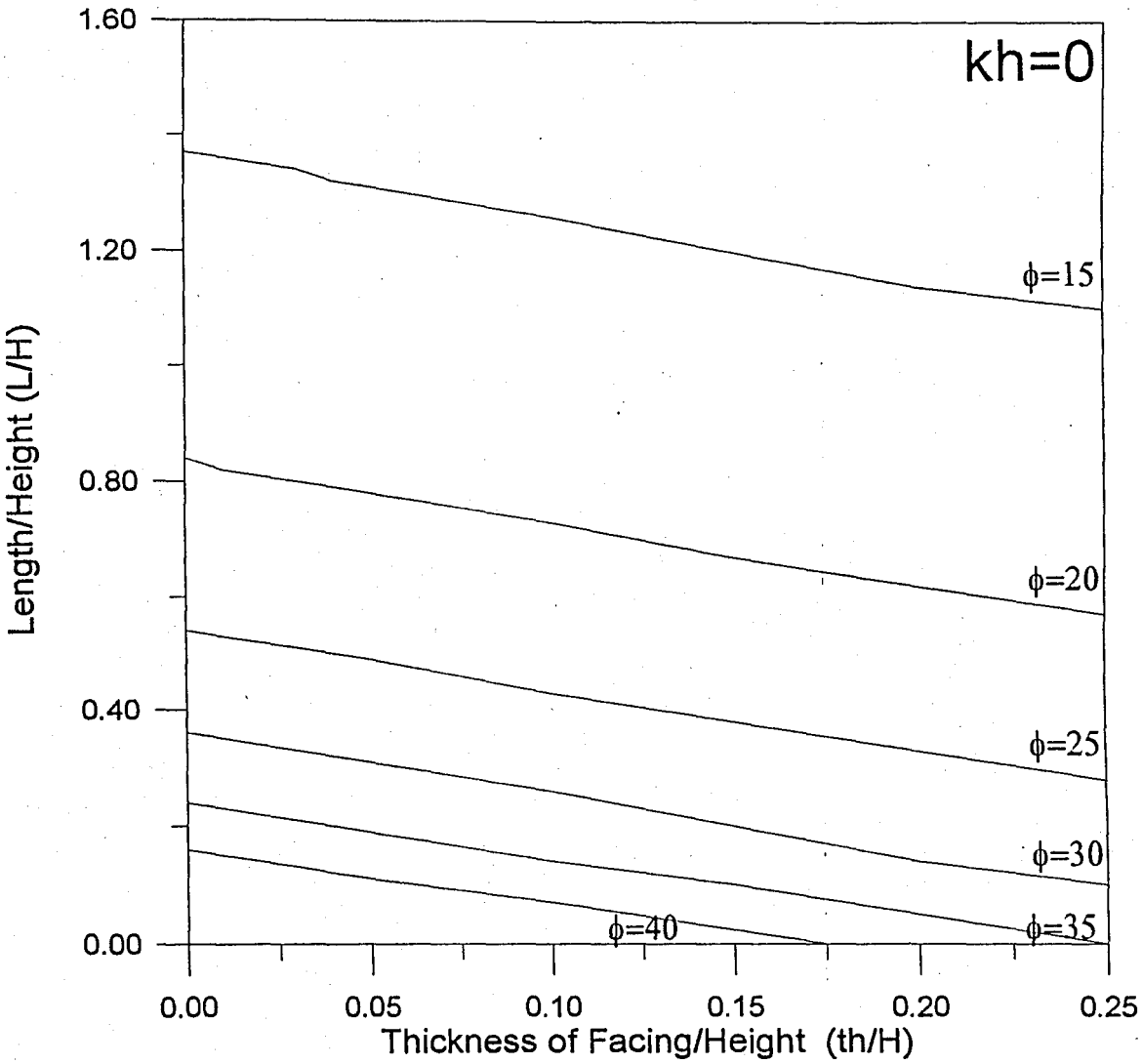

FIGURE 6.9 Length of reinforcements over Height for different soil types ($k_h = 0$)

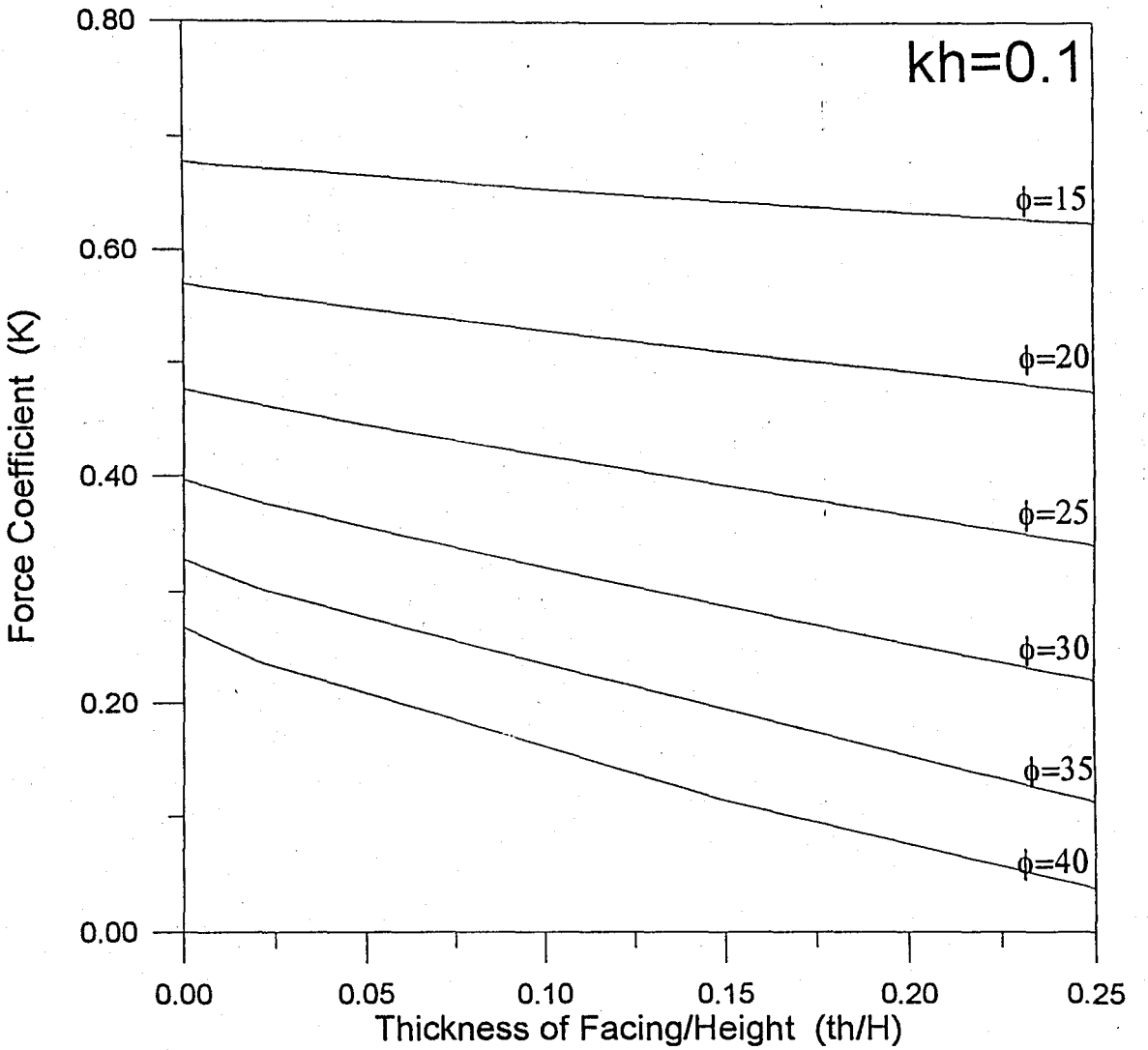

FIGURE 6.10 Force coefficients for different soil types ($k_h = 0.1$)

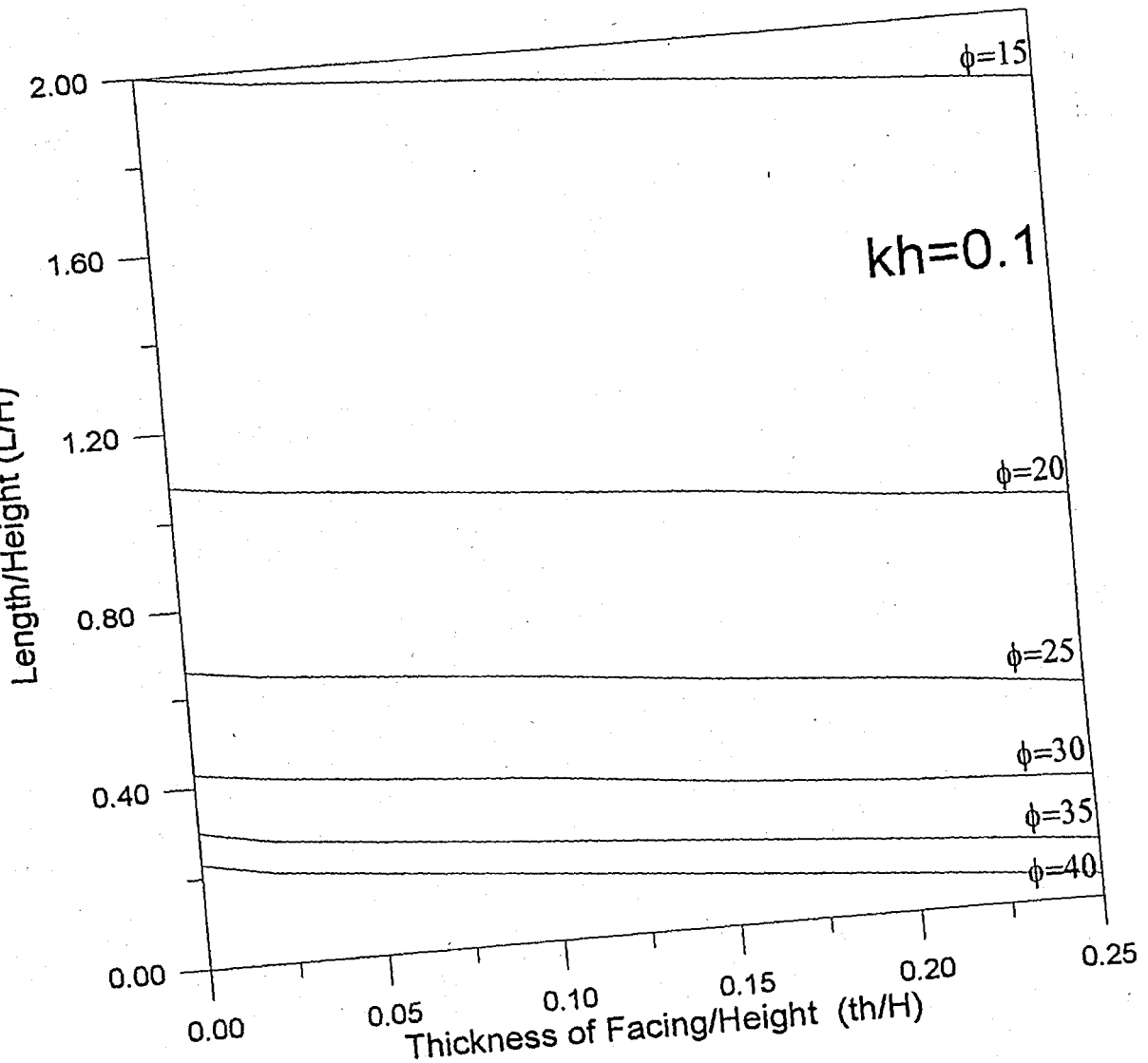

FIGURE 6.11 Length of reinforcements over Height for different soil types ($k_h = 0.1$)

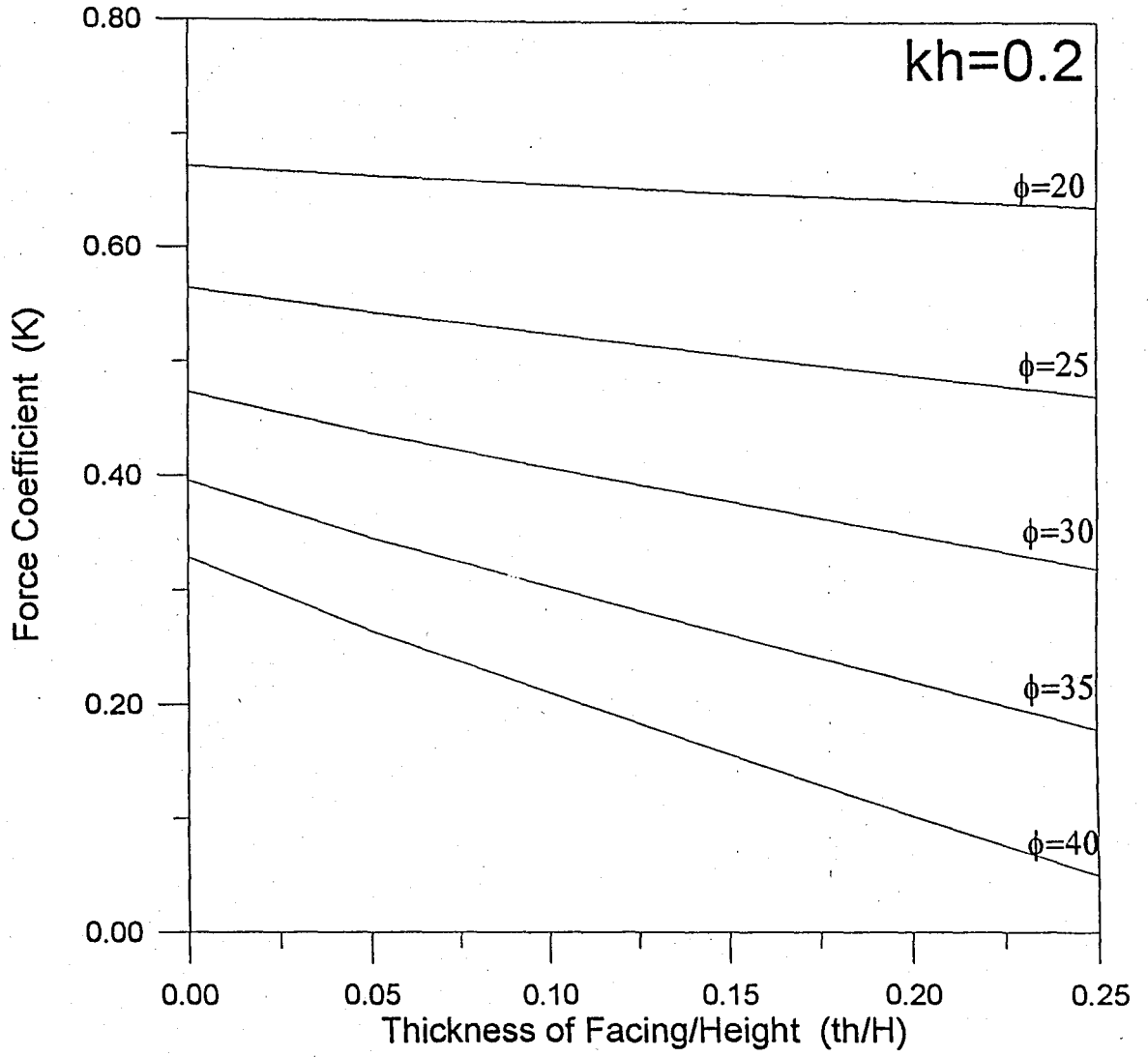

FIGURE 6.12 Force coefficients for different soil types (k_h = 0.2)

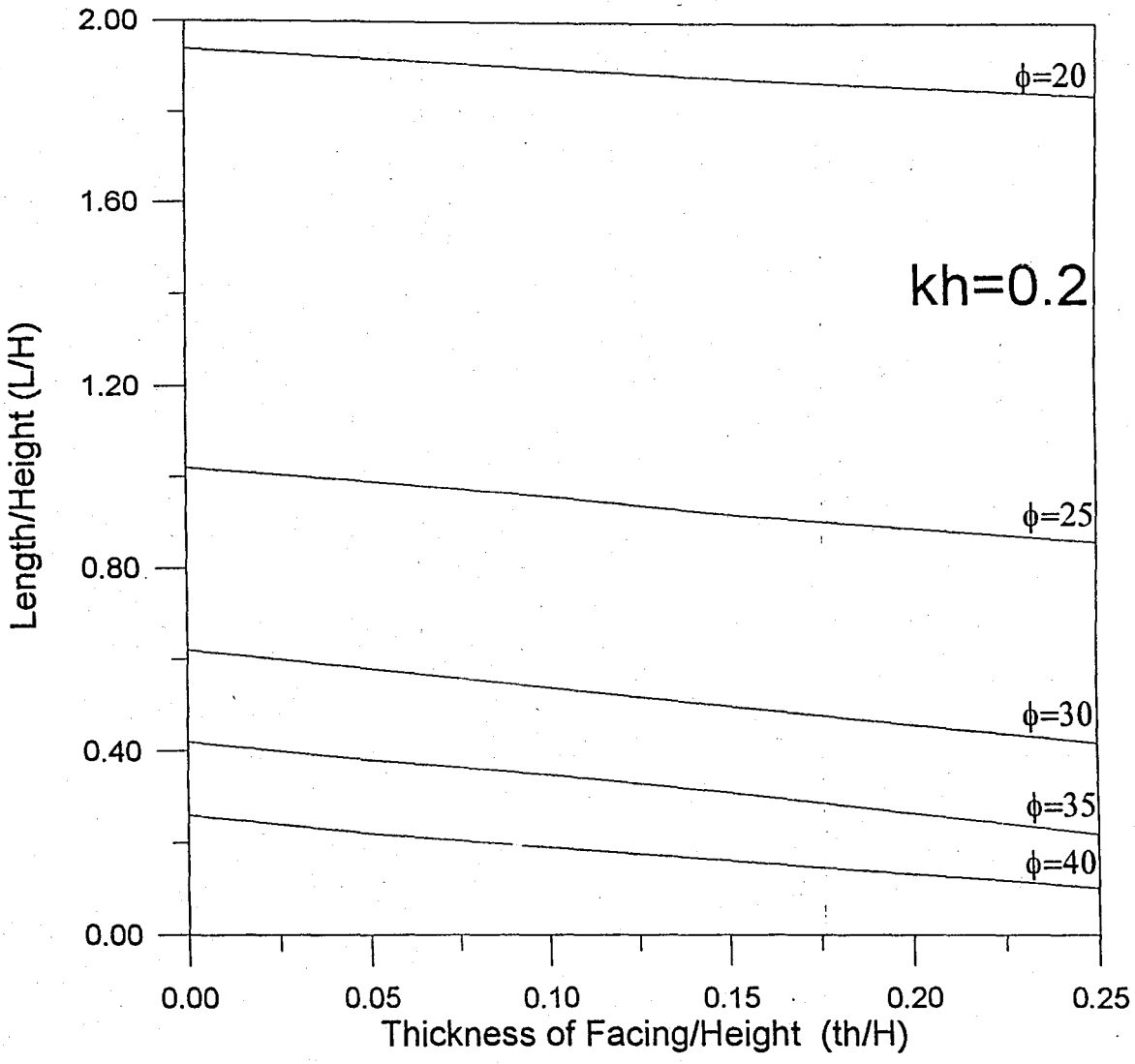

FIGURE 6.13 Length of reinforcements over Height for different soil types ($k_h = 0$)

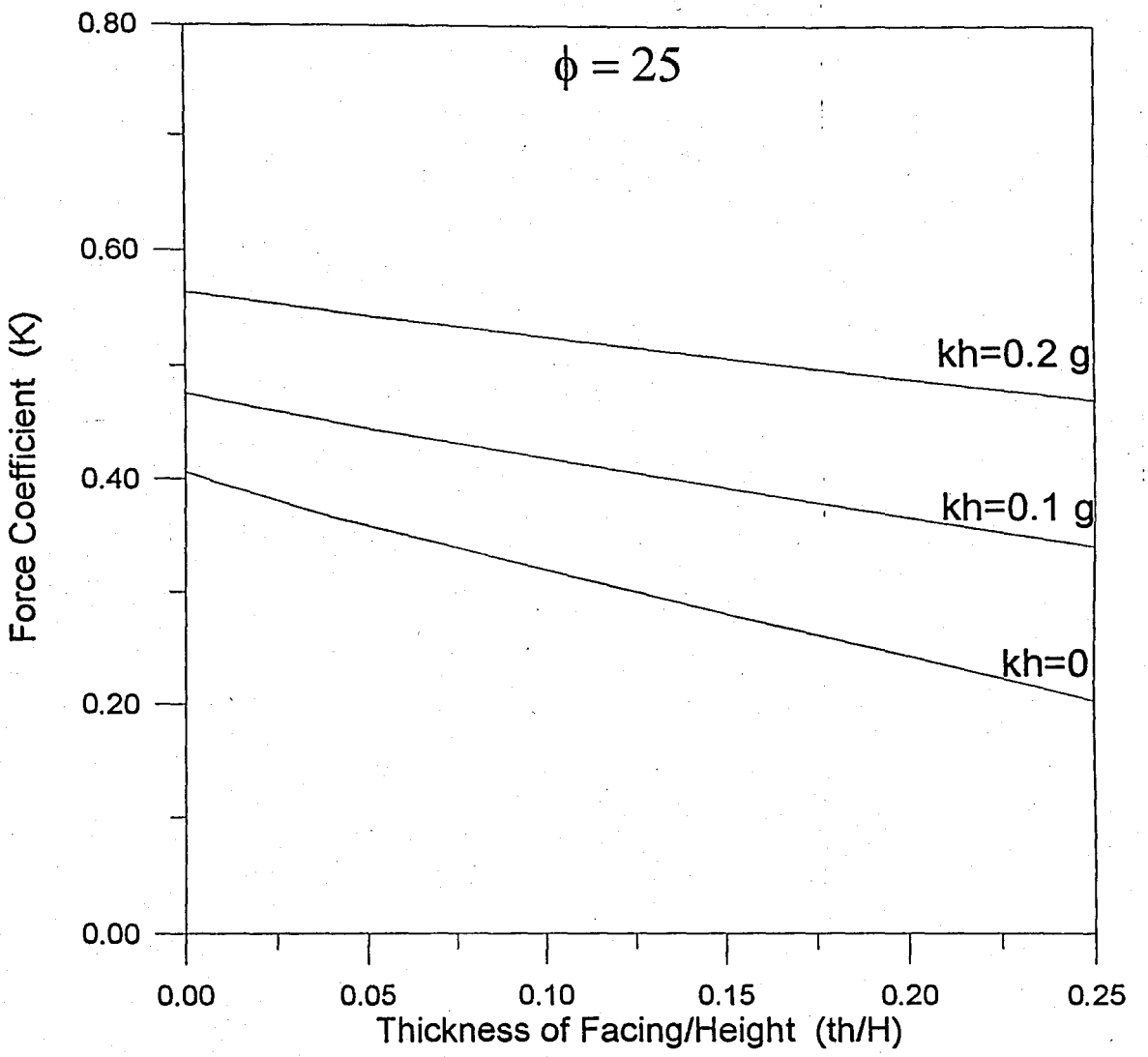

FIGURE 6.14 Comparison of force coefficients for different horizontal accelerations

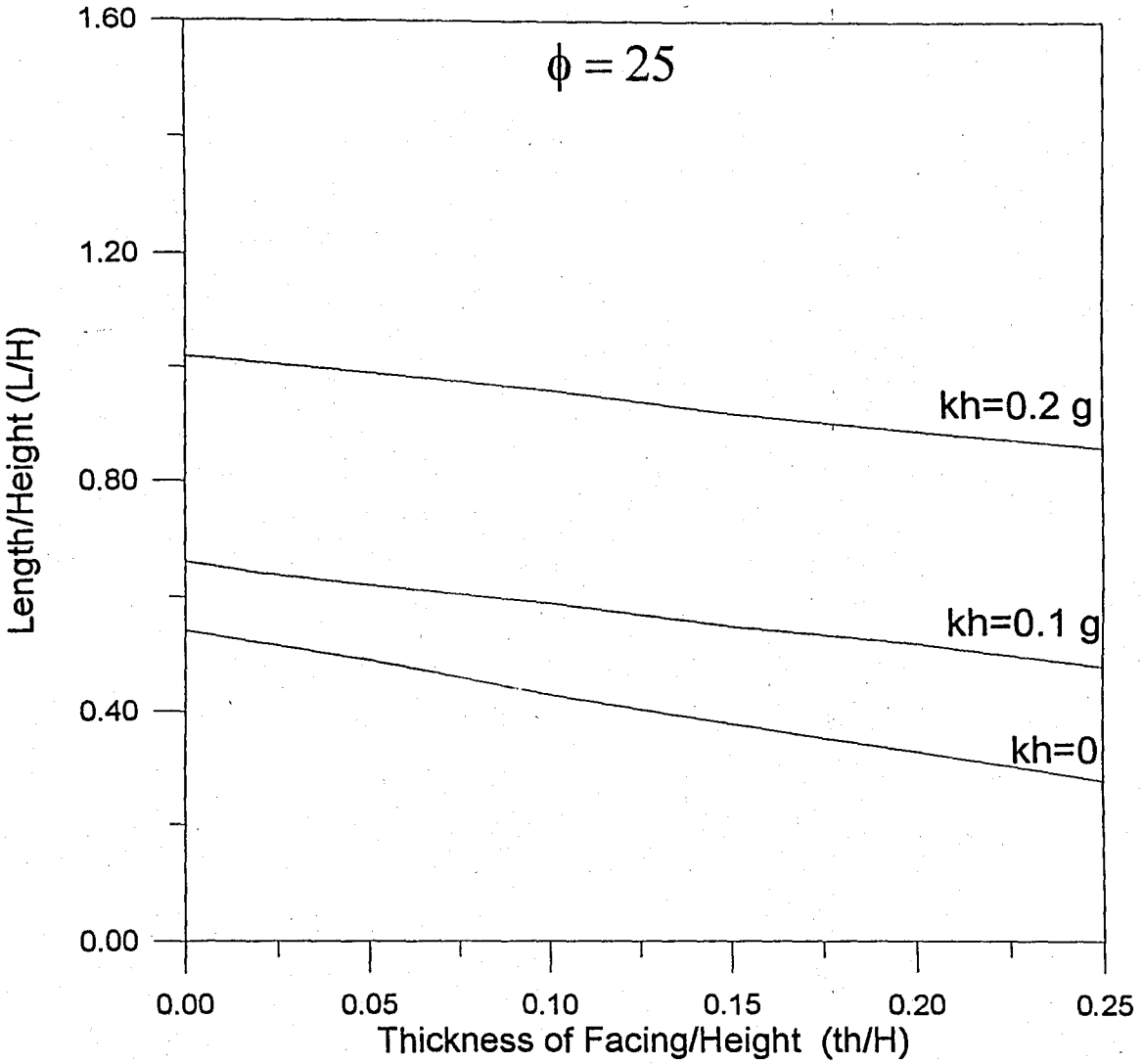

FIGURE 6.15 Comparison of Length / Height ratios for different horizontal accelerations

6.3 Summary

This study shows that the behavior of geosynthetic reinforced earth retaining walls is rather complex. So estimated stresses and deformations did not fit exactly the measured data.

Soil material properties and relevant soil reinforcement interaction parameters as data for the finite element analysis can not be determined precisely so as to produce healthy results for Finite Element Analysis either.

The currently used design method, is commonly based on restrictive assumptions pertaining to the state of stress in the soil or limit equilibrium. This leads to a very conservative design. Design of geosynthetic reinforced earth retaining walls should verify combined effect of geotextiles as reinforcement and permeable fabrics.

Attention and enough care must be given to the system as a whole. In order to have a stable reinforced wall, it is not enough to reinforce it arbitrary. Choosing good quality backfill, improving the foundation soil as well careful handling and placement of reinforcement, providing some type of facing are all very important factors during the construction. Quality control of every item used while and after construction should be checked.

7 CONCLUSIONS

In this study the performance of a geotextile reinforced wall was studied and compared to the results of a Finite Element Analysis. The Kilyos wall is unique in its focus on field measurements, and is the first known reinforced wall where the backfill consists of lime treated clay.

Clayey soils can be efficiently used as backfill for reinforced structures if the engineering characteristics are improved by appropriate treatment, and lateral drainage is provided by a suitable reinforcement type. The use of fine grained materials in reinforced soil structures will reduce the cost of projects that would otherwise require granular material to satisfy current specifications, specially if granular backfill has to be transported from a long distance.

It is noticed that the addition of lime to the clay improved its workability. This is observed clearly while mixing and transporting and compacting the mix. Also lime addition increased the cohesion of the soil, which played an important role in increasing the shear resistance of the wall.

The reinforced soil retaining structure stood for more than two years under all atmospheric conditions with and without the surcharge load. This proves that weather conditions does not affect the stability of reinforced walls under these types of conditions.

It was possible to increase the surcharge load up to three times more than typical traffic load. This suggest that the typical traffic surcharge loads are light to be considered for the design of reinforced walls. In other words, the contribution from the traffic load is small to the over all safety factors.

Good structural performance is strongly dependable on maintaining a low water content in the cohesive soil. The permeable geosynthetics embedded in clayey backfills function not only as reinforcements but also as lateral drains, thus increasing the stability of the wall. Therefore there is a strong evidence that permeable polymeric reinforcement can effectively reinforce the clay structures and increase their stability. Therefore, it is important to produce high strength geotextile with high in plane permeability as well, used as reinforcements and help in dissipation of the pore water pressure and thus increase the stability.

In the design, a constant distribution of vertical stress was assumed and measurements provided evidence to the contrary. Finite element studies and real measurements of stresses in the wall indicated nonlinear behavior. The vertical pressure along the first and second layers of the backfill are not uniformly distributed. Lateral pressures were almost constant. No conclusive data indicate a definite pattern of pressure distribution. Deviation may be due to the effect of high cohesion resulted from lime treatment, non homogeneous backfill or residual stresses created by the compaction procedure.

More field data are required to determine the relationship between vertical and lateral pressure distributions and the influencing factors such as backfill type, design and construction and the stiffness of the reinforcing system.

The developed coils system used in this study to measure deformations did not provide a sufficiently broad data base from which to draw a conclusion about the nature of the deformations inside the wall. This was due to non rapid construction of the wall which allowed the consolidation to complete immediately leaving so little deformation to occur in the long term which were beyond the sensitivity of the coil system.

Although the procedure used in the design represent the state of the art, it did not prove to be predicting well how the wall would perform in reality. The current used design methods do not account for the interaction of applied surcharge loads, transmissivity of the geosynthetic reinforcements and failure criteria for clay soils treated and untreated with lime. The current design appears to be conservative and it is important therefore, to develop

refined and improved methods, which account for all of the above factors which may lead to more economical designs of such walls.

From a qualitative stand point, both instrumentation data and observations of the actual wall performance indicated that the wall performed its intended function. The results of this study have substantiated the excellent performance of the reinforced wall and showed that lime treated clayey soils can be used to construct satisfactory reinforced soil retaining structures. The evaluations show also that proper design and construction can result in stable, durable and more economical earth structures.

Computer models of two-wedge failure mechanism based on limit equilibrium considerations has been successfully used in the design of reinforced retaining walls. This approach allows to take into account different loading and seismic forces, providing solutions for several practical situations.

The presented charts for designing reinforced vertical walls with concrete facing demonstrated analytically that the facing rigidity plays an important role in increasing the stability and produce economical designs, even under seismic loading conditions.

Current design methods should be modified or adjusted to account for the facing system. Future studies should concentrate on the facing effect since the facing may reduce the lateral earth pressure. This will result in a less reinforced structure. The load transferred to the wall face with different facing systems for vertical walls as well as near vertical walls and slopes should be quantified.

REFERENCES

Allen, T. M. and R. D. Holtz, "Design of Retaining Walls Reinforced with Geosynthetics," *Proceedings of the congress sponsored by the Geotechnical Engineering Division of the American Society of Civil Engineering*, Mclean, F., Campbell, D. A. and D. W. Harris, Editors, Vol. 2, pp. 970 - 987, Boulder, Colorado, 1991

Barrett, B., "Retaining walls," A Design Primer: Geotextiles and Related Materials, First Edition, Industrial Fabric Association International, St. Paual, pp. 40 - 48, 1992.

Billiard, J. W. and J. T. H. Wu, "Load Test of a Large Scale Geotextile Reinforced Retaining wall," *Proceedings of the Geosynthetics '91 International Conference*, Atlanta, 26 - 28 February 1991, Vol. 2 pp. 537 - 548, Industrial Fabrics Association International, Atlanta, 1991.

Brandl, H. "Alteration of Soil Parameters by Stabilization with Lime," *Proceedings of the Tenth International Conference of Soil Mechanics and Foundation Engineering*, ICSMFE, Stockholm, Vol. 3, pp. 587-594, 1981.

Broms, B. B. "Design of Fabric Reinforced Retaining Structures," *Proceedings of the International Symposium on Earth Reinforcement*, ASCE, Pittsburgh, pp. 282 - 290, 1978.

Boden, J. B., Irwin, H. M. and R. G. Pocock, "Instruction of Experimental Reinforced Earth Wall at the T. R. R. L.," *Symposium on Reinforced Earth and other Soil Composite Techniques*, Edinburgh, Scotland, 1977.

Bolton, M. D. and P. L. R. Pang "Collapse Limit States of Reinforced Earth Retaining Walls," Geotechnique 32, No. 4, pp. 349 - 367, 1982.

Bolton, M. D., Choudhury, S. P. and P. L. Pang, "Reinforced Earth Walls, a Centrifugal Model Study," *Proceedings of the Conference sponsored by the Geotechnical Engineering Division of the American Society of Civil Engineers on Reinforced Earth,* Pittsburgh, Pennsylvania, pp. 252 - 281, 1978.

Bonaparte, R., Holtz, R. D. and J. P. Giroud "Soil Reinforcement Design Using Geotextiles and Geogrids," Geotextile Testing and the Design Engineer, ASTM STP 952, American Society for Testing and Material Philadelphia, pp. 69 - 116, 1987.

Boul, I. *Personnel Communications,* 1993.

Bulut, M., "Determining Mechanical Properties of Lime Stabilized Clay," MS Thesis, Boğaziçi University, 1986.

Burwash, W. J. and J. D. Frost, "Case History of a 9 m High Geogrid Reinforced Retaining Wall Backfilled with Cohesive Soil," *Proceedings of the Geosynthetics '91 International Conference,* Atlanta, 26 - 28 February 1991, Vol. 2 pp. 485 - 493, Industrial Fabrics Association International, Atlanta, 1991.

Christopher, B. R. and R. D. Holtz *Geotextile Design and Construction Guidelines Manual,* Federal Highway Administration, Washington, DC, 1985.

Christopher, B. R., Gill, S. A., Giroud, J. P., Juran, I., Mitchell, J. K., Schlosser, F., and Dunnicliff, J., *Reinforced Soil Structures, Design and Construction Guidelines*, Volume I and II, Federal Highway Administration, Report No: FHWA-RD-89-043, Washington, DC, 1990.

Chua, L. O., Desoer, C. A. and E. S. Kuh *Linear and Nonlinear Circuits,* McGraw Hill, New York, 1987.

Claybourn, A. F. and J. T. H. Wu, "Case History of Geosynthetic Reinforced Soil Walls," *Proceedings of the Geosynthetics '91 International Conference,* Atlanta, 26 - 28

February 1991, Vol. 2 pp. 549 - 559, Industrial Fabrics Association International, Atlanta, 1991.

Claybourn, A. F. and J. T. H. Wu "Failure Loads of the Denver Walls by Current Design Methods," *Proceedings of the International Symposium on Geosynthetic Reinforced Soil Retaining Walls,* Denver, Colorado, 8 - 9, August 1991, pp. 61-77, A. A. Balkema, 1992.

Collin, J. G. " Earth Wall Design," Ph.D. Dissertation, University of California, 1986.

Edinçliler, A. *Personnel Communications,* 1994.

Floss, R. and B. R. Thamm, "Field Measurements of a Reinforced Earth Retaining Wall Under Static and Dynamic Loading," *International Conference on Soil Reinforcement; Reinforced Earth and other Techniques,* Vol. 3, pp. 183 - 188, Paris, France, 1979.

Goodings, D. J. "Effects of poorly draining backfill on geotextiles for earth reinforcement of vertical soil slopes," Final report to the Maryland Department of Transportation State Highway Administration Bureau of Research, 1989.

Güler, E., "Lime Stabilized Cohesive Soil as a Fill for Geotextile Reinforced Structures," *Proceedings of the Forth International Conference on Geotextiles, Geomembranes and Related Products,* The Hague, 28 May - 1 June 1990, Vol. 1, pp. 39-44, A. A. Balkema, New York, 1990.

Güler, E. and D. J. Goodings "Centrifuge Models of Clay Lime Reinforced Soil Walls," *Proceedings of the Conference sponsored by the Geotechnical Engineering Division of the American Society of Civil Engineers,* New Orleans, 25-28 February 1992, Geotechnical Special Publications No: 30, Vol. 2, pp. 1249-1260, ASCE, 1992.

Ismeik, M., "A Study on Slope Stability Analysis of Geosynthetic Reinforced Embankments," MS. Thesis, Boğaziçi University, 1992.

Iyidil, H. A. "Effect of Lime on Geotextiles," MS. Thesis, Boğaziçi University, 1988.

Jaber, M. B. "Behavior or Reinforced Soil Walls in Centrifuge Model Tests," Ph.D. Dissertation, University of California at Berkeley, 1989.

Jewell, R. A., Paine, N. and R. I. Woods "Design Methods for Steep Reinforced Embankments," *Proceedings of the Symposium on Polymer Grid Reinforcement*, pp. 70 - 81, Thomas Telford, London, 1984.

Jewell, R. A. "Revised Design Charts for Steep Reinforced Slopes," *Proceedings of the Symposium on Reinforced Embankments: Theory and Practice in the British Isles*, Cambridge, pp. 1- 30, Thomas Telford, London, 1990.

Juran, I. and F. Schlosser, "Theoretical Analysis of Failure in Reinforced Earth Structures," *Proceedings of the Conference sponsored by the Geotechnical Engineering Division of the American Society of Civil Engineers on Reinforced Earth*, Pittsburgh, Pennsylvania, pp. 528 - 555, 1978.

Koerner, R. M., *Designing with Geosynthetics*, second edition, Prentice-Hall, New York, 1994.

Lee, K. L., Adams, B. D. and J. M. D. Vagneron, "Reinforced Earth Retaining Walls," *Journal of Soil Mechanics and Foundation Engineering Division*, American Society of Civil Engineering, Vol. 99, No. 10, pp. 745 - 764, 1973.

Leshchinsky, D. and E. B. Perry, "A Design Procedure for Geotextiles Reinforced Walls," *Proceedings of the International Conference of Geosynthetics '87*, New Orleans, Vol. 1 pp. 95 - 107, Industrial Fabrics Association International, St. Paul, 1987.

Mitchell, J. K. "Soil Improvement, State of the Art Report," *Proceedings of the Tenth International Conference of Soil Mechanics and Foundation Engineering*, ICSMFE, Stockholm, Vol. 4, pp. 509-565, 1981.

Mitchell, J. K. and W. C. B. Villet "Reinforcement of Earth Slopes and Embankments," *National Cooperative Highway Research Program,* Report No: 290, pp. 323-330, Transportation Research Board, Washington DC, 1987.

Murata, O., Tateyama, M., Tatsuoka, F., Nakamura, K. and Y. Tamura, "A Reinforced Method for Earth Retaining Walls using Short Reinforcing Membranes and a Continuous Rigid Facing," *Proceedings of the congress sponsored by the Geotechnical Engineering Division of the American Society of Civil Engineering*, Mclean, F., Campbell, D. A. and D. W. Harris, Editors, Vol. 2, pp. 935 - 946, Boulder, Colorado, 1991

Murata, O., Tateyama, M. and F. Tatsuoka " Loading Tests of Geosynthetic Reinforced Soil Retaining Walls and Their Stability Analysis," *Proceedings of the International Symposium on Earth reinforcement Practice,* Kyushu, 11 - 13 November 1992, Vol. 1, pp. 385 - 390, A. A. Balkema, New York, 1993.

Murata, O., Tateyama, M. and F. Tatsuoka "Shaking Table Tests on a Large Geosynthetic Reinforced Soil Retaining Wall Model," *Proceedings of the Seiken Eleventh International Symposium on Recent Case Histories of Permanent Geosynthetic Reinforced Soil Retaining Walls,* Tokyo, 6 - 7 November 1992, pp. 259 - 264, A. A. Balkema, New York, 1994.

Najefzadeh, G. R. "Reinforced Earth Retaining Structures," MS. Thesis, Boğaziçi University, 1981.

Porbaha, A., "Centrifuge Modeling of Geotextile Reinforced Cohesive Soil Retaining Systems," Ph.D. Dissertation, University of Maryland, 1994.

Schmertmann, G. R., Bonaparte, R., Chouery, V. C. and R. J. Johnson, "Design Charts for Geogrid Reinforced Soil Slopes," *Proceedings of the International Conference of Geosynthetics '87,* New Orleans, Vol. 1 pp. 108 - 120, Industrial Fabrics Association International, St. Paul, 1987.

Steward, J. E., Williamson, R. and J. Mohney "Guidelines for Use of Fabrics inn Construction and Maintenance of Low Volume Roads," Earth Reinforcement , Force Service Portland, Oregon, pp. 87 - 95, 1977

Tateyama, M., Murata, O., Watanabe, K. and F. Tatsuoka "Geosynthetic Reinforced Retaining Walls for Bullet Train Yard in Nagoya" *Proceedings of the Seiken Eleventh International Symposium on Recent Case Histories of Permanent Geosynthetic Reinforced Soil Retaining Walls*, Tokyo, 6 - 7 November 1992, pp. 141 - 150, A. A. Balkema, New York, 1994.

Tatsuoka, F., Murata, O. and M. Tateyama "Permanent Geosynthetic Reinforced Soil Retaining Walls Used for Railway Embankments in Japan" *Proceedings of the International Symposium on Geosynthetic Reinforced Soil Retaining Walls*, Denver, 8 - 9 August 1991, pp. 101 - 130, A. A. Balkema, New York, 1992.

Tatsuoka, F. "Keynote Lecture: Roles of Facing Rigidity in Soil Reinforcing," *Proceedings of the International Symposium on Earth reinforcement Practice*, Kyushu, 11 - 13 November 1992, Vol. 2, pp. 831 - 870, A. A. Balkema, New York, 1993.

Task Force 27 Report, AASHTO / AGC / ARTBA, Joint Committee, "*In Situ Soil Improvement Techniques: Design Guidelines for use of Extensible Reinforcements (Geosynthetics) for Mechanically Stabilized Earth Walls in Permanent Applications*," Washington, D. C., pp. 28 - 38, 1990.

Tompkins, W. J. and T. G. Webster *Interfacing Sensors to the IBM PC*, Prentice-Hall, New York, 1988.

Vidal, H., "The Principal of Reinforced Earth," Highway Research Record 282, Highway Research Board, National Research Council, Washington, DC, 1969.

Wu, J. T. H., "Construction and Instrumentation of Denver Walls," *Proceedings of the International Symposium on Geosynthetic Reinforced Soil Retaining Walls,* Denver, Colorado, 8 - 9, August 1991. pp. 21 - 30, A. A. Balkema, 1992 a.

Wu, J. T. H., "Measured Behaviour of the Denver Walls," *Proceedings of the International Symposium on Geosynthetic Reinforced Soil Retaining Walls,* Denver, Colorado, 8 - 9, August 1991, pp. 31 - 41, A. A. Balkema, 1992 b.

Wu, J. T. H., Qi, X., Chou, N., Ksouri, I. and M. B. Helwany "Comparisons of Predications for the Denver Walls," *Proceedings of the International Symposium on Geosynthetic Reinforced Soil Retaining Walls,* Denver, Colorado, 8 - 9, August 1991, pp. 43 - 60, A. A. Balkema, 1992.

REFERENCES NOT CITED

Britto, A. M. and M. J. Gunn *Critical State Soil Mechanics Via Finite Elements,* Ellis Horwood Limited, 1987

Britto, A. M. and M. J. Gunn *User's and Programmer's Guide to CRISP,* Vol. 1,2, University of Cambridge , 1987.

Cascone, E., Maugeri, M. and E. Motta "Seismic Design of Earth Reinforced Embankments," *Proceedings of the First International Conference on Earthquake Geotechnical Engineering,* Tokyo, 14- 16 November 1995, Vol. 2, pp. 1129 - 1134, A. A. Balkema, New York, 1995.

Durukan, Z. S., "A study on Reinforced Soil Retaining Walls," MS Thesis, Boğaziçi University, 1986.

Giroud, J. P., "Geotextiles and Related Products," in S. M. Sayed (Editor), *Geotechnical Modeling and Applications,* pp. 355-390, Houston: Gulf Publishing Company, 1986.

Görken, N. Y., "Comparison of Different Design Procedures Used in Reinforced Slope Design," MS. Thesis, Boğaziçi University, 1995.

Hausmann, M. R., *Engineering Principles of Ground Modification,* McGraw Hill Publishers, New York, 1990.

Organ, N. S., Innes, J., Hawker, B. H. and D. Ohagan, *Design Manual for Roads and Bridges,* HMSO Publishers, London, 1994.

Sen, P. C. *Principals of Electric Machines and power Electronics,* John Wiley, New York, 1989.

Serway, R. A. *Physics for Scientists and Engineers,* Sounders College Publishing, New York, 1990.

Tatsuoka, F., Koseki, J. and M. Tateyama "Performance of Geogrid Reinforced Soil Retaining Walls during the Great Hanshin Awaji Earthquake, January 17, 1995," *Proceedings of the First International Conference on Earthquake Geotechnical Engineering,* Tokyo, 14- 16 November 1995, Vol. 1, pp. 55 - 62, A. A. Balkema, New York, 1995.

Wu, J. T. H. *Design and Construction of Low Cost Retaining Walls; The Next Generation in Technology,* Colorado Transportation Institute, 1994

APPENDIX 1

Photographs

Photograph 1 Mixing the Soil with Lime

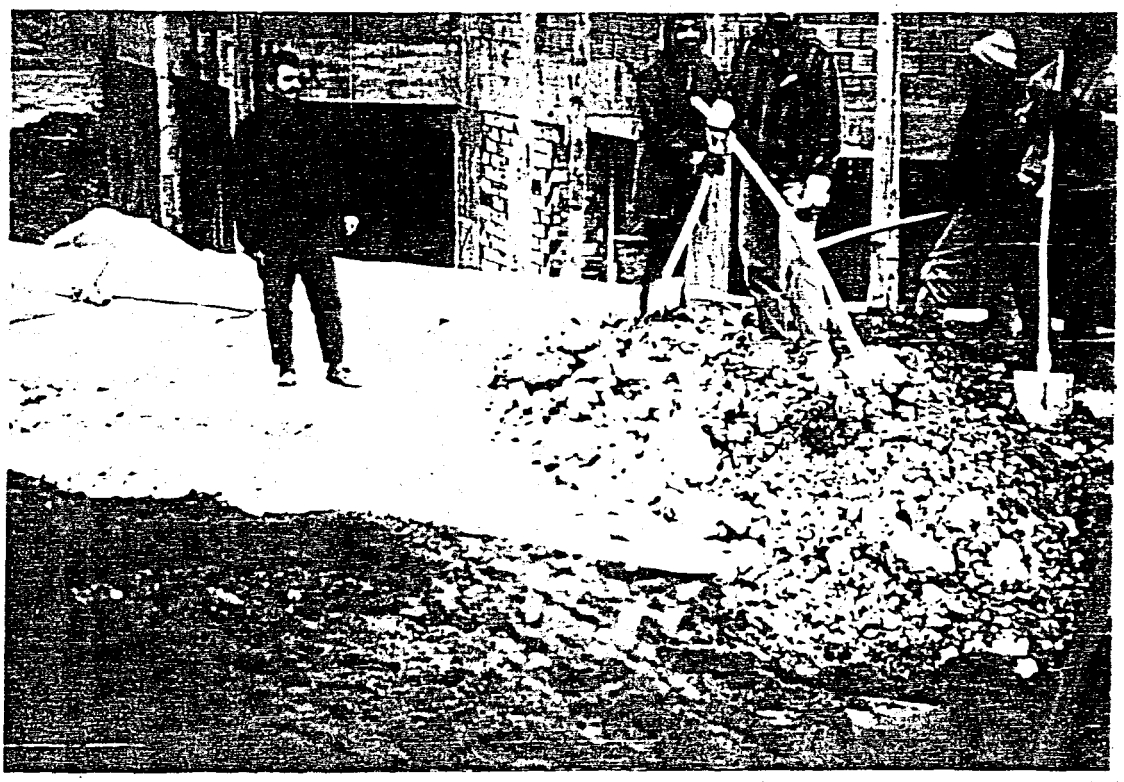

Photograph 2 Distributing the Mixed Soil over the Geotextile Layer

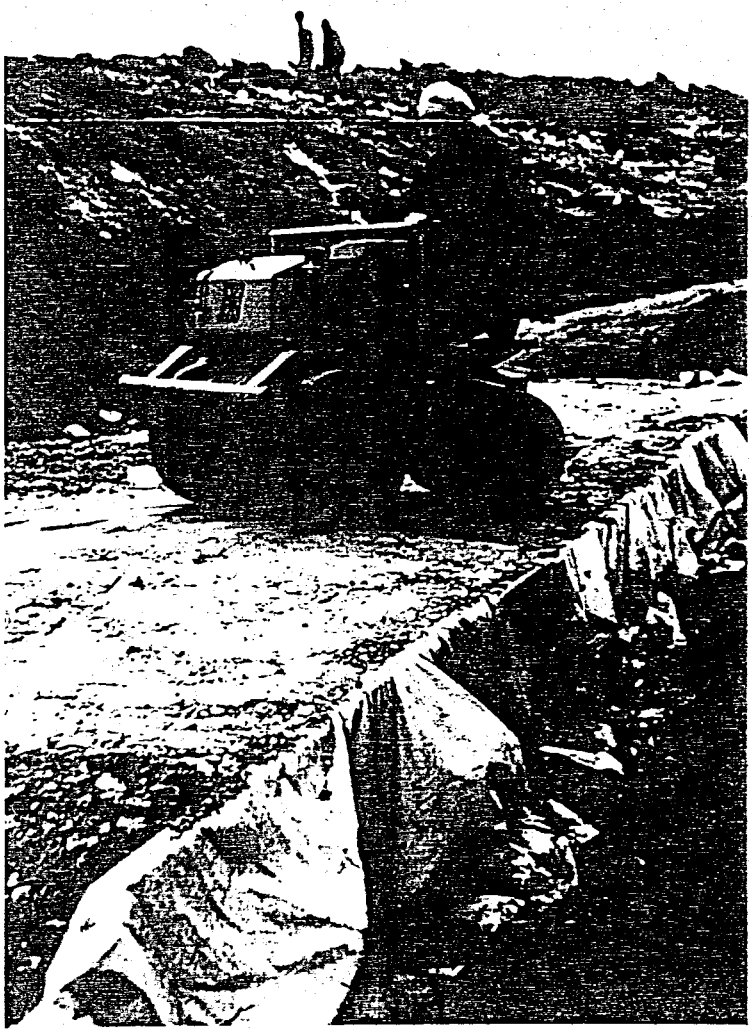

Photograph 3 Compacting the Layer by Using a Smooth Wheeled Roller

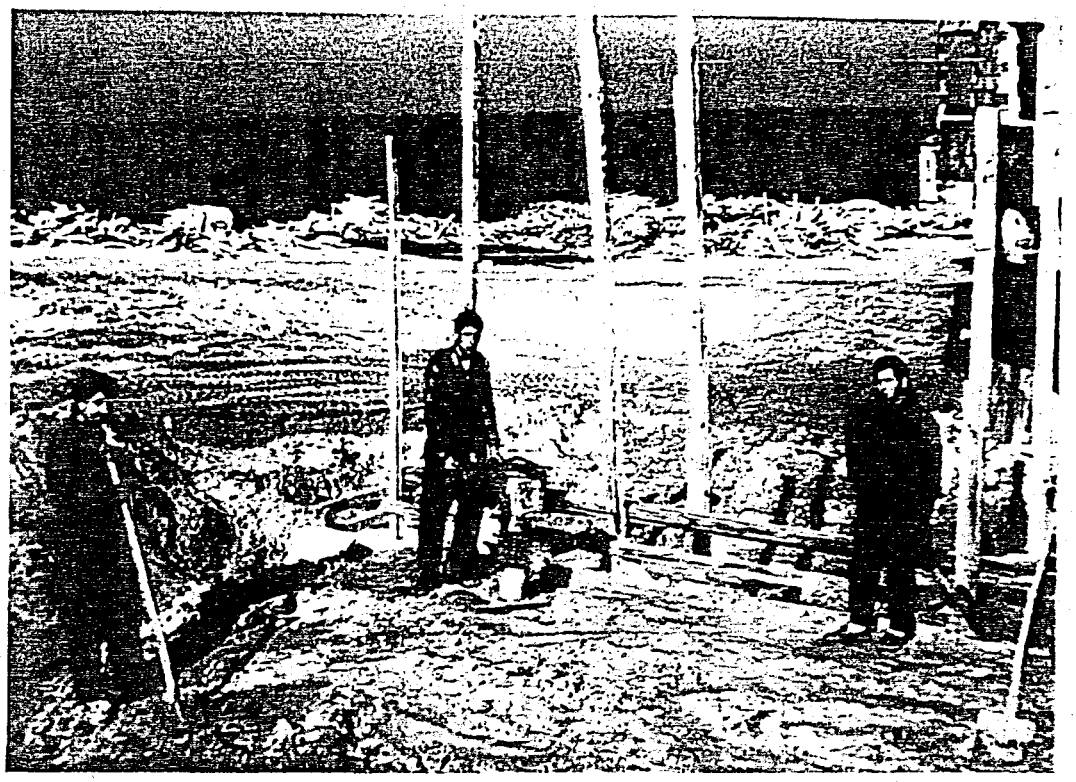

Photograph 4 Compacting the Layer by Using a Wacker Vibro Rammer Compactor

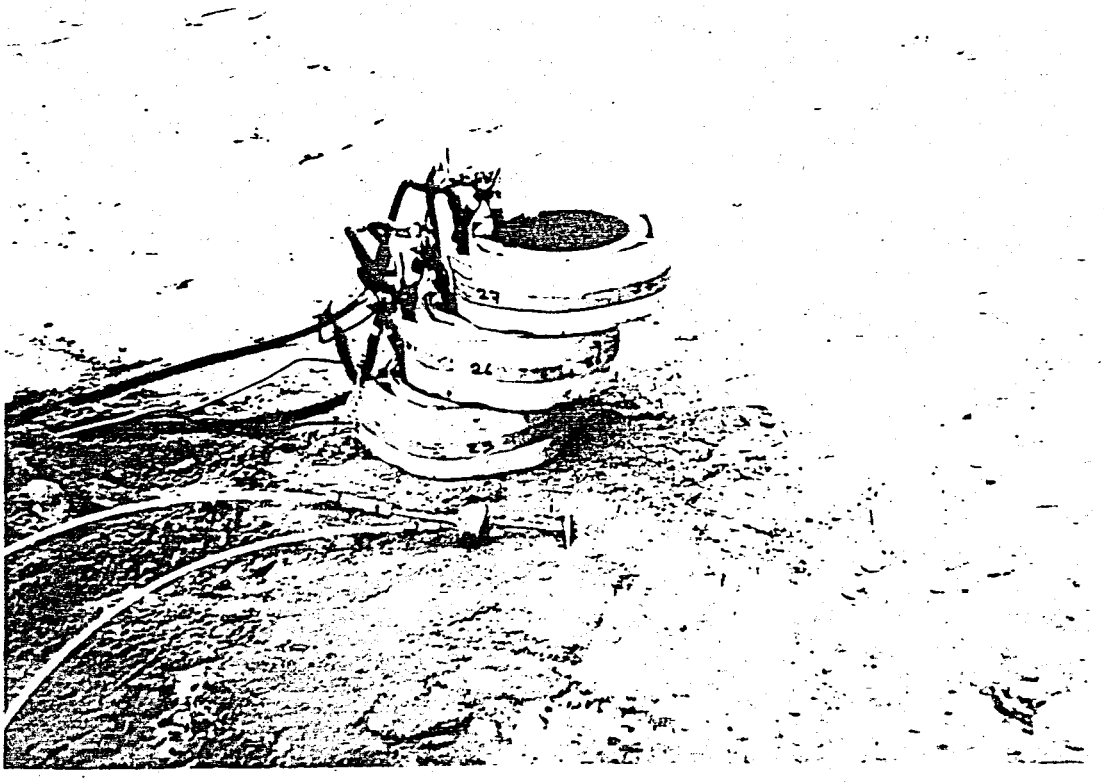

Photograph 5 The Coil Set and Glötzl Pressure Cell

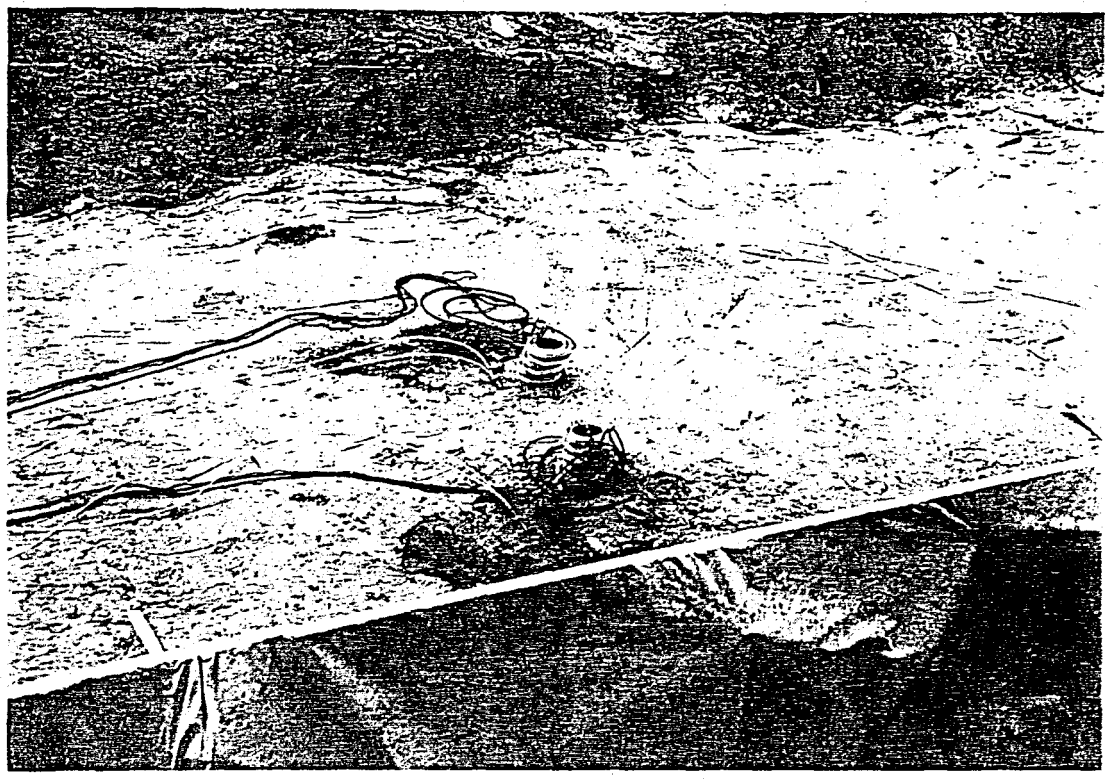

Photograph 6 Instrumenting the Coil Set and Glötzl Pressure Cell

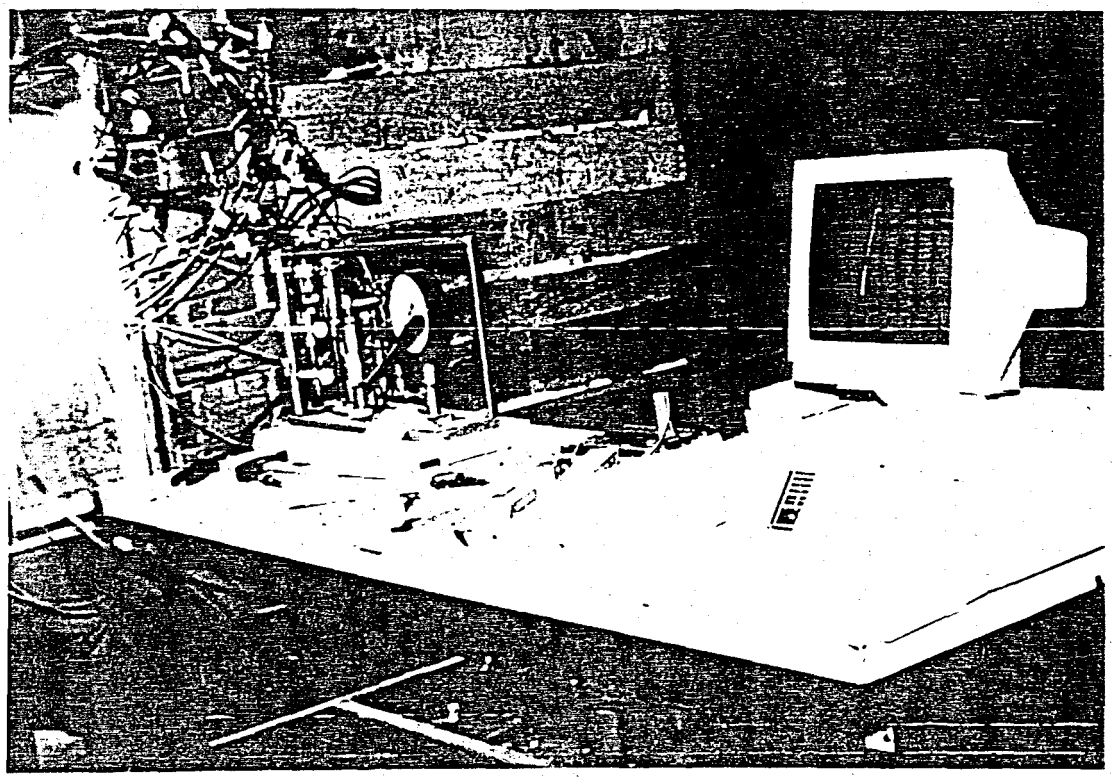

Photograph 7 The Computer Room Where all Measurements are Recorded

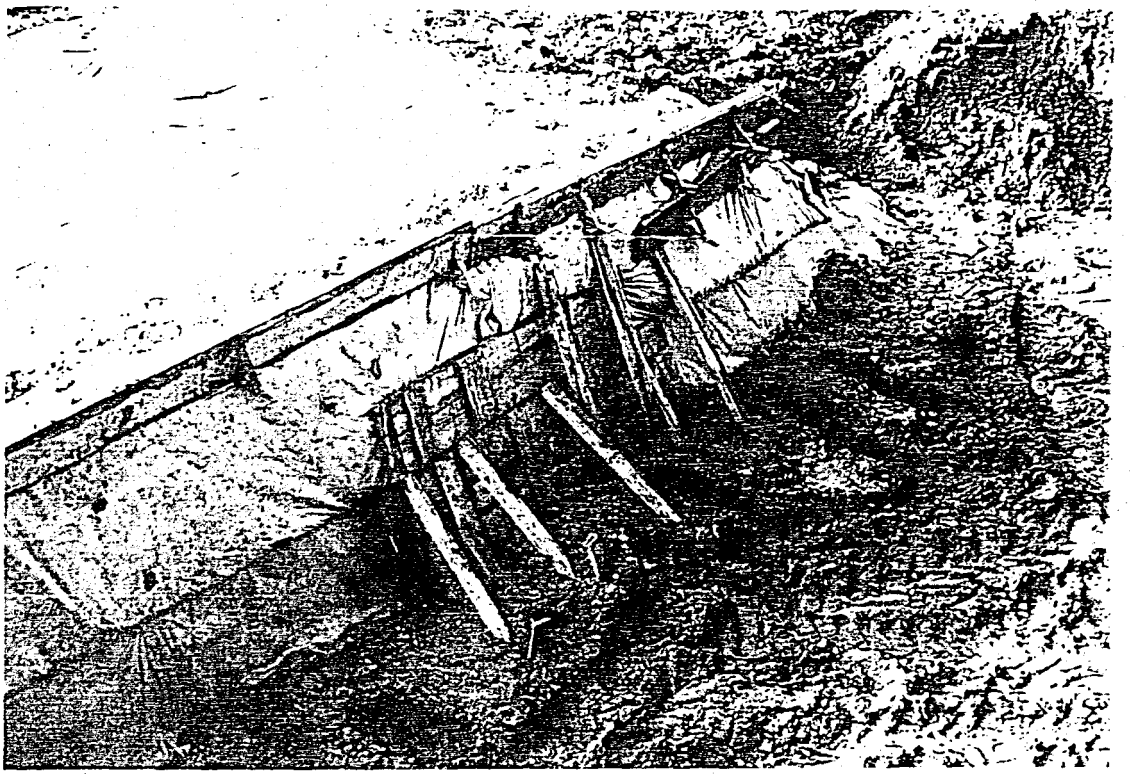

Photograph 8 II layer is completed

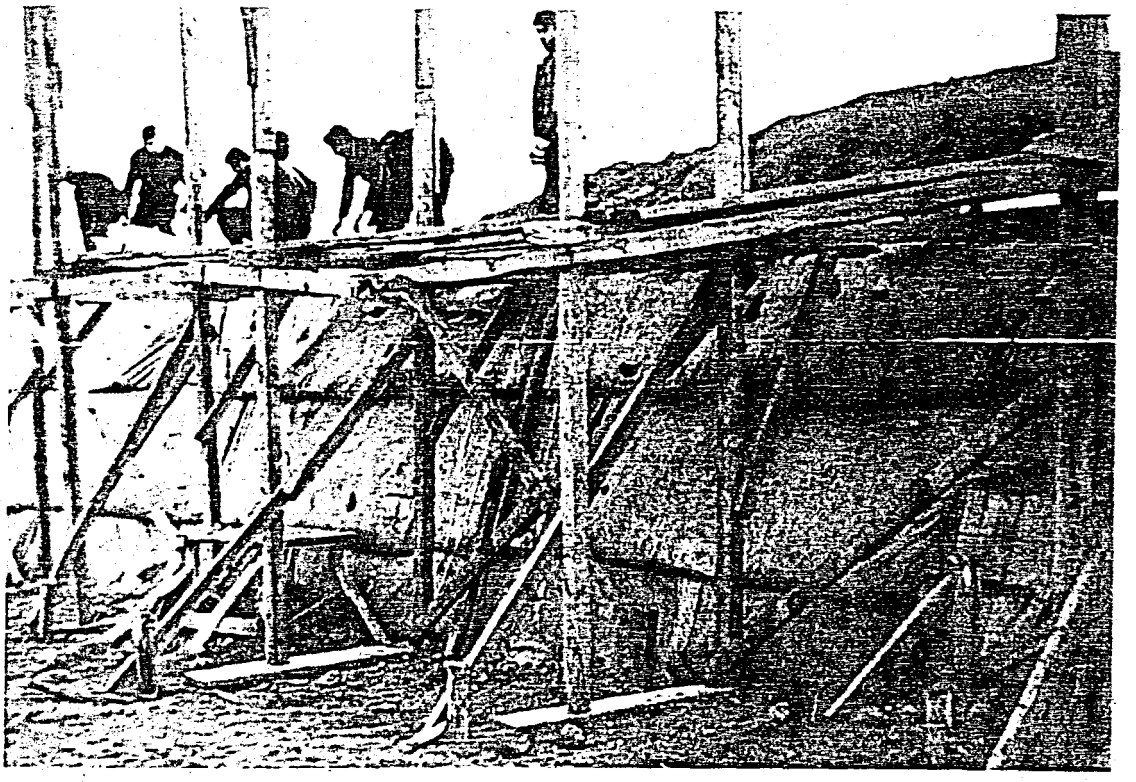

Photograph 9 III layer is completed

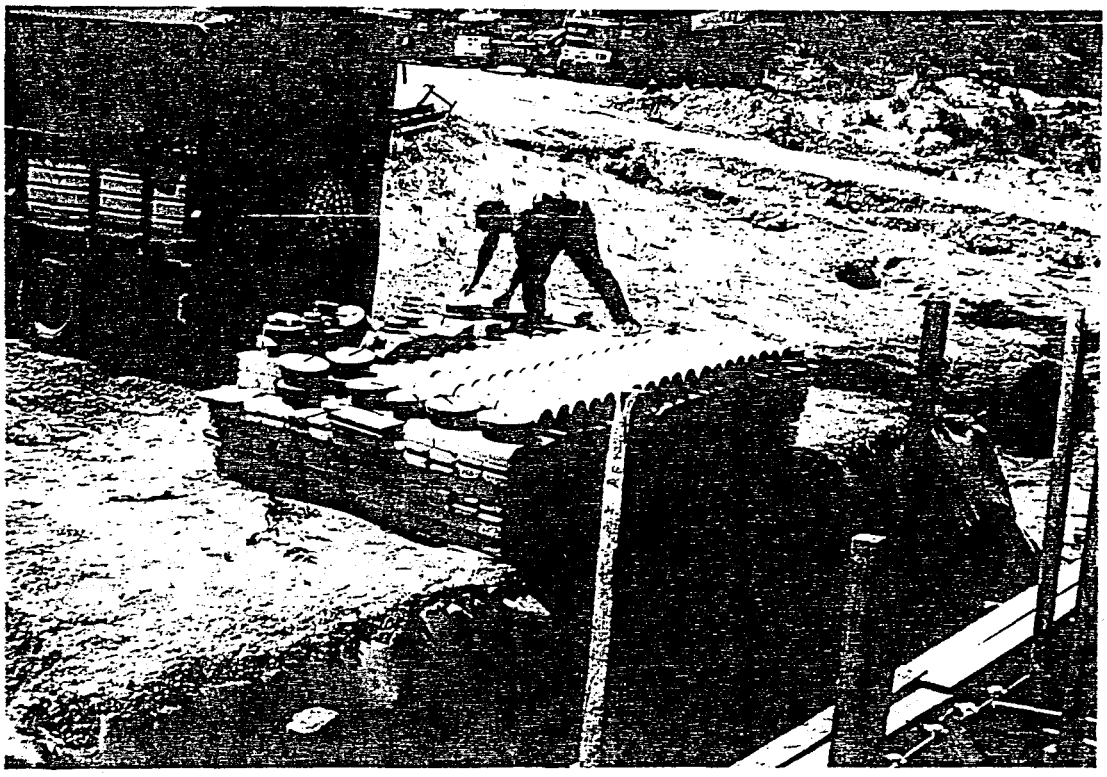

Photograph 10 The First Overloading Stage

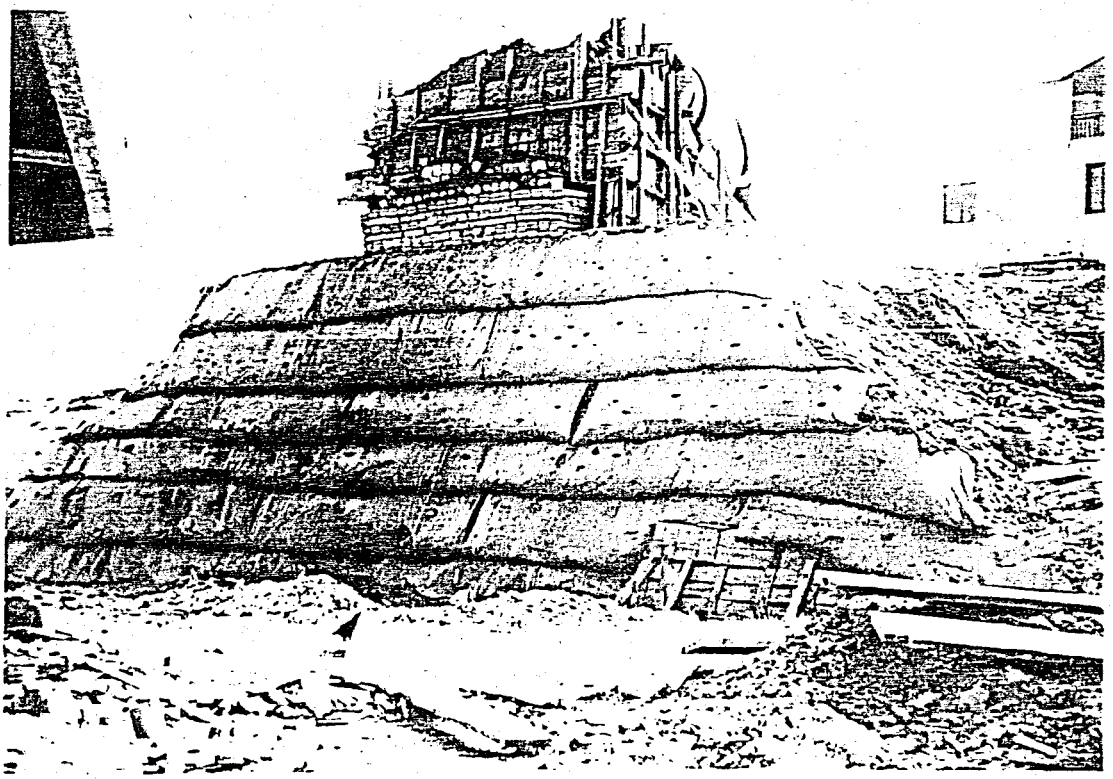

Photograph 11 The Instrumented Kilyos Wall with the Maximum Possible Surcharge Load

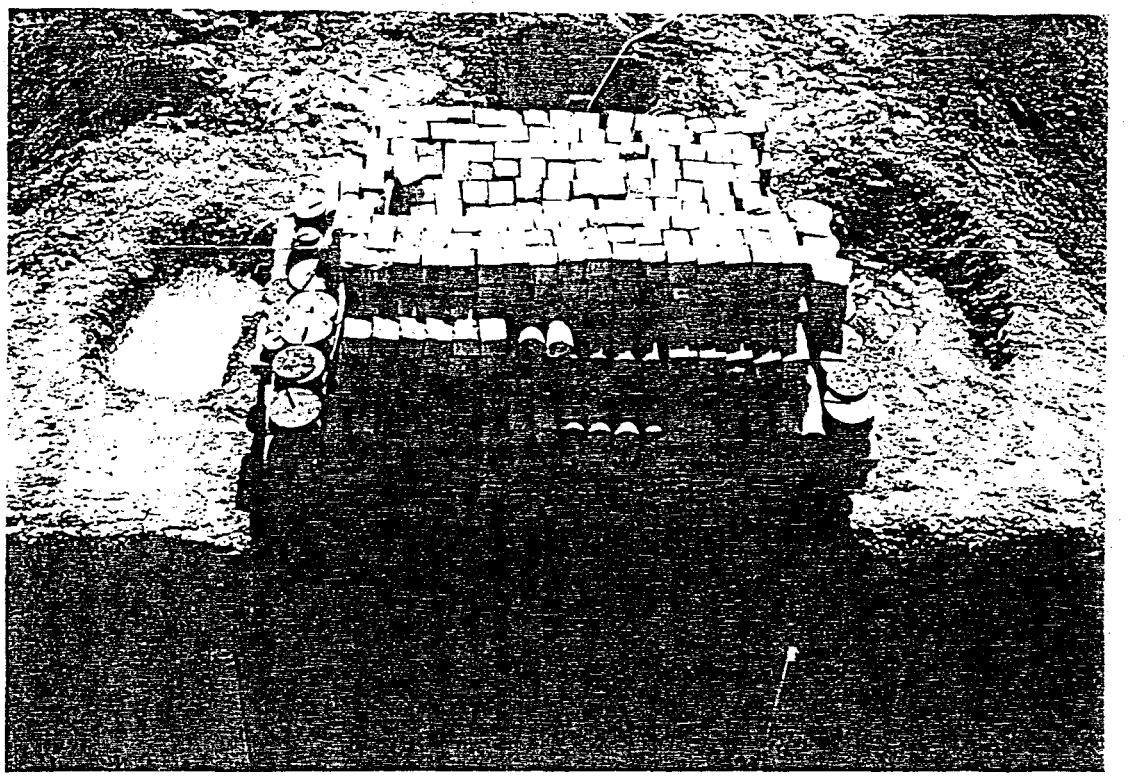

Photograph 13 Wetting the Soil by Continuos Flow of Water through the Excavated Holes

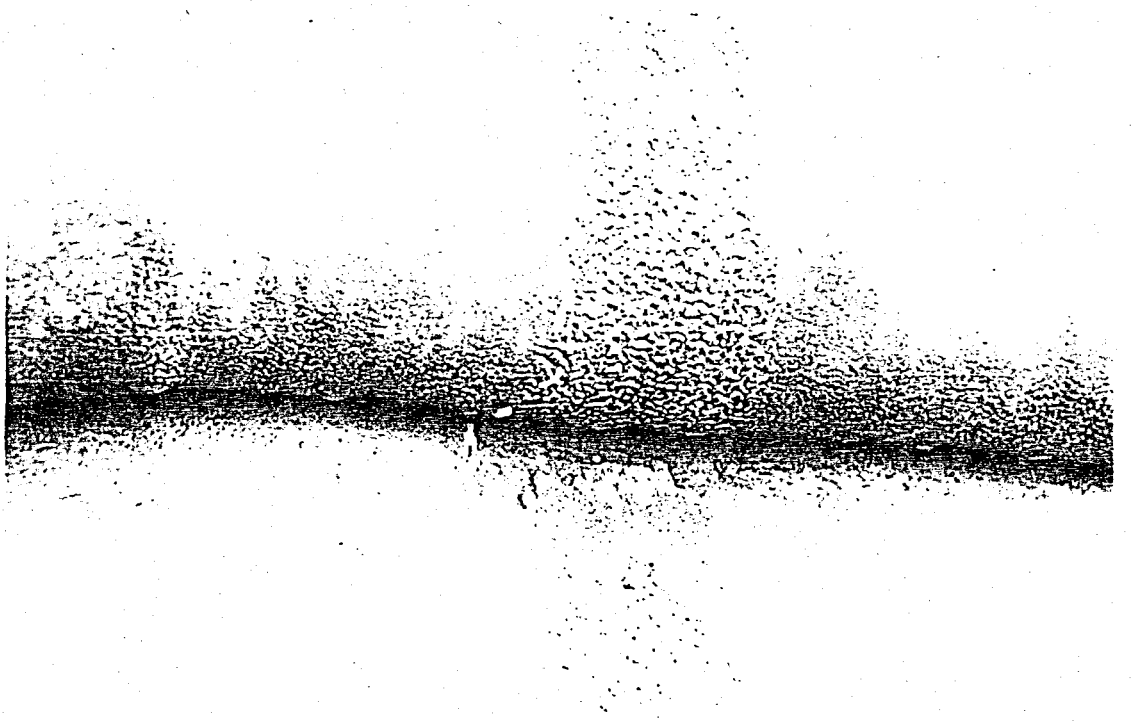

Photograph 14 The Horizontal Drainage of Water through the Geotextile Layer

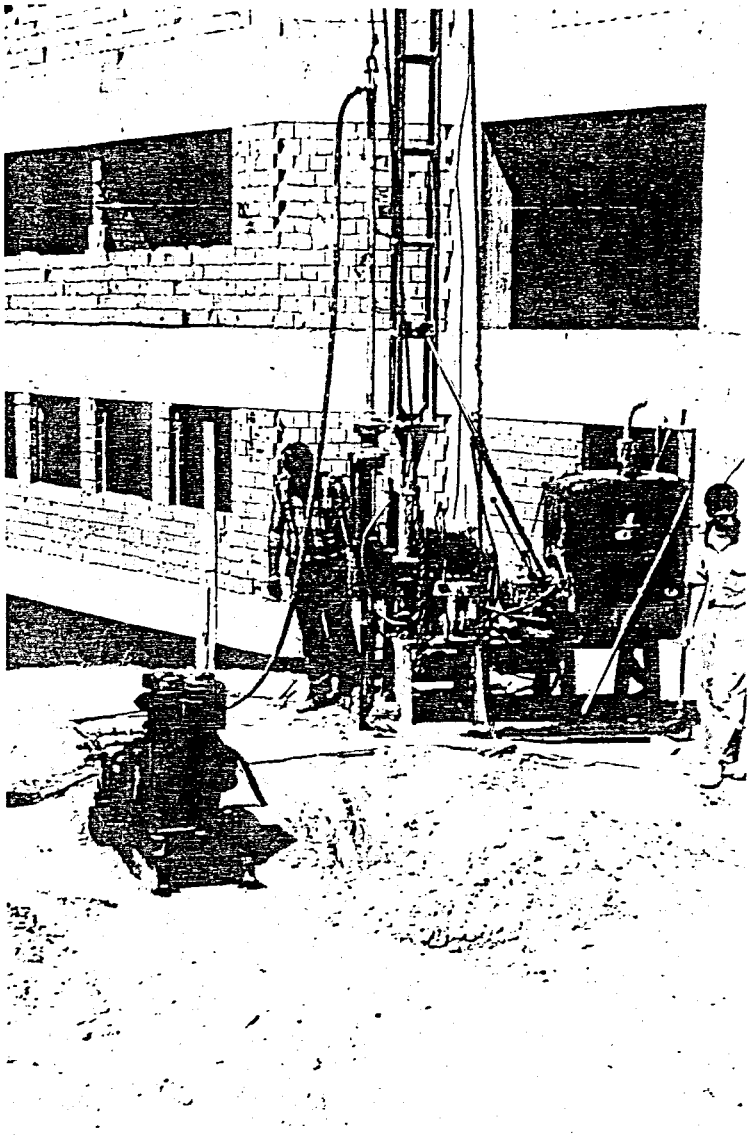

Photograph 12 Boreholes Sampling

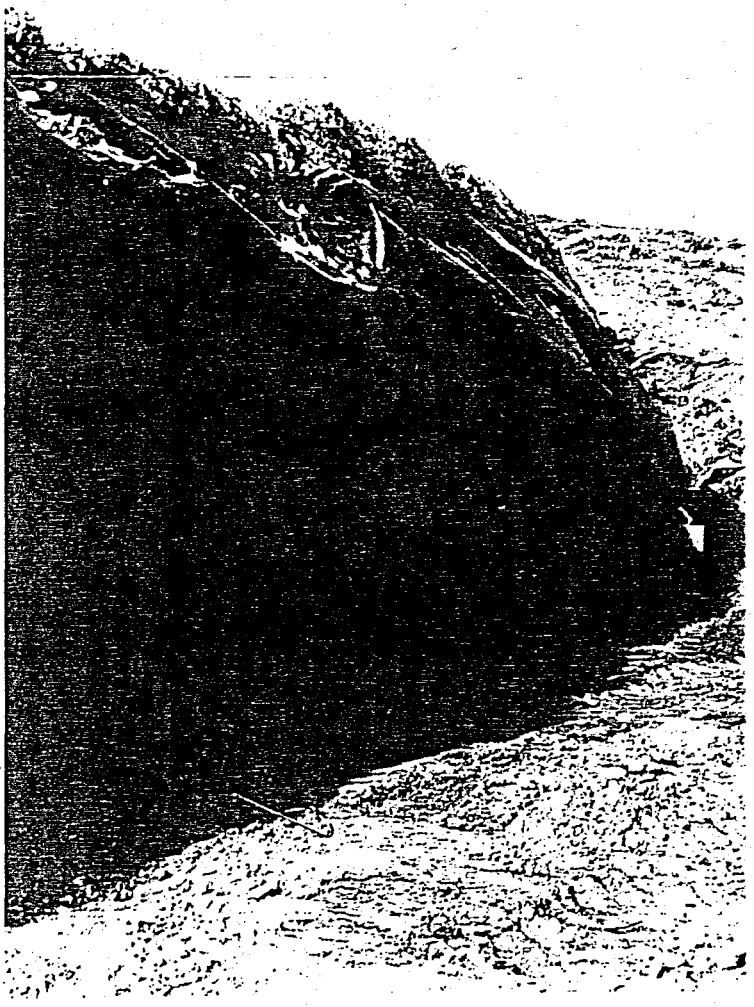

Photograph 15 The 4 Layer Wall after Removing the Upper Two Layers

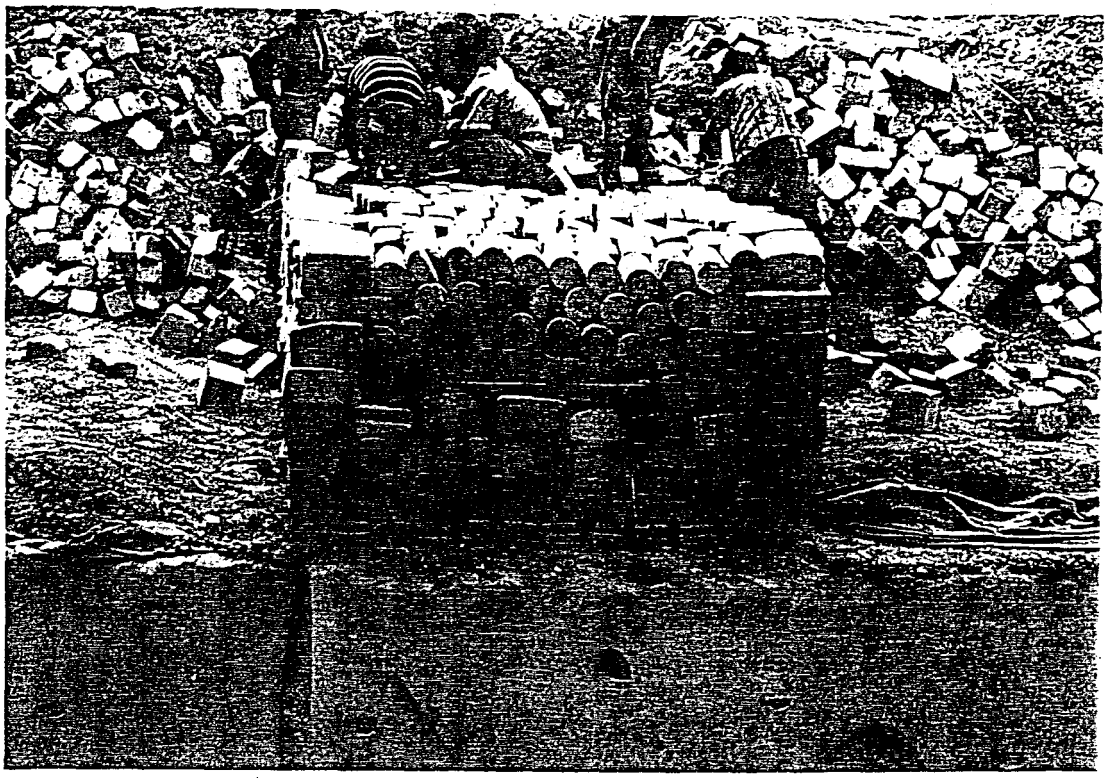

Photograph 16 Second Overloading Stage of the 4 Layer Wall

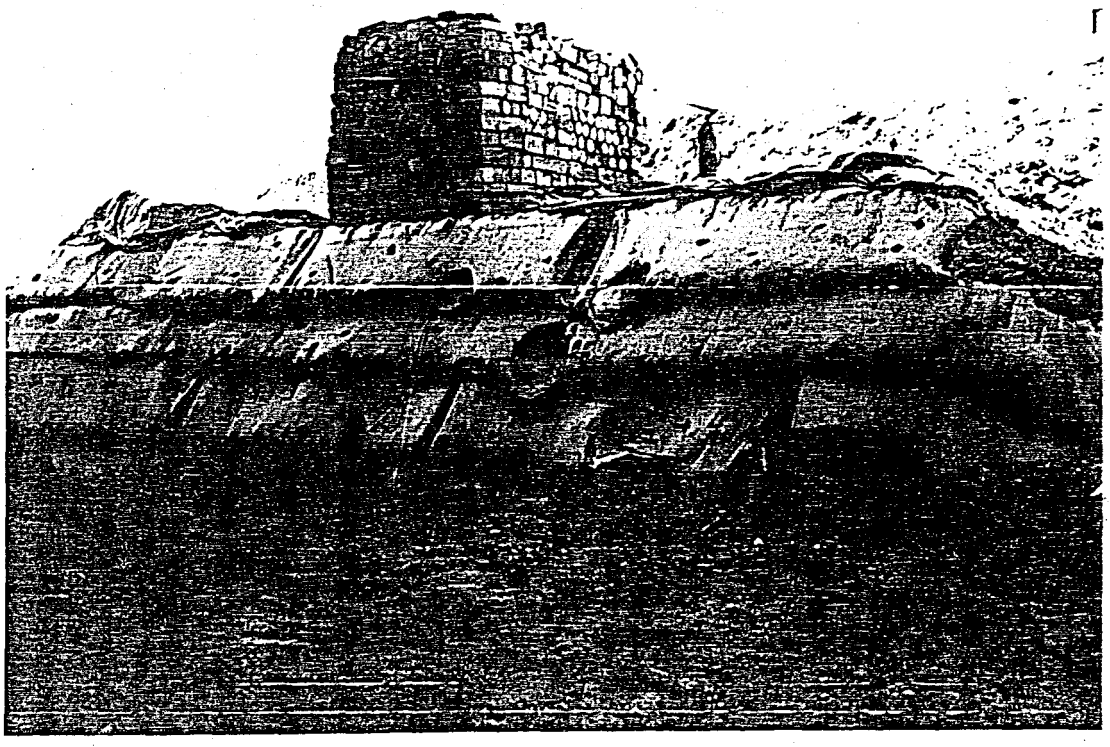

Photograph 17 The Surcharge Load over the Kilyos Wall

APPENDIX 2

Pressure Reading Measurements

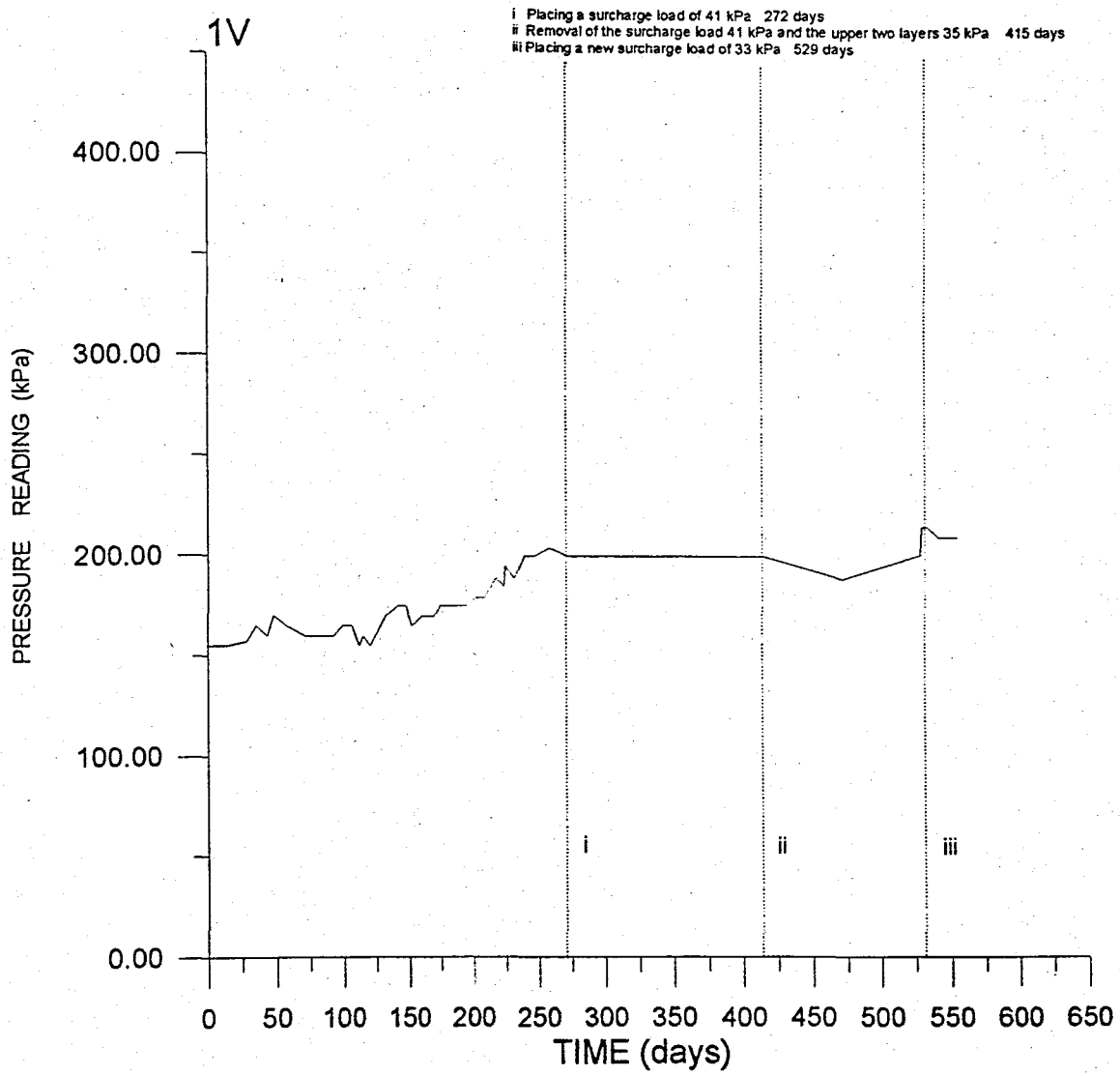

Graph 1 The Measurements of Glötzl Pressure Cell 1V

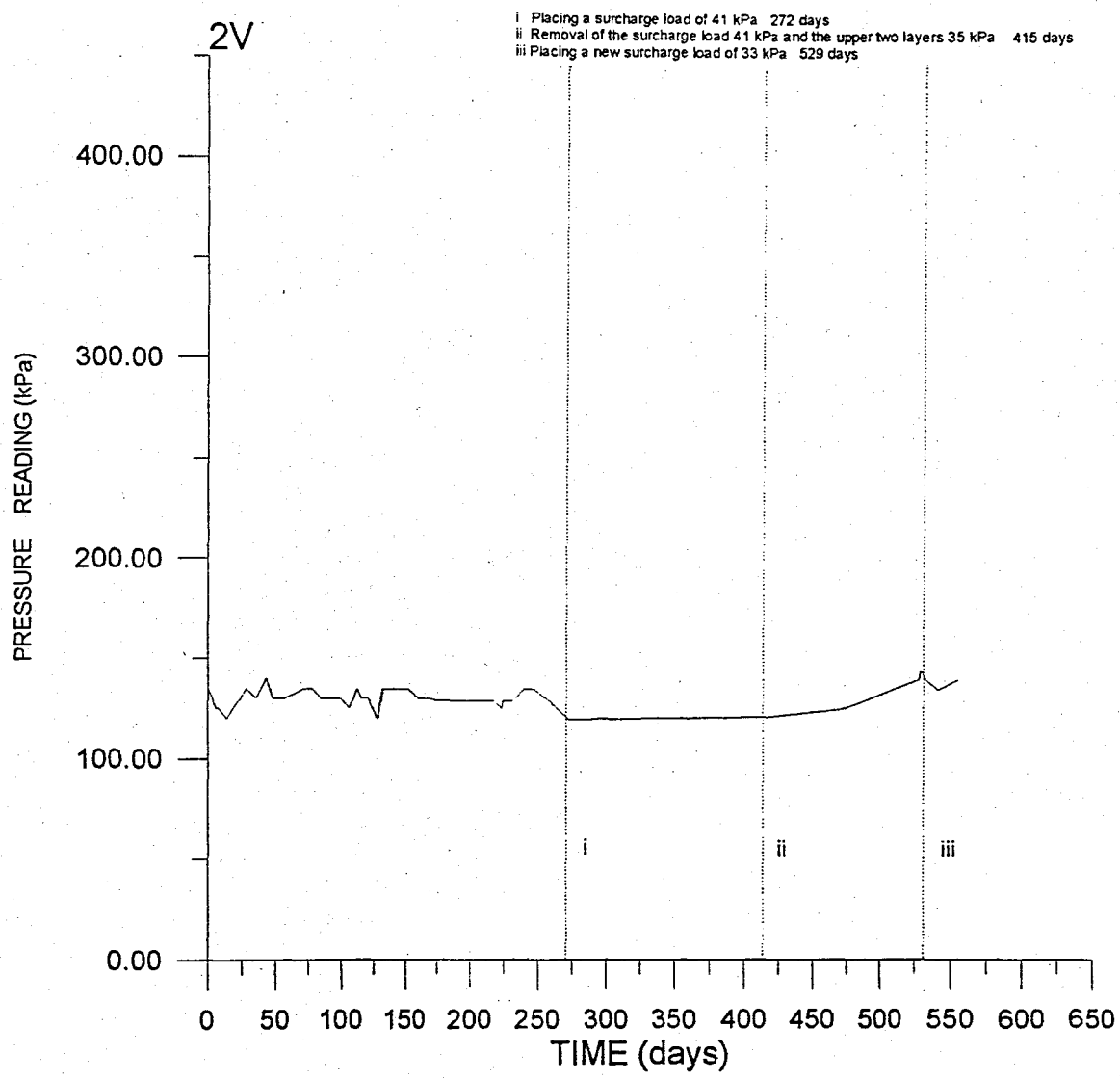

Graph 2 The Measurements of Glötzl Pressure Cell 2V

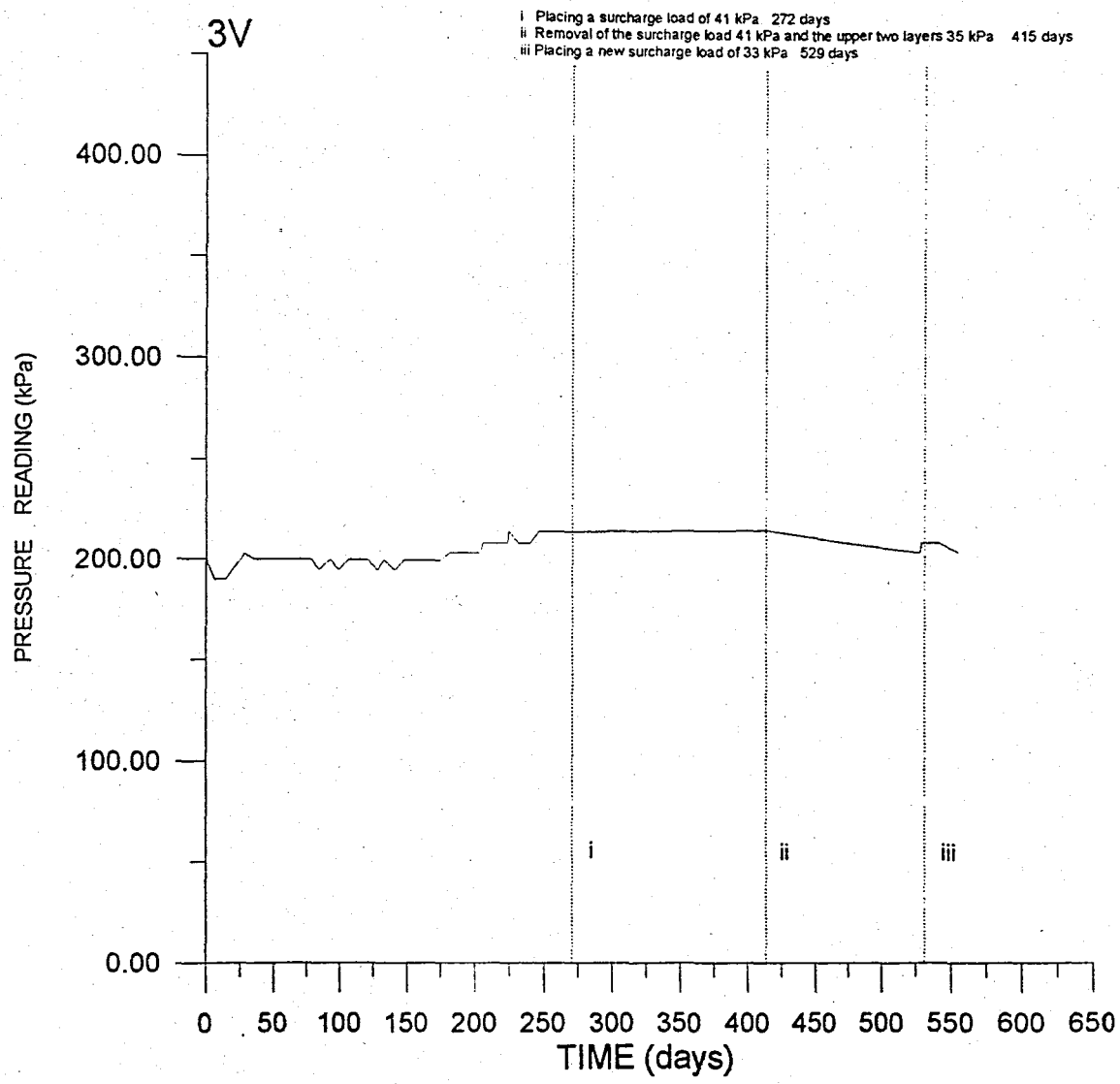

Graph 3 The Measurements of Glötzl Pressure Cell 3V

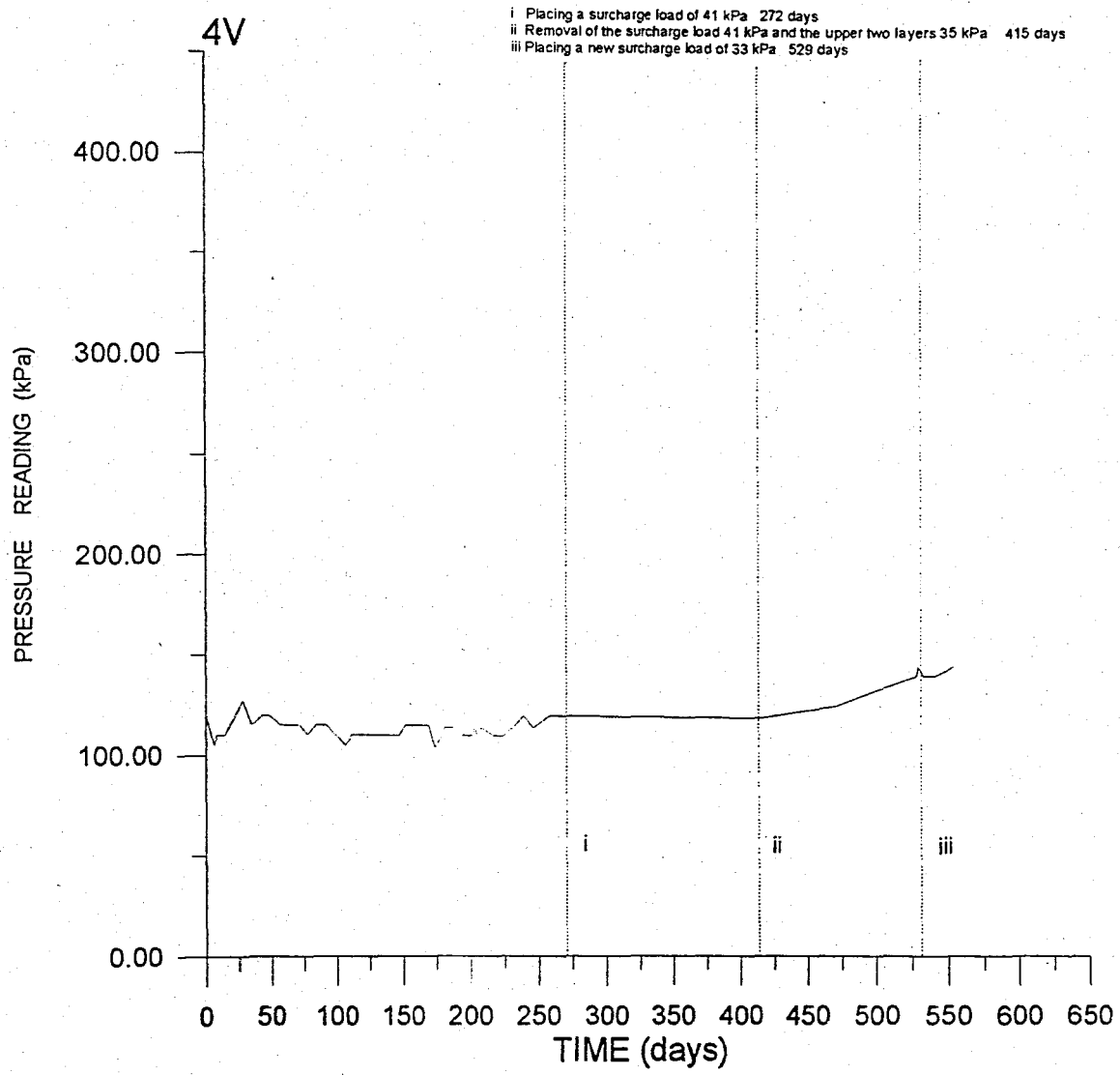

Graph 4 The Measurements of Glötzl Pressure Cell 4V

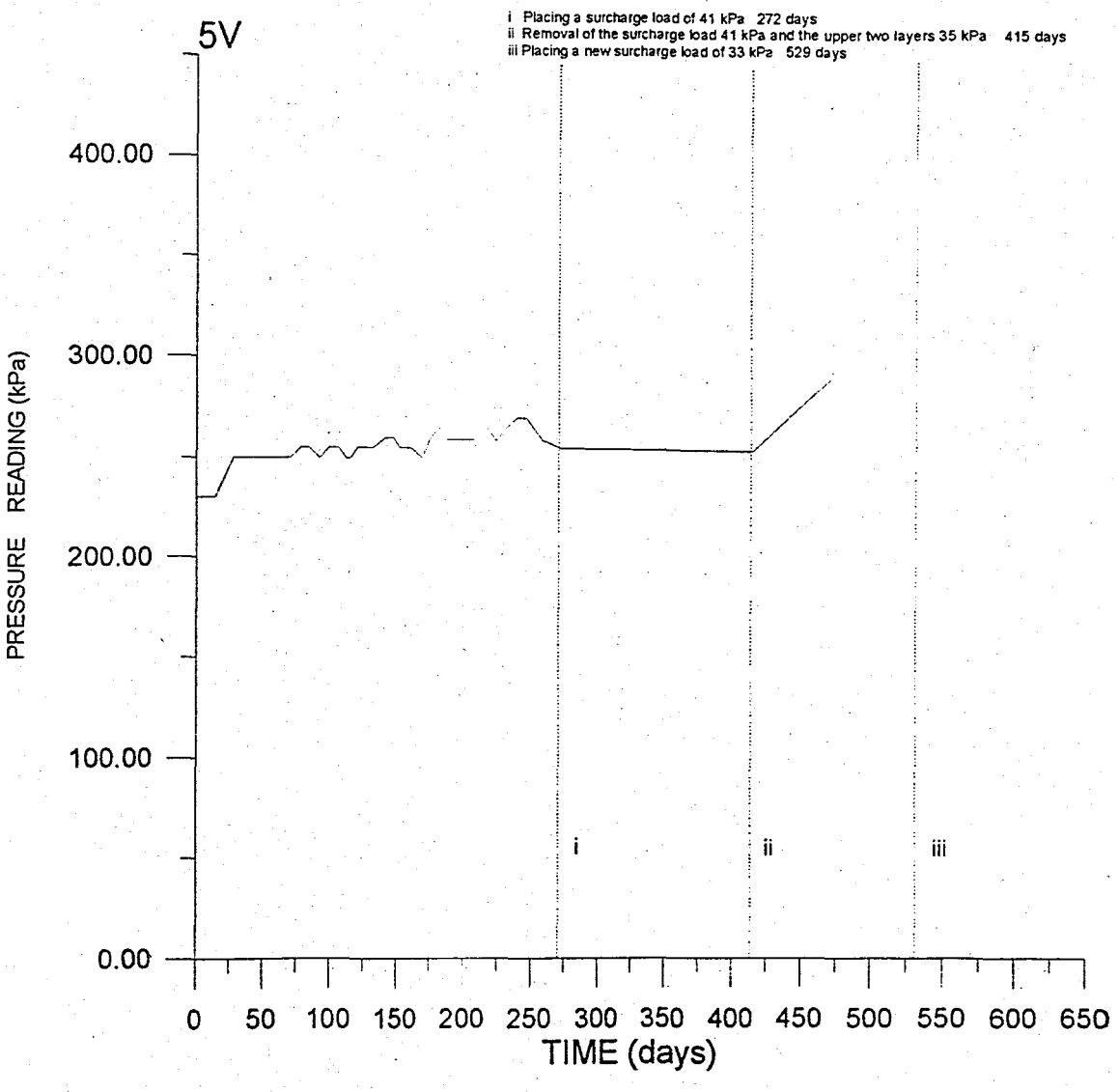

Graph 5 The Measurements of Glötzl Pressure Cell 5V

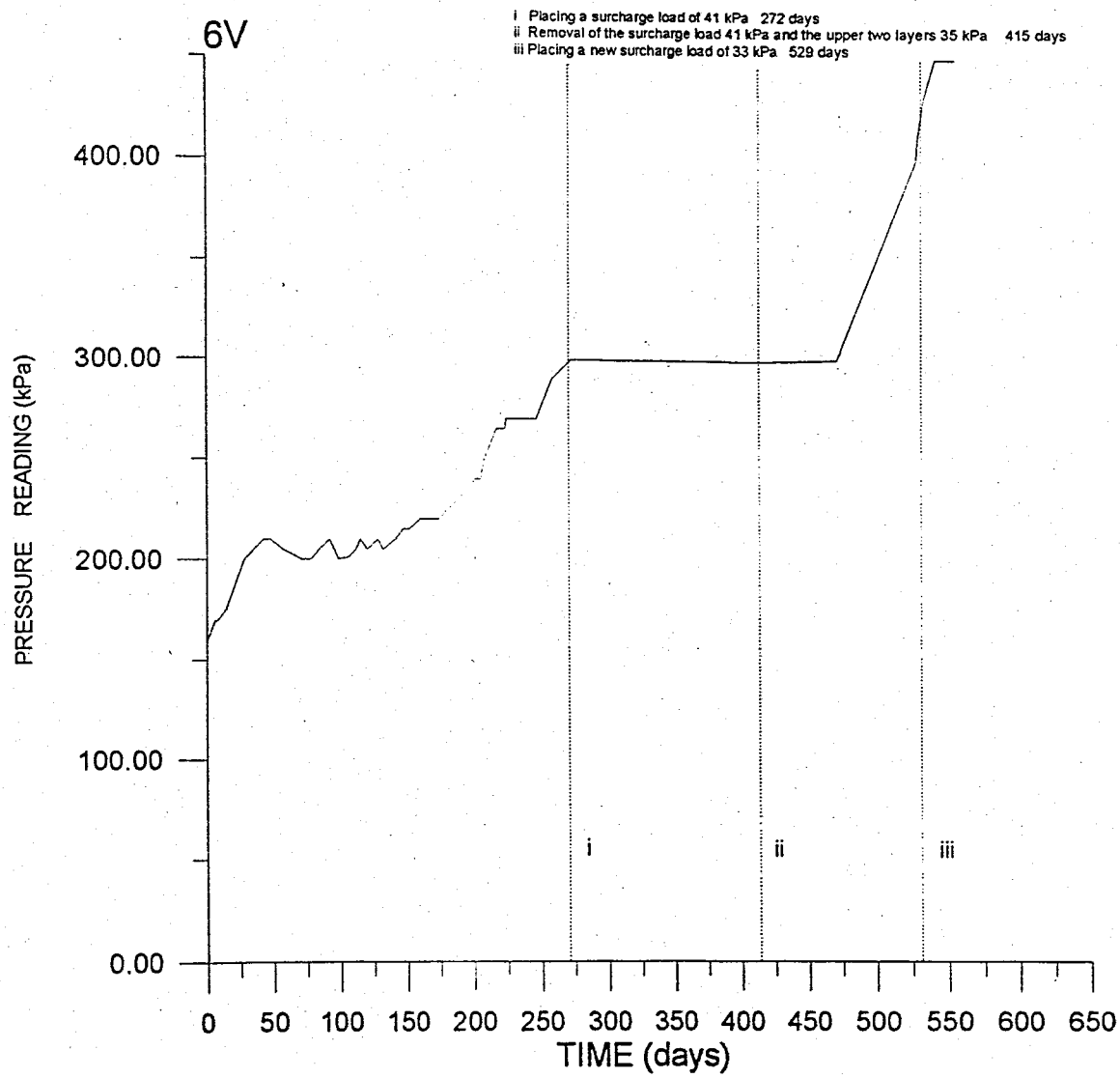

Graph 6 The Measurements of Glötzl Pressure Cell 6V

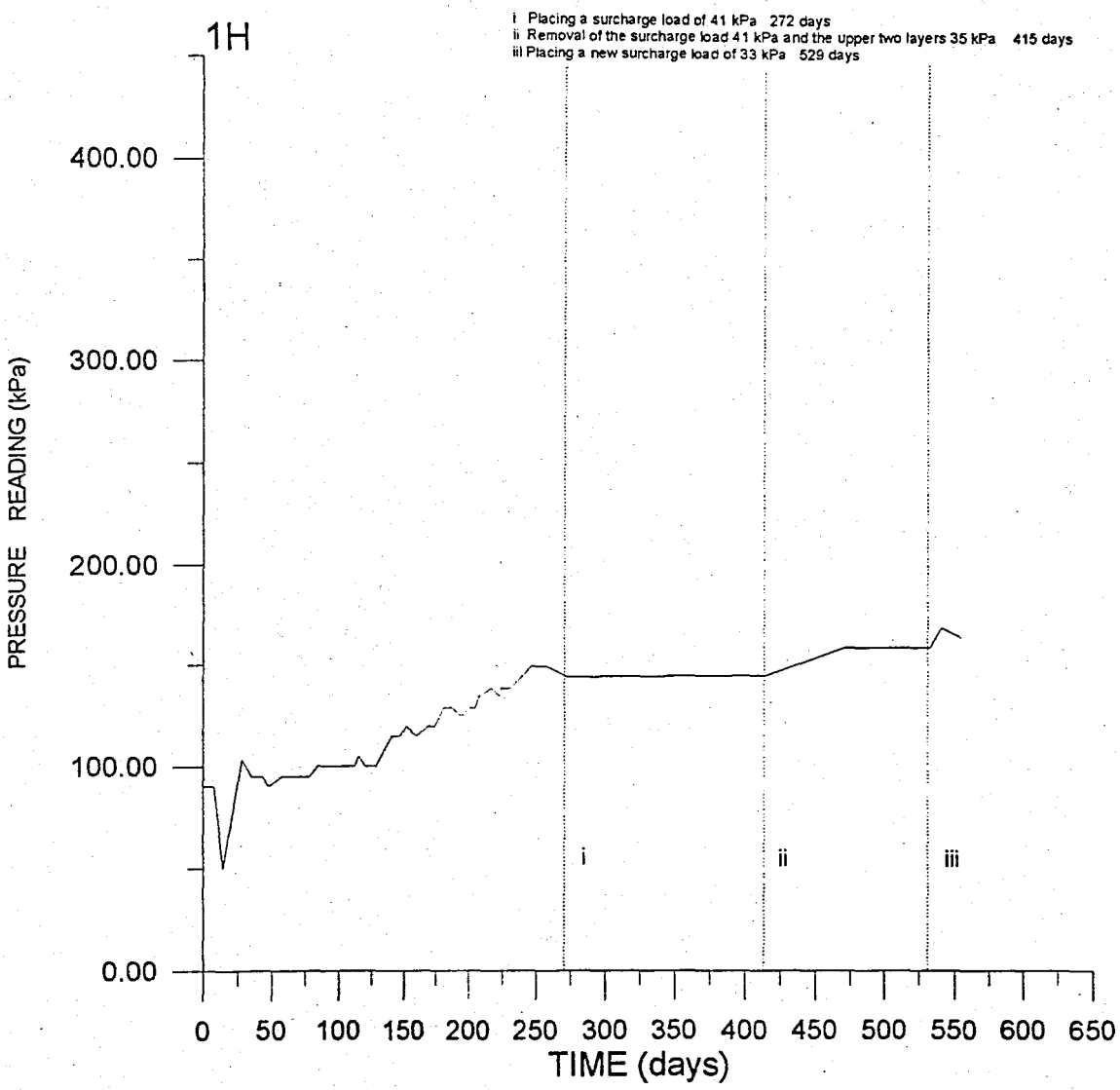

Graph 7 The Measurements of Glötzl Pressure Cell 1H

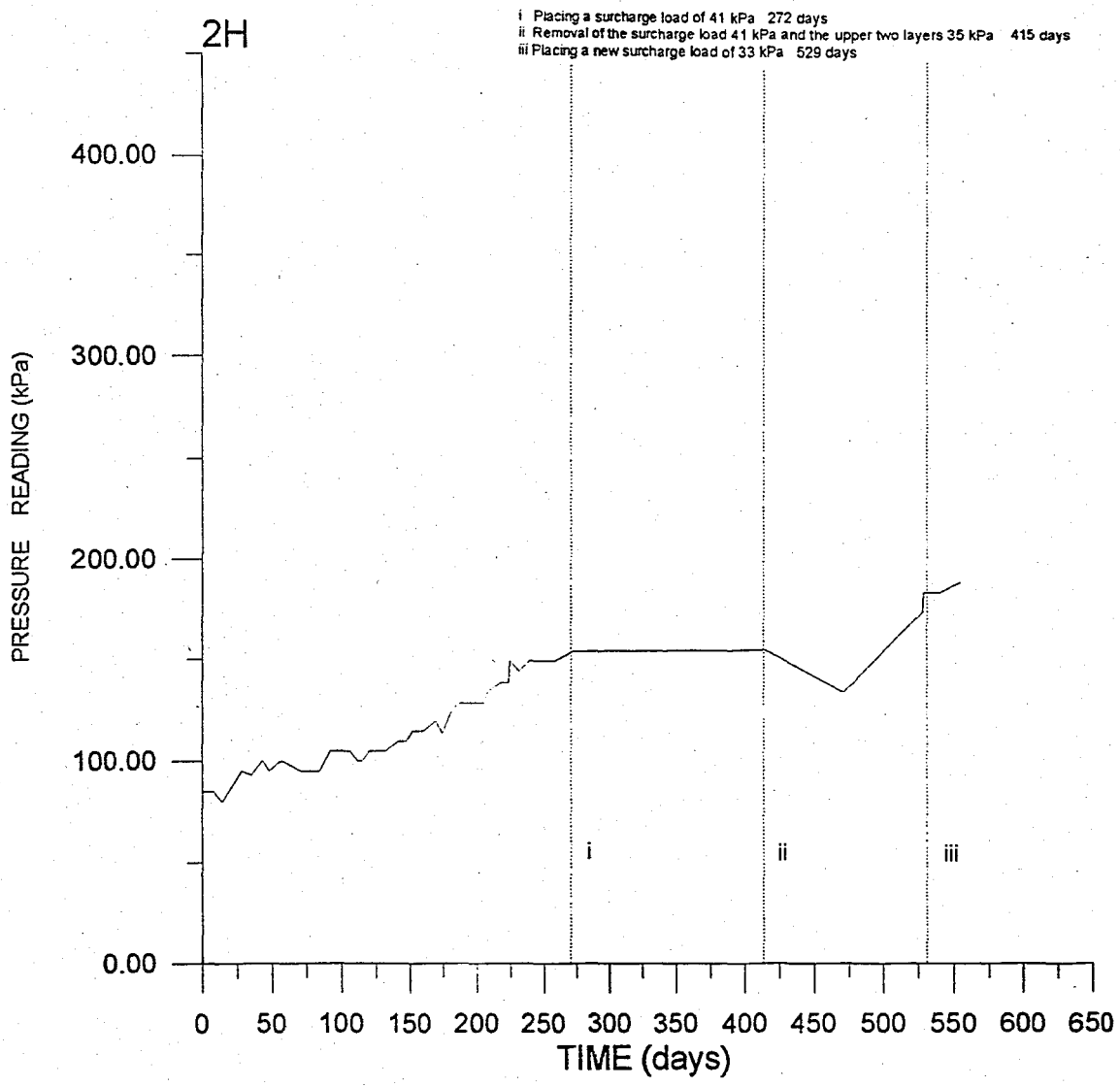

Graph 8 The Measurements of Glötzl Pressure Cell 2H

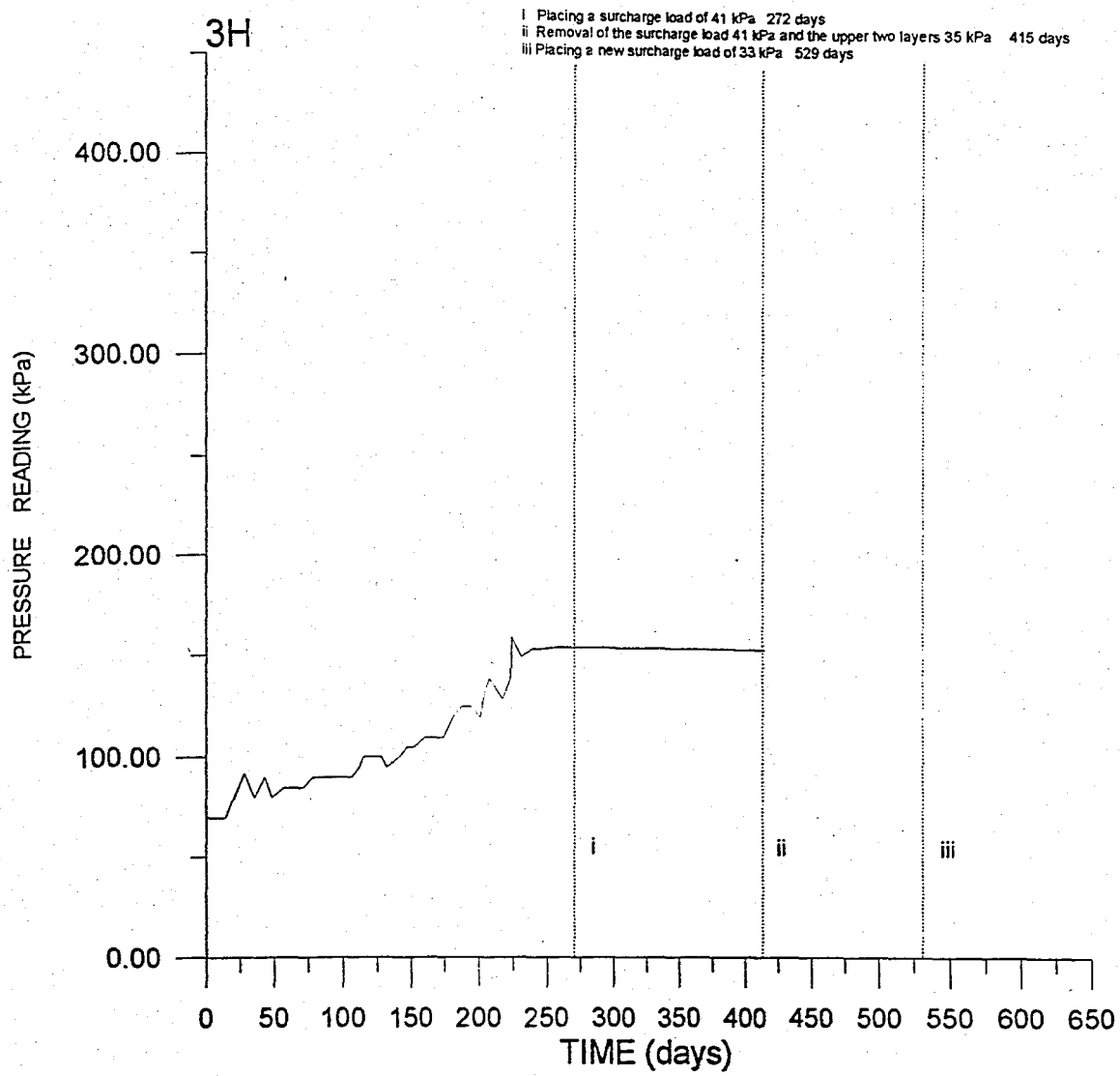

Graph 9 The Measurements of Glötzl Pressure Cell 3H

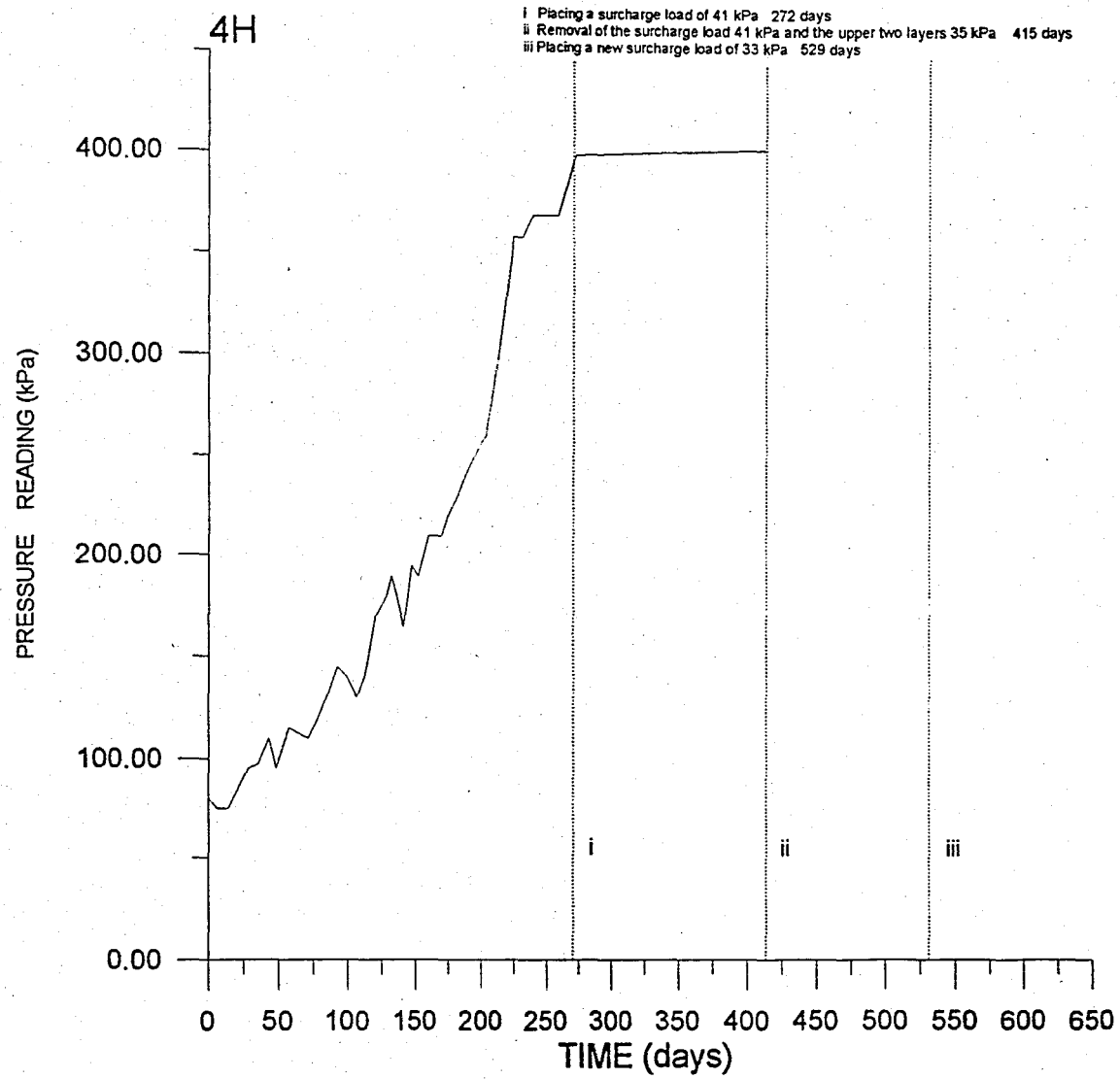

Graph 10 The Measurements of Glötzl Pressure Cell 4H

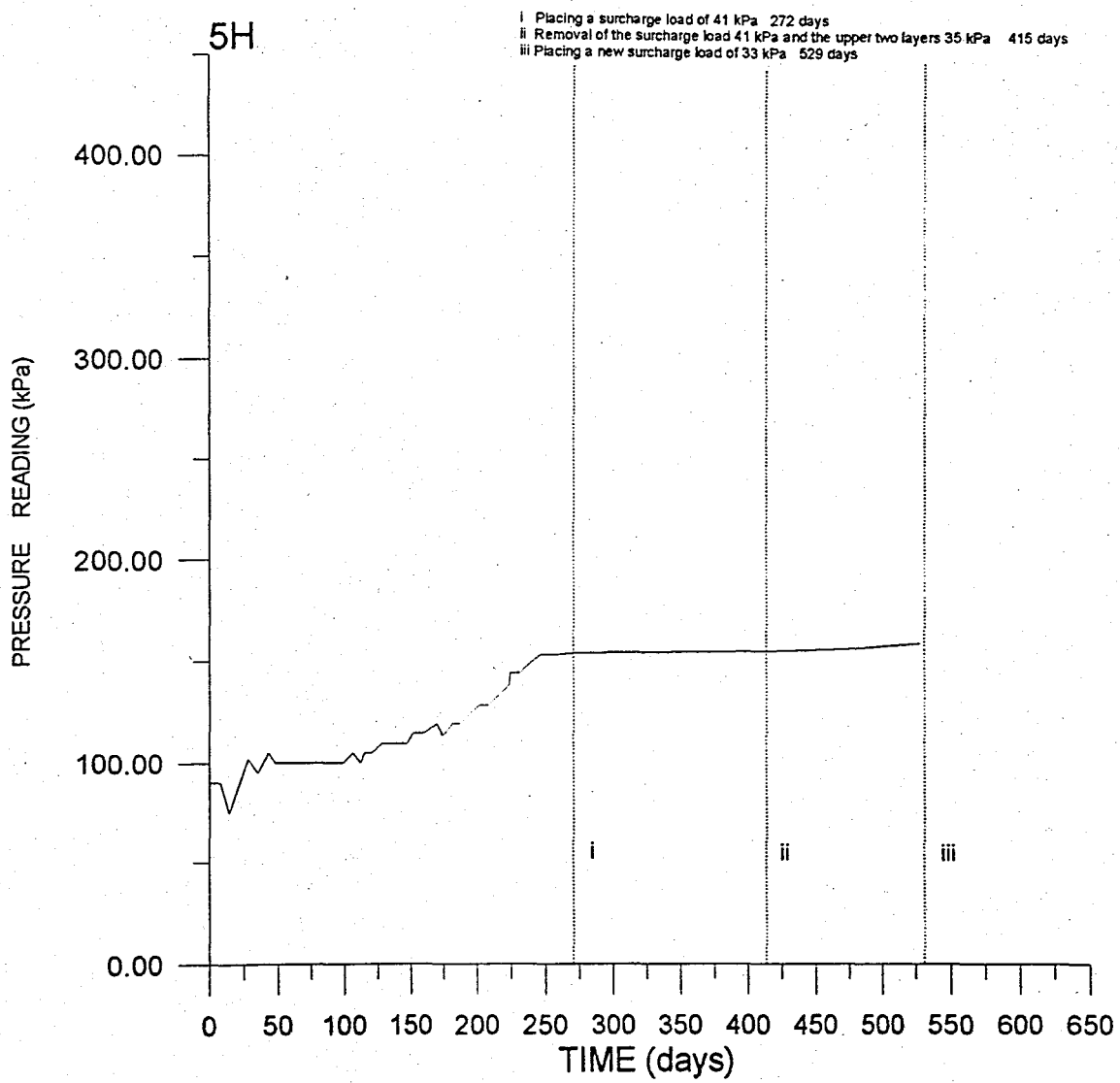

Graph 11 The Measurements of Glötzl Pressure Cell 5H

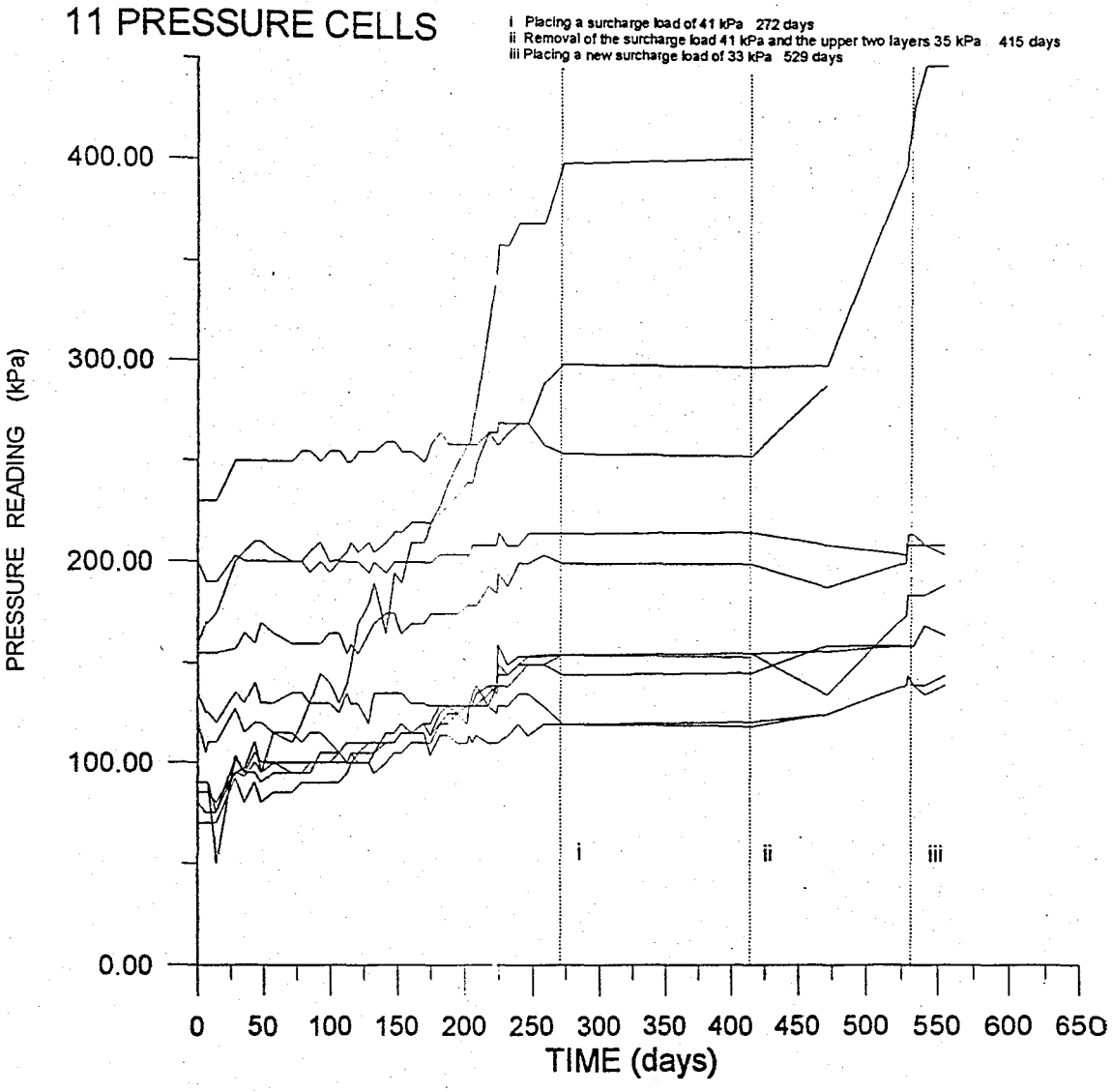

Graph 12 Measurements of all Pressure Cells

APPENDIX 3

Finite Element Analysis Results

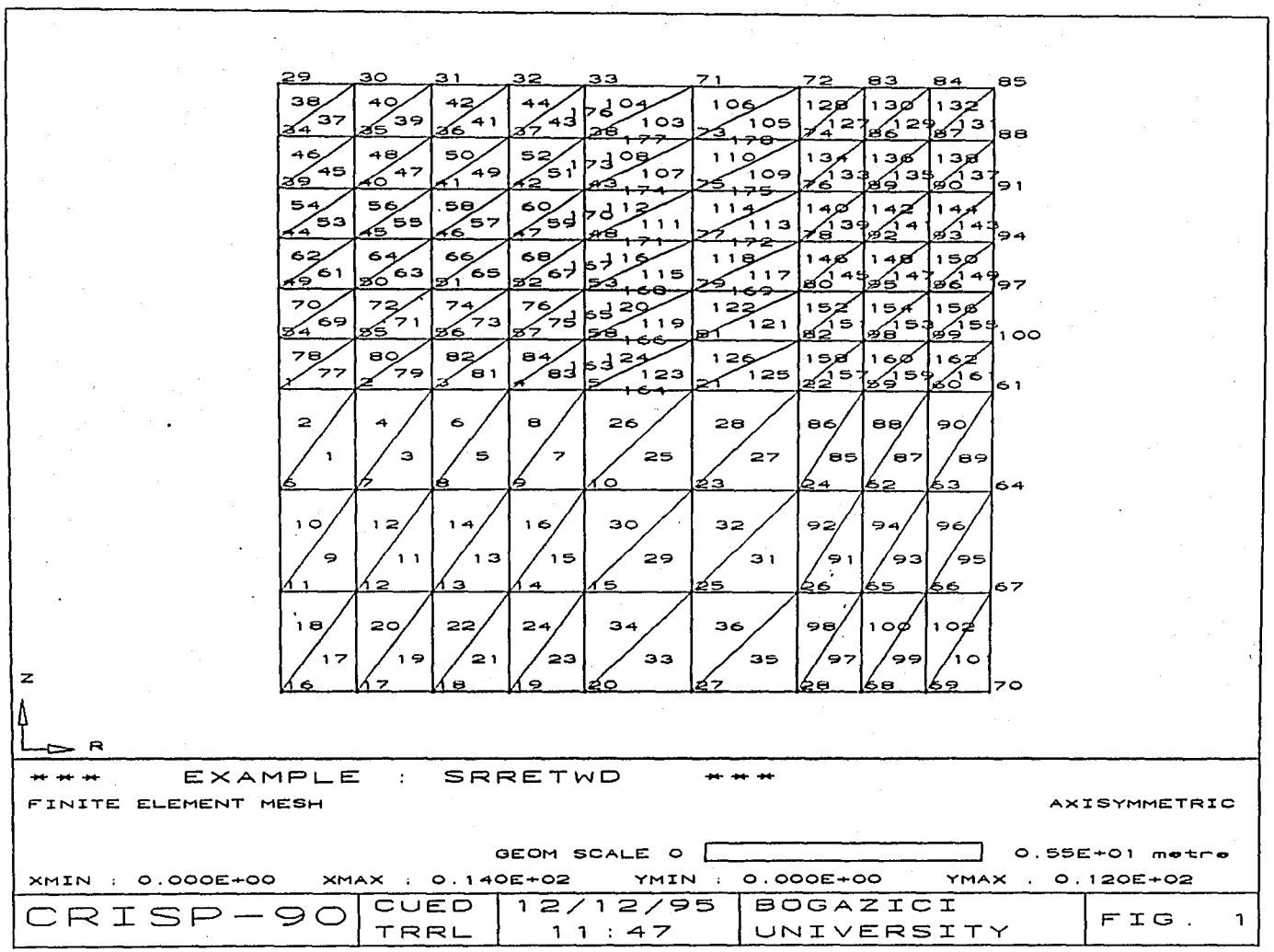

Figure A3.1 Finite Element Mesh

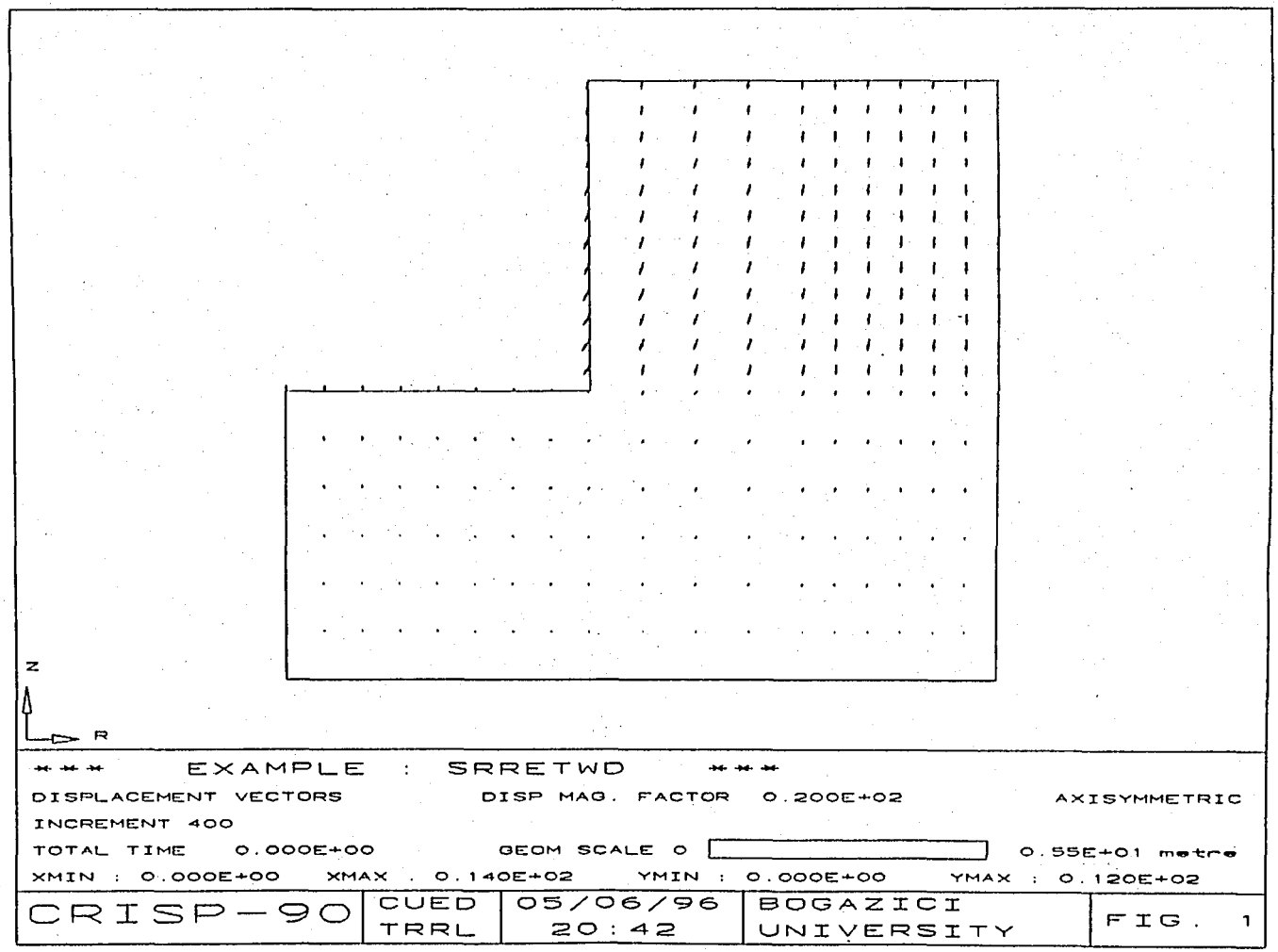

Figure A3.2 Displacement Vectors

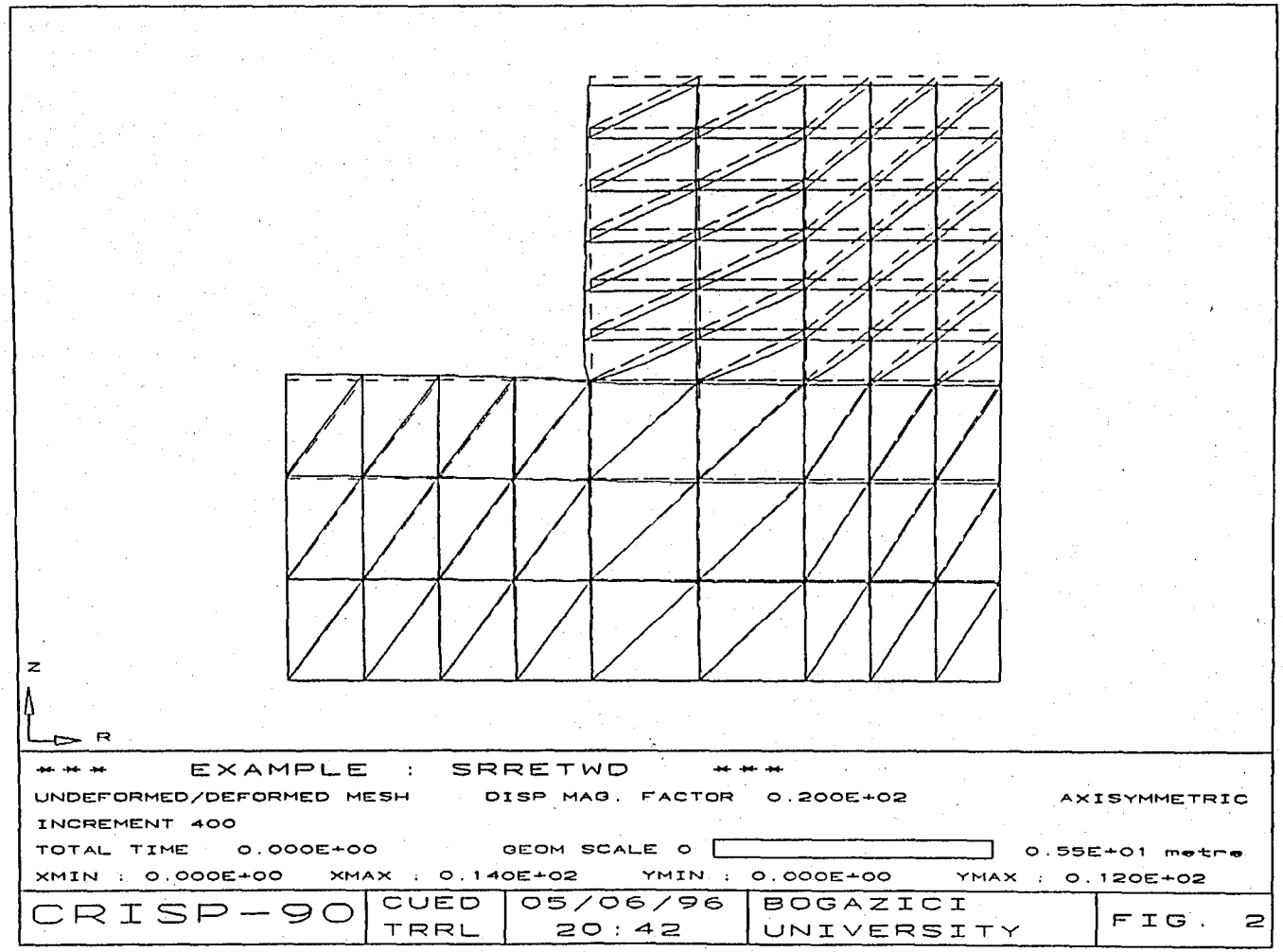

Figure A3.3 Undeformed / Deformed Mesh

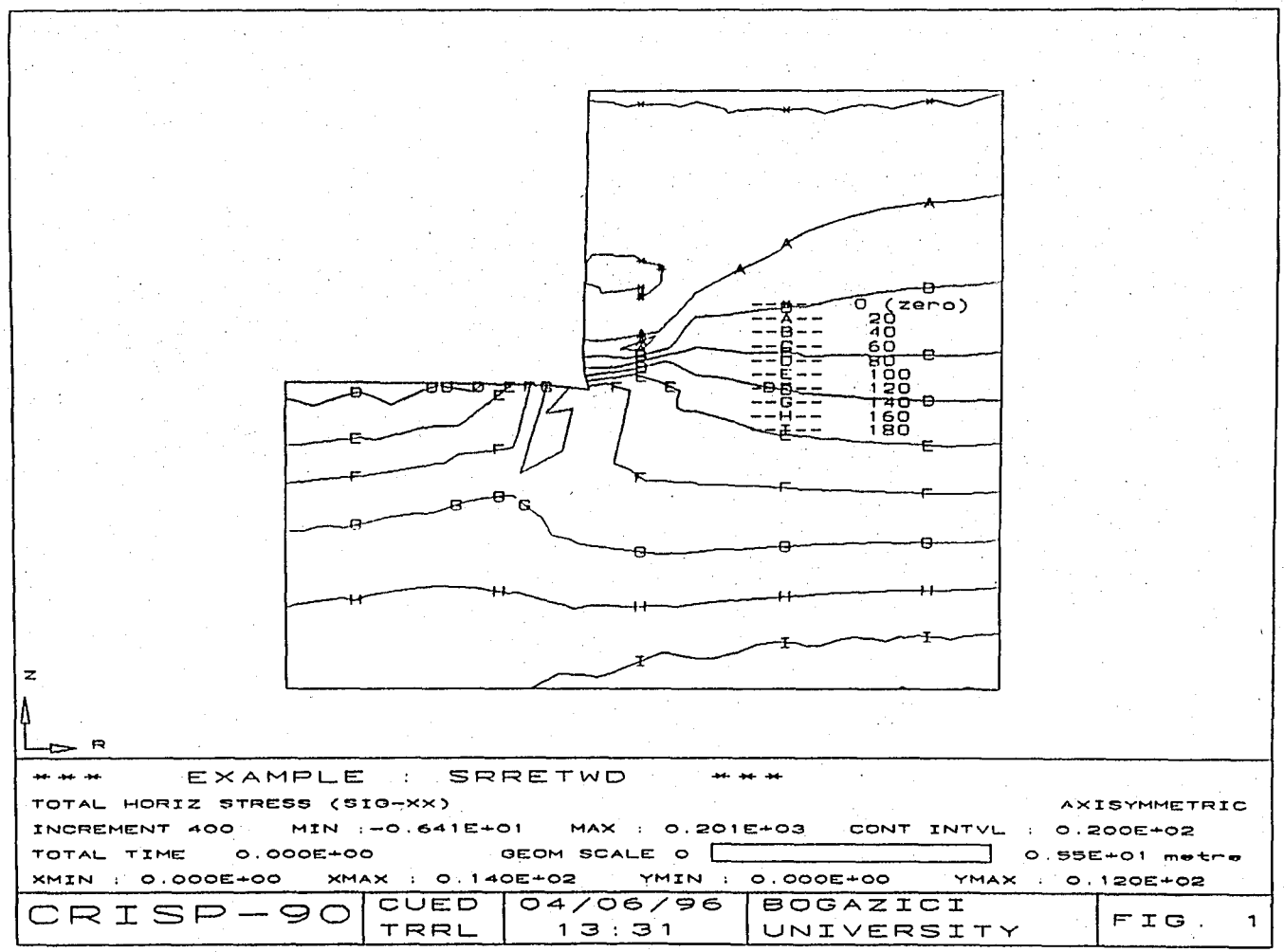

Figure A3.4 Total Horizontal Stress

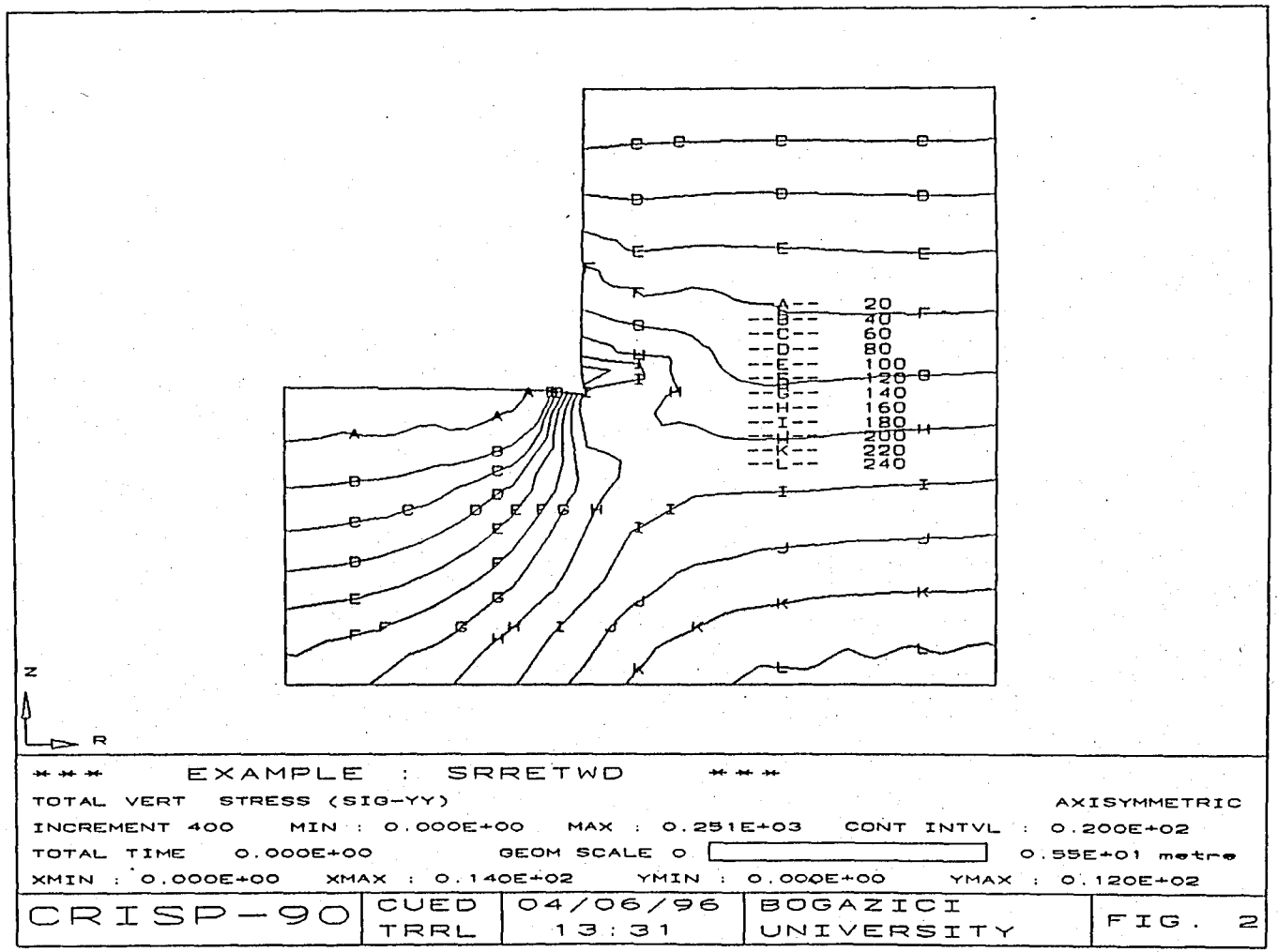

Figure A3.5 Total Vertical Stress

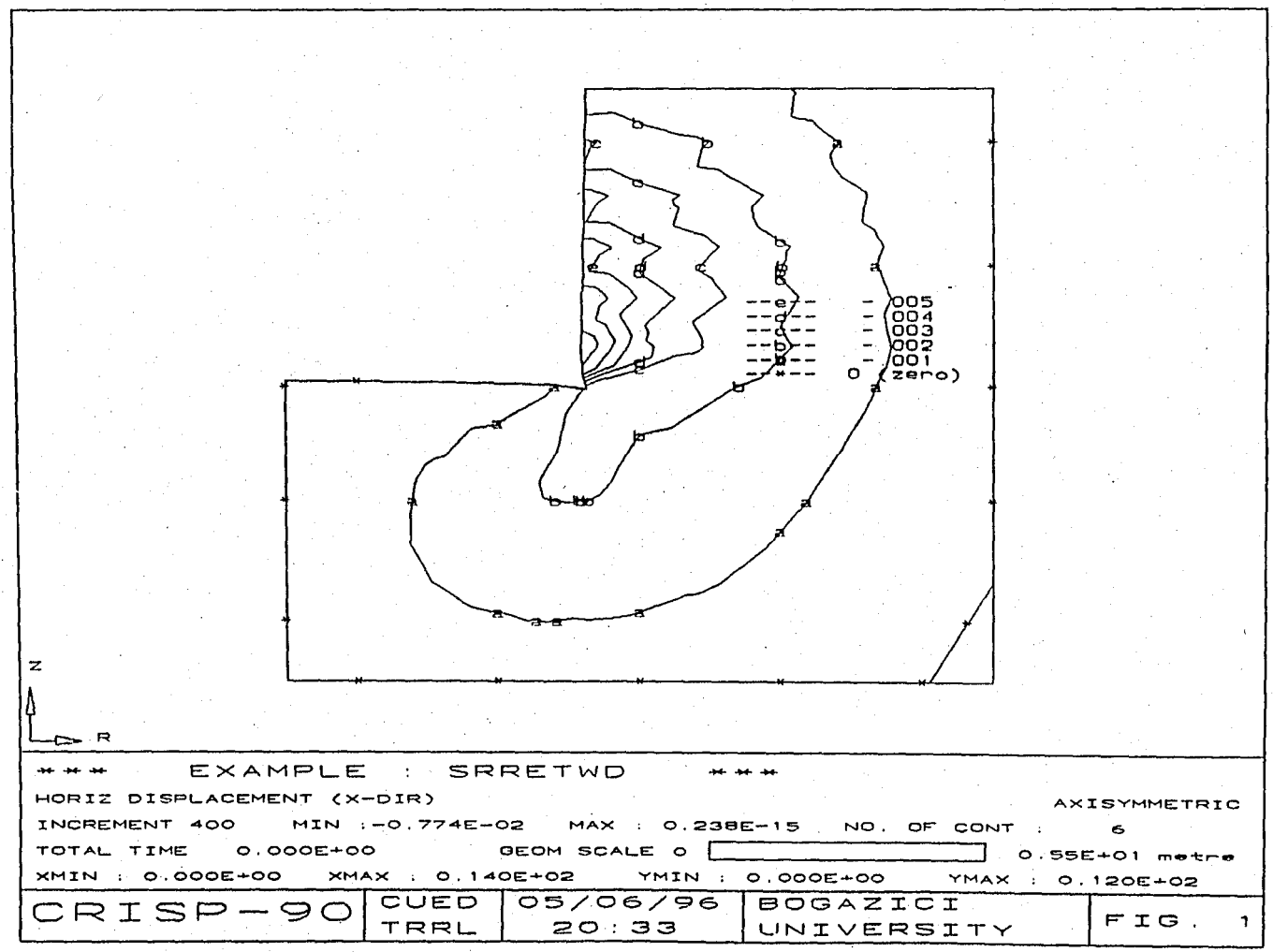

Figure A3.6 Horizontal Displacement

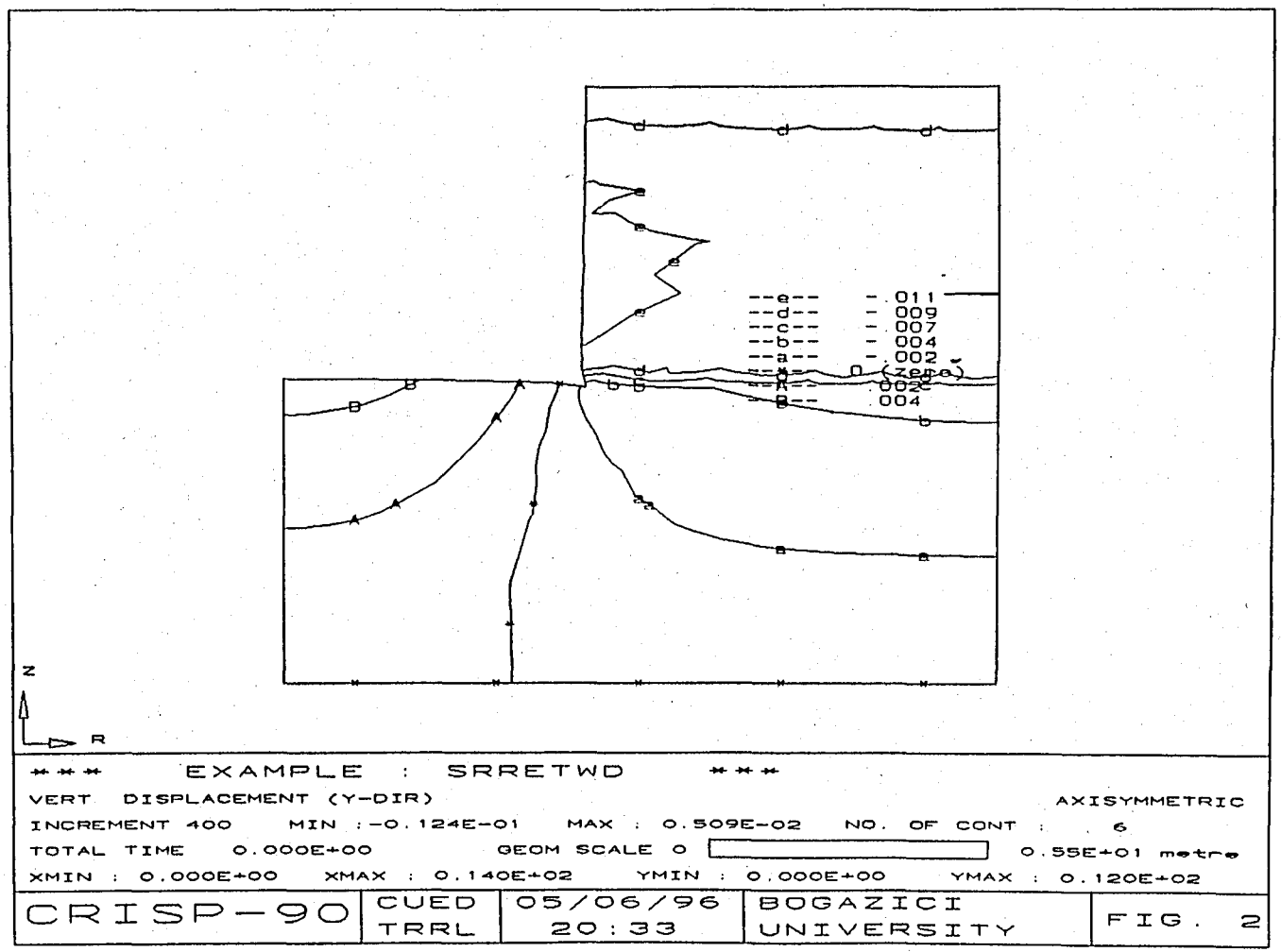

Figure A3.7 Vertical Displacement